Astronomy & Astrophysics manuscript no. Bonomoetal˙2017
October 11, 2018
© ESO 2018

arXiv:1704.00373v1 [astro-ph.EP] 2 Apr 2017

The GAPS Programme with HARPS-N@TNG ⋆

XIV. Investigating giant planet migration history via improved eccentricity and mass determination for 231 transiting planets

A. S. Bonomo[1], S. Desidera[2], S. Benatti[2], F. Borsa[3], S. Crespi[4], M. Damasso[1], A. F. Lanza[5], A. Sozzetti[1], G. Lodato[4], F. Marzari[6], C. Boccato[2], R. U. Claudi[2], R. Cosentino[7], E. Covino[8], R. Gratton[2], A. Maggio[9], G. Micela[9], E. Molinari[7], I. Pagano[5], G. Piotto[6], E. Poretti[3], R. Smareglia[10], L. Affer[9], K. Biazzo[5], A. Bignamini[10], M. Esposito[8], P. Giacobbe[1], G. Hébrard[11,12], L. Malavolta[6,2], J. Maldonado[9], L. Mancini[13,1], A. Martinez Fiorenzano[7], S. Masiero[9,14], V. Nascimbeni[6,2], M. Pedani[7], M. Rainer[3], and G. Scandariato[5]

(Affiliations can be found after the references)

Received 12 October 2016 / Accepted 1 March 2017

ABSTRACT

We carried out a Bayesian homogeneous determination of the orbital parameters of 231 transiting giant planets (TGPs) that are alone or have distant companions; we employed differential evolution Markov chain Monte Carlo methods to analyse radial-velocity (RV) data from the literature and 782 new high-accuracy RVs obtained with the HARPS-N spectrograph for 45 systems over ∼3 years. Our work yields the largest sample of systems with a transiting giant exoplanet and coherently determined orbital, planetary, and stellar parameters.

We found that the orbital parameters of TGPs in non-compact planetary systems are clearly shaped by tides raised by their host stars. Indeed, the most eccentric planets have relatively large orbital separations and/or high mass ratios, as expected from the equilibrium tide theory. This feature would be the outcome of planetary migration from highly eccentric orbits excited by planet-planet scattering, Kozai-Lidov perturbations, or secular chaos. The distribution of $\alpha = a/a_{\rm R}$, where a and $a_{\rm R}$ are the semi-major axis and the Roche limit, for well-determined circular orbits peaks at 2.5; this agrees with expectations from the high-eccentricity migration (HEM), although it might not be limited to this migration scenario. The few planets of our sample with circular orbits and $\alpha > 5$ values may have migrated through disc-planet interactions instead of HEM. By comparing circularisation times with stellar ages, we found that hot Jupiters with $a < 0.05$ au have modified tidal quality factors $10^5 \lesssim Q'_{\rm p} \lesssim 10^9$, and that stellar $Q'_{\rm s} \gtrsim 10^6 - 10^7$ are required to explain the presence of eccentric planets at the same orbital distance.

As a by-product of our analysis, we detected a non-zero eccentricity $e = 0.104^{+0.021}_{-0.018}$ for HAT-P-29; we determined that five planets that were previously regarded to be eccentric or to have hints of non-zero eccentricity, namely CoRoT-2b, CoRoT-23b, TrES-3b, HAT-P-23b, and WASP-54b, have circular orbits or undetermined eccentricities; we unveiled curvatures caused by distant companions in the RV time series of HAT-P-2, HAT-P-22, and HAT-P-29; we significantly improved the orbital parameters of the long-period planet HAT-P-17c; and we revised the planetary parameters of CoRoT-1b, which turned out to be considerably more inflated than previously found.

Key words. Planetary systems – Techniques: radial velocities – Stars: fundamental parameters – Planet-star interactions

1. Introduction

Despite two decades of observational efforts to discover extrasolar planets with a variety of techniques, many fascinating issues concerning the properties and orbital evolution of giant planets are still open questions. Among these are the migration of hot Jupiters, the origin of the frequently observed spin-orbit misalignments, and the architecture of planetary systems with close-in giant planets. These planets are thought to be formed beyond the water-ice line ($a \gtrsim 1 - 3$ au) in the protoplanetary disc, where solid material is abundant because of ice condensation, and then migrate towards their host stars (Bodenheimer et al. 2000; Rafikov 2006). Two main scenarios are usually invoked to explain the migration of hot giant planets: disc-driven migration and high-eccentricity migration (HEM).

The former would yield mainly circular orbits and spin-orbit alignments because of damping by the disc (e.g. Goldreich & Tremaine 1980; Papaloizou & Larwood 2000; Kley & Nelson 2012). Nevertheless, modest eccentricities $e \lesssim 0.1$ might be excited by disc-planet interactions for high disc surface densities and planet masses (e.g. Dunhill et al. 2013) or for less massive discs and planets with initial non-zero eccentricities ($e \sim 0.04$, Duffell & Chiang 2015). Actually, even significant obliquities can be observed after smooth disc migration if the disc was primordially misaligned for instance by a distant stellar companion (Batygin 2012) or chaotic star formation (Bate et al. 2010).

According to the HEM scenario, giant planets can move very close to their stars because of tidal dissipation of highly eccentric orbits occurring at periastron (e.g. Rasio & Ford 1996). Initial high eccentricities and spin-orbit misalignments are thought to be produced after disc dissipation by planet-planet scattering (e.g. Chatterjee et al. 2008), Kozai-type perturbations induced by a distant stellar or planetary companion on a highly inclined orbit (e.g. Fabrycky & Tremaine 2007, Naoz et al. 2011), secular dynamics in multi-planet systems (e.g. Wu & Lithwick 2011;

Send offprint requests to: A. S. Bonomo
e-mail: bonomo@oato.inaf.it

⋆ Tables 1, 2, 7, 8, and 9 are available in electronic form at the CDS via anonymous ftp to cdsarc.u-strasbg.fr (130.79.128.5) or via http://cdsweb.u-strasbg.fr/cgi-bin/qcat?J/A+A/

Hamers et al. 2017), or a combination of these processes (e.g. Nagasawa et al. 2008). Tidal dissipation inside the planet mainly acts to circularise and shrink the planetary orbit, while tides inside the star act to realign the orbital plane with the stellar equator (Lai 2012). This explains why circularisation and spin-orbit re-alignment may procede with different timescales according to the different dissipation rates inside the stars and the planets (e.g. Ogilvie 2014).

The current distribution of eccentricities of known giant planets – with circular orbits prevalently found at small distances from their host stars and significant eccentricities at wider separations where tidal interactions are much weaker – seem to support the high-eccentricity scenario against migration in the disc (see e.g. Matsumura et al. 2010; Pont et al. 2011, hereafter P11; Husnoo et al. 2012, hereafter H12). Moreover, planets that migrated from highly eccentric orbits through tidal dissipation and underwent orbit circularisation without significant mass or orbital angular momentum loss are expected to be found at a distance from their stars greater than or equal to twice the Roche limit $a_{\rm R} = 2.16 \cdot R_{\rm p} \cdot (M_{\rm s}/M_{\rm p})^{1/3}$ (e.g. Faber et al. 2005; Ford & Rasio 2006). It has recently been argued that this condition might also explain the sub-Jovian desert, the dearth of sub-Jupiter-mass planets on short-period orbits (Matsakos & Königl 2016; however, see also Mazeh et al. 2016).

Further support for the HEM is likely provided by the eccentricity-metallicity relation for warm Jupiters, that is Jovian planets with orbital periods $10 \lesssim P \lesssim 200$ d, first noticed by Dawson & Murray-Clay (2013). They pointed out that eccentric warm Jupiters are mainly found around metal-rich stars because in metal-rich environments more Jovian planets can form and thus more frequent gravitational interactions among them may occur via scattering or secular perturbations and raise their eccentricities. The finding that planets with an outer companion have higher average eccentricites than their single counterparts has been recently claimed by Bryan et al. (2016) from results of a Doppler survey of non-transiting systems carried out with the HIgh Resolution Echelle Spectrometer (HIRES) on the Keck telescope.

However, migration of close-in planets may also occur via interactions with the protoplanetary disc. Evidence for disc migration is mainly provided by i) giant planets orbiting very young stars and ii) hot and warm giant planets in compact systems, that is tightly packed multi-planet systems with minimum mutual inclinations:

i. Young giant planets such as V830 Tau b (Donati et al. 2016) with an age of ∼2 Myr likely migrated through interactions with the protoplanetary disc because HEM would usually require longer times (e.g. Nagasawa et al. 2008; Petrovich 2015; Petrovich & Tremaine 2016).
ii. Two examples of hot giant planets in compact systems are the planetary systems Kepler-101 (Bonomo et al. 2014) and WASP-47 (Becker et al. 2015). The former is composed of an inner super-Neptune (Kepler-101b) with an orbital period $P = 3.49$ d and an outer Earth-size planet with $P = 6.03$ d. The latter contains four planets, with its hot Jupiter WASP-47b between an inner super-Earth ($P = 0.79$ d) and an outer Neptune-size planet ($P = 9.03$ d), and an additional long-period companion (Neveu-VanMalle et al. 2016). The giant planets Kepler-101b and WASP-47b almost certainly underwent disc migration otherwise the HEM would have destabilised the orbits of their close planetary companions. However, systems like Kepler-101 and WASP-47 seem to represent the exception rather than the rule because high-precision space-based data from Kepler and CoRoT have revealed that the vast majority of hot giant planets do not have close companions (e.g. Latham et al. 2011; Steffen et al. 2012). The same considerations apply to warm Jupiters whose multiplicity rate appears to be significantly higher than hot giant planets (Huang et al. 2016).

Alternative theories to both high-eccentricity and disc migration to explain the presence of hot and warm giant planets in compact systems foresee in situ formation (Batygin et al. 2016; Huang et al. 2016), although these theories need observational corroboration (Batygin et al. 2016).

To yield more observational constraints to theoretical models of giant planet migration and star-planet tidal interactions, it is important to determine accurate and precise orbital and physical parameters, hopefully in a uniform way, for a large sample of giant planets. Among the known giant planets, those seen in transit are the most interesting because transits allow us to determine the planet radii and, when combined with RV measurements, their true masses, which are fundamental physical quantities for investigating tidal effects (e.g. Hut 1981). This work aims precisely to perform a homogeneous analysis of orbital and physical parameters of the known transiting giant planets (hereafter, TGPs) published before 1 January 2016 that do not belong to compact planetary systems. A particular attention is given to the orbital eccentricity which is a key parameter for understanding planetary evolution (e.g. Damiani & Lanza 2015). This analysis is of particular importance for several reasons:

- planet eccentricities are often fixed at zero in the discovery papers when found consistent with zero or different from zero but with a low significance. Even though in some cases this assumption may be justified (see e.g. Sect. 6 in Anderson et al. 2012), it prevents us from determining the uncertainty on the eccentricity and, when this uncertainty is large, small but significant eccentricities in principle cannot be excluded;
- radial-velocity (RV) data of some planetary systems discovered by independent groups and obtained with different spectrographs were never combined to improve the orbital solution;
- RV jitter terms (see e.g. Gregory 2005) were not included as free parameters in the orbital fit of several known TGPs. This may lead to an underestimation of the eccentricity uncertainty and, in the worst cases, even to spurious eccentricities (H12);
- previous homogeneous analyses by P11 and H12 were limited to less than 70 systems while about 300 well-characterised TGPs are known today.

For these reasons, we undertook a homogeneous Bayesian analysis of RV data published in the literature and new RVs we collected for forty-five TGPs with the High Accuracy Radial velocity Planet Searcher for the Northern hemisphere (HARPS-N) spectrograph on the 3.6 m Telescopio Nazionale Galileo in La Palma island since mid-2012. We determine the orbital and physical parameters of 231 known TGPs in a consistent way, estimate upper and lower limits of their modified tidal quality factors, and, in general, attempt to understand better the orbital evolution/migration of close-in gaseous giant planets. We also report improved constraints on some long-term trends caused by distant companions of known TGPs with the HARPS-N observations we obtained so far.

2. Giant planet sample and radial-velocity datasets

2.1. Sample selection

The sample of the TGPs for our homogeneous analysis was chosen as follows. First, we selected only transiting planets with masses $0.1 < M_p < 25$ M_{Jup} and uncertainty on the mass lower than 30%. We set the mass upper limit following Schneider et al. (2011) and, to discard low-mass planets that may undergo a completely different evolution, we used a lower limit that is more conservative than the value of 0.3 M_{Jup} adopted by Hatzes & Rauer (2015). Indeed, in addition to the fact that the mass range of TGPs between 0.1 and 0.3 M_{Jup} is not well populated, the transition between low-mass and giant planets may not occur sharply at 0.3 M_{Jup} (see Fig. 2 in Hatzes & Rauer 2015). We are interested in TGPs that are alone or have distant companions (if any) with orbital separations from the inner planet greater than 0.5 au. So TGPs with $M_p > 0.1$ M_{Jup} in compact multi-planet systems, such as the already mentioned WASP-47 and Kepler-101 systems, but also Kepler-9 (Holman et al. 2010; Borsato et al. 2014) and Kepler-89 (Weiss et al. 2013), were excluded. We took into account the TGPs satisfying the aforementioned criteria that were published before 1 January 2016 and found 235 systems from which we excluded four systems, namely HAT-P-44, HAT-P-46, Kepler-14, and WTS-1. This yields 231 systems for our sample which are listed in Table 5.

The HAT-P-44 and HAT-P-46 systems were excluded because, after preliminary analyses of the HIRES RV data, we noticed their orbital parameters strongly depend on those of their outer companions, but the latter are not well constrained by the HIRES RVs (Hartman et al. 2014). We removed Kepler-14 from our catalogue because the RV semi-amplitude cannot be simply derived by the orbital fit (Sect. 3), but requires an ad hoc correction for the contamination by the visual stellar companion (Buchhave et al. 2011b). Finally, we noticed that some of the epochs of the RV data of WTS-1 listed in the discovery paper (Cappetta et al. 2012) are incorrect[1]. For this reason, we excluded it as well.

2.2. HARPS-N radial-velocity data

As mentioned in Sect. 1, we obtained new RVs for 45 of the selected 231 systems with the fibre-fed cross-dispersed HARPS-N echelle spectrograph on the Telescopio Nazionale Galileo (Cosentino et al. 2012, 2014). These data were obtained by the Global Architecture of Planetary Systems (GAPS) Consortium (Poretti et al. 2015). The high-resolution (R = 115 000) HARPS-N spectrograph is located in a vacuum vessel which ensures temperature and pressure stability and thus provides very accurate RV measurements with instrumental drifts $< 1\,m\,s^{-1}$ per night.

These 45 systems were chosen from the list of dwarf stars with TGPs known at the time of the start of our programme (April 2012) that are brighter than $V = 12.0$ and further north than −20 deg. Very fast rotators or well-studied hosting stars that already had many RV measurements were excluded. A few individual targets were added to the sample during the execution of the programme for RV monitoring after dedicated Rossiter-McLaughlin observations or for other specific reasons of interest.

[1] Unfortunately, the leading author was unable to recover the correct epochs even though the reported orbital phases in Table 8 of Cappetta et al. (2012) should not be affected by errors.

Table 1. HARPS-N radial-velocity measurements and associated photon-noise uncertainties.

Target	Epoch $BJD_{UTC} - 2,450,000$	RV $m\,s^{-1}$	σ_{RV} $m\,s^{-1}$
HAT-P-1	6147.708176	-2627.69	1.53
HAT-P-1	6566.590673	-2679.27	1.77
...	...	...	...

Notes. HARPS-N RV data are available at the CDS. A portion is shown here for guidance regarding its form and content.

At least seven RVs were taken for each of the 45 systems; for some of them we obtained more than 30 RV measurements. These observations are spread over $\sim 2.5 - 3$ yr and were gathered with typical exposure times of 15 min with a simultaneous Thorium-lamp spectrum for stars with $V < 10.5$ or in obj_AB observing mode, that is with fibre A on target and fibre B on sky, for fainter stars. Indeed, the simultaneous Thorium lamp does not provide a real improvement in the accuracy of RVs for $V \gtrsim 10.5$. Radial velocities were extracted from the high-resolution spectra with the standard online pipeline that performs a weighted cross-correlation with the numerical mask closer to the stellar spectral type (Pepe et al. 2002). Their typical photon-noise errors range from 2 to 10 $m\,s^{-1}$, depending on the stellar brightness and projected rotational velocity $V \sin i$ (Bouchy et al. 2009). The RVs of HAT-P-2 and XO-3, which are moderately fast rotators, were obtained by fitting the cross-correlation function with a Gaussian function over a window of 50 $km\,s^{-1}$ instead of the default value of 20 $km\,s^{-1}$. The reprocessing was performed using the Yabi interface at the Trieste Observatory (Borsa et al. 2015).

In total, we collected 782 HARPS-N RVs, which are listed in Table 1 along with their epochs given in BJD_{UTC} and photon-noise uncertainties. Some of them have already been published such as those acquired for Qatar-1 (Covino et al. 2013), HAT-P-18 (Esposito et al. 2014), XO-2N (Damasso et al. 2015a), TrES-4 (Sozzetti et al. 2015), and KELT-6 (Damasso et al. 2015b). The RVs of Qatar-1 and HAT-P-18 in Table 1 are slightly different from those reported in Covino et al. (2013) and Esposito et al. (2014) because they were extracted with the latest version of the HARPS-N pipeline (version 3.7), not available at the time of the original publications. We derived the RVs of HD 17156 from the HARPS-N spectra that were collected by Maggio et al. (2015) to search for possible variations in the $\log R'_{HK}$ activity indicator from periastron to apoastron; for this reason, these data have a specific sampling, with many observations being concentrated in four nights close to periastron or apoastron (see Table 1).

2.3. Literature radial-velocity data

For each system, we used the available RV datasets published in the literature before 1 January 2016 with at least four RV observations at different orbital phases and excluded all the in-transit measurements because the Rossiter effect was not modelled along with the orbital fit (Sect. 3). We list the total number of RVs used, their timespan, and the number of independent datasets for each of the 231 host stars in Table 5. The maximum number of independent RV datasets for a single system is five (WASP-14).

In a few cases, considerably noisy RV datasets were not used when they do not yield any improvement in the orbital solution and more precise data taken with other spectro-

Table 2. TRES radial-velocity measurements of Qatar-2 and associated photon-noise uncertainties.

Epoch	RV	σ_{RV}
$BJD_{UTC} - 2,450,000$	$m\,s^{-1}$	$m\,s^{-1}$
5580.0116	431.38	38.54
5581.0271	537.21	33.54
...	...	...

Notes. Data are available at the CDS. A portion is shown here for guidance regarding its form and content.

graphs are available. In two cases, such as Qatar-1 and TrES-4, the literature RV measurements of Alsubai et al. (2011) and Mandushev et al. (2007) were not included because they yield RV semi-amplitudes that are inconsistent with the HARPS-N data (see Covino et al. 2013 and Sozzetti et al. 2015 for Qatar-1 and TrES-4, respectively).

2.4. Additional radial-velocity data

For the present work we used an updated set of RVs for Qatar-2, consisting of 42 Tillinghast Reflector Echelle Spectrograph (TRES) RVs spanning 153 days from the discovery paper (Bryan et al. 2012) after correcting for a minor bug in the barycentric correction (Bryan et al. 2014), plus 27 new TRES RVs spanning 316 additional days (C. A. Latham, private communication). These RVs are listed in Table 2.

We also included new HARPS data of CoRoT-9 that are presented in Bonomo et al. (2017) and that allow us to derive more precise orbital parameters and, in particular, non-zero eccentricity.

3. Bayesian data analysis

The literature data and our new HARPS-N RV measurements were fitted with i) a Keplerian orbit model; ii) a Keplerian orbit and a long-term linear drift when residuals obtained with the simple Keplerian orbit show a significant ($\geq 3\sigma$) slope caused by either an outer planetary/stellar companion or an activity cycle; iii) two non-interacting Keplerians with a possible long-term drift if the inner TGP has a known long-period companion, as in the case of HAT-P-13, HAT-P-17, WASP-8, etc.; iv) a Keplerian orbit and a curvature if data cover less than half of the period of the outer companion or the activity cycle, as for HAT-P-2, HAT-P-22, HAT-P-29, WASP-34, XO-2N (Sect. 5.2).

The free parameters of model i) are the transit epoch T_c, the orbital period P, the RV semi-amplitude K, $e\cos\omega$ and $e\sin\omega$ (where e and ω are the eccentricity and the argument of periastron), a jitter term s_j and a RV zero point for each dataset (which accounts for the RV offsets among different spectrographs). The slope $\dot{\gamma}$ is the extra parameter in model ii), with the addition of the quadratic trend $\ddot{\gamma}$ for model iv). Model iii) obviously includes the orbital parameters of the outer planet as well.

The posterior distributions of the orbital parameters were obtained in a Bayesian framework by means of a differential evolution Markov chain Monte Carlo (DE-MCMC) technique, which is the MCMC version of the differential evolution genetic algorithm (ter Braak 2006). This guarantees an optimal exploration of the parameter space and fast convergence through the automatic choice of step scales and orientations to sample the posterior distributions (Eastman et al. 2013). For each system, a number of chains equal to twice the number of free parameters were initialised close to the values of the orbital parameters reported in the literature and run simultaneously. The scales and directions of the jumping distribution for a given chain are determined from two of the other chains that are randomly selected at each step according to the prescriptions given by ter Braak (2006). Then, by considering the Gaussian likelihood function given in Eq. 9 of Gregory (2005), a proposed step for each chain is accepted or rejected according to the Metropolis-Hastings algorithm.

Gaussian priors were imposed on T_c and P from transit ephemeris and on the times of the secondary eclipses T_e, by using Eq. 18 in Jordán & Bakos (2008), when these times are available from ground- and/or space-based photometry. The epochs of secondary eclipses provide important constraints on $e\cos\omega$ that must be properly taken into account in the orbital fit. The adopted priors on T_c, P, and T_e are reported in Table 6. We used a maximum of three T_e measurements per target, if more than three observations of secondary eclipses were performed, which only concerns a few systems[2]. In a few cases, priors were directly imposed on $e\cos\omega$ when their values instead of T_e measurements are reported in the literature (Table 6). Uniform priors were considered for all the other orbital parameters except for the jitter terms for which Jeffrey's priors were adopted (e.g. Gregory 2005). The uniform prior on the eccentricity was ensured by weighting the stepping probability by the Jacobian of the transformation from $[e\cos\omega, e\sin\omega]$ to $[e, \omega]$ (Ford 2006). This is practically equivalent to fitting $[\sqrt{e}\cos\omega, \sqrt{e}\sin\omega]$ (e.g. Anderson et al. 2011d), but we preferred $[e\cos\omega, e\sin\omega]$ since these quantities appear directly in the expression of the time difference $\Delta T = T_e - T_c$ (e.g. Jordán & Bakos 2008).

The DE-MCMC chains were stopped after achieving convergence and good mixing according to Ford (2006), in other words, as soon as the Gelman-Rubin statistic is lower than 1.01 and the number of independent steps is greater than 1000. Burn-in steps were identified following Eastman et al. (2013) and removed. The medians and the 15.86% and 84.14% quantiles of the posterior distributions are taken as the best values and 1σ uncertainties of the fitted and derived parameters. When the modes (or the medians) of the distributions of the eccentricity or the RV jitter were found to be consistent with zero within 1σ (2σ), we provided their 1σ upper limits (and 2σ upper limits for the eccentricity) estimated as the 68.27% (95.45%) confidence intervals starting from zero. The best-fit model and the RV residuals were visually checked for each system to be sure that everything in the analysis worked properly and that the residuals did not show any clear deviation from the expected symmetric distribution.

Since eccentricities cannot take negative values, observational uncertainties will yield systematically $e > 0$ even for circular orbits. This is a well-known bias in estimating eccentricities, as outlined by e.g. Lucy & Sweeney (1971). To overcome the bias, these authors analytically derived the theoretical eccentricity probability function and found that an eccentricity should be considered significant at a level of 95% if $\hat{e} \geq 2.45\ \sigma_e$ rather than simply $\hat{e} \geq 2\ \sigma_e$, where $\hat{e}$ is the eccentricity expectation value and σ_e is the 1σ error. Here we make use of the obtained

[2] This choice is motivated by some tests we made for TGPs with more than three observations of T_e. Actually, just a single accurate measurement of T_e already provides a strong constraint on $e\cos\omega$ so that Gaussian priors on more than three T_e observations do not really improve the accuracy and precision of e, while they often slow down the convergence of the DE-MCMC chains. Therefore, the maximum of three T_e mid-times was chosen as a trade-off between convergence speed and the amount of prior information contained in these measurements.

DE-MCMC posterior distributions and Bayesian model selection between circular and eccentric models to establish which model is preferred when the eccentricity is found with a low significance, that is between 2 and 3.5σ. To estimate the model likelihoods and thus to compute the Bayes factors between the two models, we sampled the posterior distributions obtained for both the circular and eccentric models with the Perrakis et al. (2014) method and its implementation as described in Díaz et al. (2016). Bayes factors greater than 20 in favour of the eccentric model usually provide strong evidence for a non-zero eccentricity (Kass & Raftery 1995) and, in those cases, we considered the orbit as eccentric. In general, we found that Bayes factors greater than 20 correspond to $\hat{e} > 3\ \sigma_e$, where $\hat{e}$ is computed as the median of the eccentricity posterior distribution.

Other indicators such as the Bayesian Information Criterion (BIC) or the Akaike Information Criterion (AIC) (Liddle 2007) largely used in the literature (e.g. by P11 and H12) may suffer from several problems. First of all, they just provide a proxy for the Bayesian evidence because they take only the maximum likelihood into account and not its integral over the parameter space. Moreover, they rely on the assumption on Gaussianity or near-Gaussianity of the posterior distributions, which may not be respected in several cases; they have an asymptotic behaviour as a function of the number of measurements and it is not clear whether this behaviour is reached with 10-20 measurements, as is the case for several systems of our sample (however, the corrected AICc indicator should partly overcome this problem). Even more importantly, the BIC may often overestimate the odds ratio by a great extent, as shown by Díaz et al. (2016).

We classify the orbit of a TGP as decisively circular if its eccentricity is consistent with zero and $\sigma_e < 0.050$ to use a quite stringent criterion, although inevitably any criterion such as this is somewhat arbitrary. Eccentricities consistent with zero but with larger uncertainties are considered 'undetermined' (Sect. 5).

4. System parameters

Our updated values of the RV semi-amplitude were combined with transit and stellar parameters from the literature to redetermine the physical planetary parameters, mass M_p, density ρ_p, and gravity $\log g_p$. In Table 7 we list the adopted values of stellar and transit parameters and the corresponding references. In general, we gave preference to the discovery papers unless more recent analyses yielded significantly revised and/or much more precise parameters. We used stellar parameters derived from asteroseismology for the very few targets for which asteroseismic analyses could be performed. For the adopted literature values of system parameters we employed split-normal distributions, with the option of taking asymmetric error bars into account, and combined them with the DE-MCMC posterior distributions of the orbital parameters.

System ages are crucial in order to understand the orbital evolution of planetary systems (Sect. 5.5) and to estimate upper and lower limits of the planetary modified tidal quality factors for well-determined circular and eccentric orbits (Sect. 5.6). While collecting the system parameters from the literature, we noticed strong inhomogeneity in computing stellar ages and a lack of age estimates (or age uncertainties) for some systems. System ages are usually derived via stellar evolutionary tracks by using constraints on the stellar density from the transit fitting and on the metallicity and the effective temperature of the host stars from spectral analysis (e.g. Sozzetti et al. 2007). However, for several planetary systems such as those discovered by the WASP/SWASP surveys, stellar ages have been mainly estimated through gyrochronology. Even though, in some cases, estimates from gyrochronology and stellar evolutionary tracks agree closely (see e.g. Bonomo et al. 2015), gyrochronological ages may not be accurate, in general (Angus et al. 2015) and because of possible spin-up of the host stars by their close-in planets (Pont 2009; Maxted et al. 2015). For uniformity, in the case of age values derived from gyrochronology or lack of system ages (or their errors), we computed new stellar parameters, radius, mass, and age, and associated uncertainties, by using the Yonsei-Yale evolutionary tracks (Demarque et al. 2004) and determinations of transit stellar density, metallicity, and effective temperature from the literature (values and references are given in Table 7; see also Bonomo et al. 2014, 2015 for more details). This concerns 37 host stars (see Table 7). For all these stars except three, i.e. CoRoT-1, WASP-63, and WASP-78, we found radii and masses in good agreement, within 2σ, with the literature values even when the latter were computed with empirical relations (Torres et al. 2010a; Enoch et al. 2010) instead of stellar models. Our R_s and M_s of WASP-63 and WASP-78 derived with the Y2 evolutionary tracks differ by more than 2σ from the values of the discovery papers that were instead estimated with empirical relations. The disagreement about the parameters of CoRoT-1 has a different origin: we used the updated value of stellar $T_{eff} = 6298 \pm 66$ K determined by Torres et al. (2012). This value of T_{eff} is consistent with that found by Mortier et al. (2013), but is hotter than the T_{eff} previously reported by Barge et al. (2008). We also used our R_s and M_s values for WASP-79 because our larger uncertainties encompass the solutions given in Smalley et al. (2012) both with and without the main-sequence constraint. For the other thirty-three hosting stars we used the literature values of R_s and M_s (Table 7).

For the systems for which we significantly improved the eccentricity determination (Sect. 5.1), new combined analyses of RV data and literature transit photometry might be worthwhile as they could lead to slightly improved stellar parameters, and hence planetary parameters. However, this goes beyond the scope of the present work.

5. Results

In Table 8 we report the RV orbital parameters and their 1σ uncertainties for the 231 TGPs of our sample. For eccentricities consistent with zero, we provide both the 1σ and 2σ upper limits. In the second column, we designate the orbit of each planet as circular (C), eccentric (E), or undetermined (U) on the basis of the criteria discussed in Sect. 3. In the second last column we report the long-term trends detected with significance greater than or equal to 3σ and/or indicate with 'PLC' (planetary companion) and 'CURV' the systems that show the presence of an outer planet or a curvature in the RV residuals, respectively. Trends and curvatures are usually caused by distant stellar or planetary companions, but in some cases may also be due to stellar activity cycles. In the last column we list the RV jitter for each host star found for the dataset with the lowest median formal uncertainty. Indeed, stellar jitter, which is mostly caused by stellar activity (e.g. Boisse et al. 2009; Dumusque et al. 2011; Lanza et al. 2011a), can be more accurately estimated in RV data that are not dominated by photon noise or are dominated very little.

Physical planetary parameters (mass, density, and surface gravity) were derived as explained in Sect. 4 and are listed in Table 9 along with the planet orbital periods and eccentricities; for this last value we report only the 1σ upper limits in the case of circular or undetermined orbits.

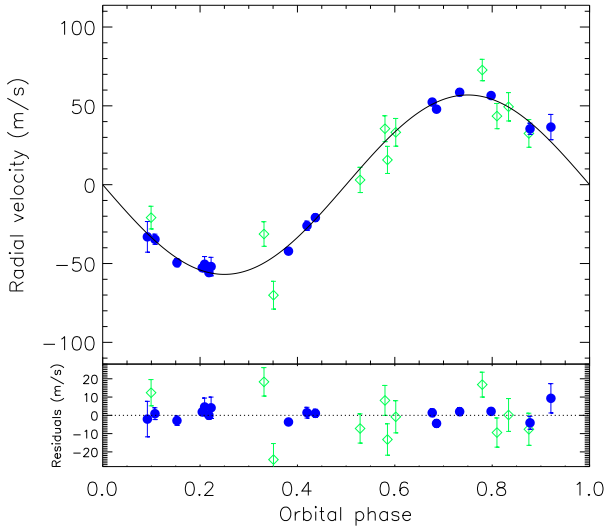


Fig. 1. HARPS-N (blue circles) and SOPHIE (green circles) RV measurements of WASP-13 phase-folded with the photometric ephemeris along with the best-fit Keplerian model. We note the high-accuracy and high-precision radial velocities collected with HARPS-N with respect to the literature data.

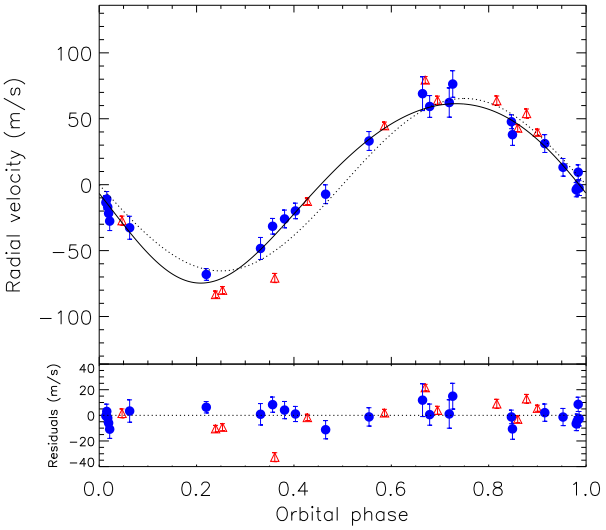


Fig. 2. Phase-folded radial-velocity curve of HAT-P-29, after removing the quadratic trend (see text). The blue circles and red triangles indicate the HARPS-N and HIRES RV measurements, respectively. The solid line shows the preferred eccentric orbit, while the dotted line displays the circular model for comparison.

We first discuss significant differences and new discoveries with respect to the literature (Sect. 5.1, 5.2, and 5.3) and then report on ensemble analyses to investigate tidal evolution and tidal star-planet interactions (Sect. 5.4, 5.5, and 5.6).

5.1. Eccentricities

Several measures of the orbital eccentricities reported in Table 8 are the most accurate and precise ever obtained because they were derived by i) combining for the first time different RV datasets published in the literature; ii) including for the first time priors on the epochs of secondary eclipses in the Keplerian fit (for instance, those recently observed by Kammer et al. 2015); and iii) adding our new high-accuracy and high-precision HARPS-N data for 45 systems.

An example of the improvement on the measure of the orbital eccentricity in case iii), especially in the absence of constraints from observations of planetary occultations, is WASP-13: we found $e < 0.017$, to be compared with $e = 0.14 \pm 0.10$ by using only the literature (SOPHIE) values (Skillen et al. 2009), although the eccentricity was fixed to zero in the discovery paper. Figure 1 shows our HARPS-N RV data of WASP-13 (blue circles) along with the SOPHIE measurements (green circles).

With 25 high-precision and high-accuracy HARPS-N radial velocities we found a small but significant (5.8σ) eccentricity for HAT-P-29b, that is $e = 0.104^{+0.021}_{-0.018}$ (Table 8). This cannot be revealed with previous HIRES data only (Buchhave et al. 2011a; Knutson et al. 2014). Radial-velocity data are shown in Fig. 2 along with the eccentric and circular best fits for comparison. Figure 3 displays the posterior distributions of $e\cos\omega$ versus $e\sin\omega$, and the derived e and ω, showing the evident eccentricity detection. The non-zero eccentricity is not dependent on the way the long-term trend seen in HIRES RVs is modelled, that is with a quadratic trend (Sect. 5.2) or by fitting two independent slopes for the HIRES and HARPS-N data.

A few significant eccentricities or remarkable hints of non-zero eccentricity reported in the literature were found consistent with zero and/or were designated as 'undetermined' in our analysis. These concern CoRoT-2b ($e = 0.0143^{+0.0077}_{-0.0076}$, Gillon et al. 2010b), CoRoT-23b ($e = 0.16 \pm 0.02$, Rouan et al. 2012), TrES-3b ($e = 0.170^{+0.032}_{-0.031}$, Knutson et al. 2014), HAT-P-23b ($e = 0.106 \pm 0.044$, Bakos et al. 2011), and WASP-54b ($e = 0.067^{+0.033}_{-0.025}$, Faedi et al. 2013). As reported in Table 8, we found a circular orbit for CoRoT-2b and TrES-3b, while the eccentricities of CoRoT-23b, HAT-P-23b, and WASP-54b are not well determined according to the adopted criteria in Sect. 3.

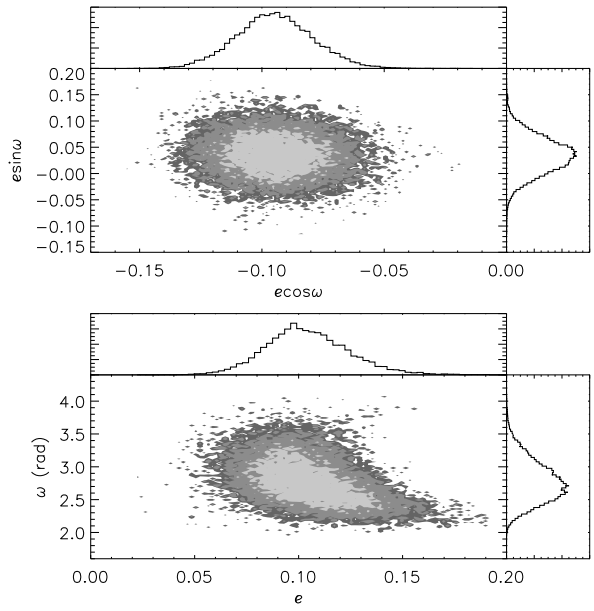


Fig. 3. DE-MCMC posterior distributions of $e\sin\omega$ vs $e\cos\omega$ (upper panel), and the derived ω vs e (bottom panel), from our analysis of the HIRES and new HARPS-N RVs, showing the small but significant eccentricity of HAT-P-29b: $e = 0.104^{+0.021}_{-0.018}$.

For the last object we acquired thirteen new HARPS-N RVs (Table 5).

In particular, the hint for a significant eccentricity of CoRoT-2b mainly came from the timing of the Spitzer secondary eclipse at 4.5 μm by Gillon et al. (2010b) that pointed to $e\cos\omega$ significantly different from zero. However, the two Spitzer observations of planetary occultation at 3.6 and 8.0 μm by Deming et al. (2011) do not indicate any significant phase shift from 0.5 (see their Table 2). The argument of periastron is unconstrained from our orbital fit including priors imposed on the secondary eclipse timings, thus questioning further a possible non-zero eccentricity.

The disagreement with the eccentricity of TrES-3b found by Knutson et al. (2014) is remarkable, but, unlike these authors, we included all the RV measurements collected in the discovery paper (Sozzetti et al. 2009, see Table 5) where the eccentricity was fixed to zero. Our eccentricity $e < 0.043$ is in agreement with the timing of the secondary eclipses indicating $e\cos\omega$ consistent with zero (Fressin et al. 2010; Croll et al. 2010b).

More RV observations are required to unveil possible small but non-zero eccentricities for CoRoT-23b, HAT-P-23b, and WASP-54b. The same obviously applies to other systems with undetermined eccentricities, especially those with relatively long orbital periods ($P \gtrsim 7$ days) such as Kepler-39b and Kepler-74b (Bonomo et al. 2015).

Figure 4 shows our derived eccentricities as a function of the orbital period for the 123 TGPs of our sample with well-determined eccentricities. Black empty circles show circular orbits, orange triangles small ($e < 0.1$) but significant eccentricities, and blue squares higher ($e \geq 0.1$) eccentricities.

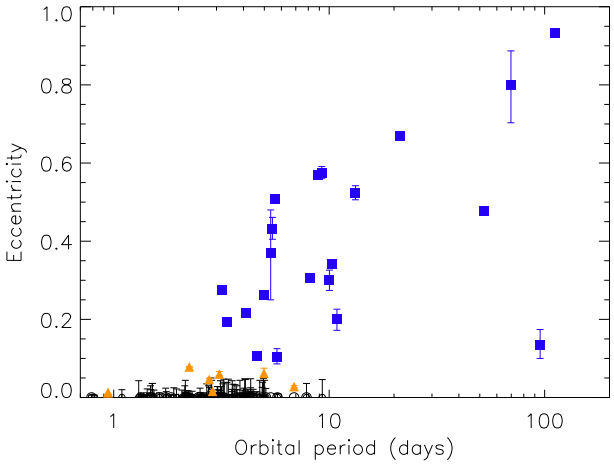


Fig. 4. Period-eccentricity diagram for the 123 TGPs in our sample with well-determined eccentricities, hence systems with undetermined eccentricities in Table 8 are not shown. Black empty circles refer to circular orbits, orange triangles indicate small ($e < 0.1$) but significant eccentricities, and blue squares $e \geq 0.1$.

5.2. Long-term trends and constraints on long-period companions

Seven of the 45 systems we followed up with HARPS-N were known to show RV drifts attributed to outer companions or stellar activity cycles: HAT-P-2, HAT-P-4, HAT-P-7, HAT-P-22, HAT-P-29, WASP-11/HAT-P-10, and XO-2N. Their slopes were discovered or better characterised with the HIRES long-term monitoring by Knutson et al. (2014).

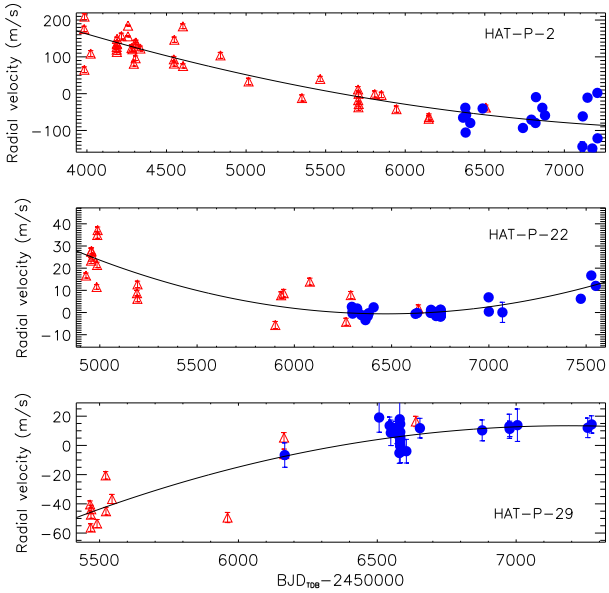


Fig. 5. Radial-velocity residuals of HAT-P-2 (top), HAT-P-22 (middle), and HAT-P-29 (bottom) after removing the orbital signal of their inner giant planets (HAT-P-2b, HAT-P-22b, and HAT-P-29b). Red triangles and blue circles indicate the HIRES and HARPS-N measurements. The SOPHIE RVs of HAT-P-2 are not displayed here because of their relatively short timespan, although they were used for the orbital fit (Table 5 and 8). Formal error bars that are lower than symbol sizes cannot be seen.

With our HARPS-N data, we are able to confirm the trends of HAT-P-4, HAT-P-7, and WASP-11 with the same slope as found with HIRES. For two systems, namely HAT-P-22 and XO-2N, we see different or inverted slopes and thus evidence for a curvature in the RV residuals, after subtracting the inner planet signal (see Fig. 5, middle panel, for HAT-P-22 and Fig. 11 in Damasso et al. 2015a for XO-2N). We do not detect any significant trend in the HARPS-N RVs of HAT-P-2 and HAT-P-29, which is consistent with the RV drifts found by Knutson et al. (2014) if our data sampled the maximum (HAT-P-29) or minimum (HAT-P-2) of the long-term RV modulation. The literature and HARPS-N RV data of HAT-P-2 and HAT-P-29 were thus fitted by including a quadratic long-term trend (see Fig. 5).

We report in Table 3 the values of the coefficients of the curvature for HAT-P-2, HAT-P-22, and HAT-P-29 as well as the resulting improved constraints on the orbital parameters of their outer companions, which were derived by following the same procedure as Kipping et al. (2011) and using their Eqs. 1, 3, and 4. In Damasso et al. (2015a) we already discussed the curvature of XO-2N in the HARPS-N data and found that it might also be due to a stellar activity cycle because of a significant correlation between the RV residuals and the activity index $\log(R'_{HK})$ (see their Figs. 12 and 13). We did not notice any such correlation for the other systems showing long-term trends in our data, that is HAT-P-4, HAT-P-7, HAT-P-22, and WASP-11, which would indicate that these trends are due to outer companions. The same applies to HAT-P-2 and HAT-P-29 given that no slopes were seen in the S-index time series by Knutson et al. (2014).

Concerning drifts and trends that we determined only with literature RVs, most of which are due to outer companions, we

Table 3. Parameters of the curvatures shown in Fig. 5 and derived constraints on the orbital period, RV semi-amplitude, and minimum mass of the outer companions HAT-P-2c, HAT-P-22c, and HAT-P-29c. The reference time $t_{\rm pivot}$ chosen as the average epoch of the RV time series, and the linear $\dot{\gamma}$ and quadratic $\ddot{\gamma}$ trends are related through Eq. 1 in Kipping et al. (2011).

Name	$t_{\rm pivot}$ BJD$_{\rm TDB}$ - 2,450,000	$\dot{\gamma}$ ms^{-1}day^{-1}	$\ddot{\gamma}$ ms^{-1}day^{-2}	P years	K m s^{-1}	$M \sin i$ M$_{\rm Jup}$
HAT-P-2c	5595.65816	$-0.077^{+0.011}_{-0.012}$	$3.04^{+1.39}_{-1.85}$E-05	≥ 49.2	≥ 249	≥ 39.5
HAT-P-22c	5612.28617	$-0.0052^{+0.0017}_{-0.0019}$	2.26E-05 $\pm$ 3.0E-06	≥ 20.8	≥ 32.9	≥ 3.0
HAT-P-29c	5816.36464	0.0328 $\pm$ 0.0064	$-$4.0E-05 $\pm$ 1.4E-05	≥ 20.9	≥ 59.3	≥ 5.4

Table 4. Improved parameters of HAT-P-17c.

Orbital Parameters	This work	Fulton et al. (2013)
Orbital period P [days]	3972^{+185}_{-146}	5584^{+7700}_{-2100}
Inferior conjunction epoch T_0[BJD$_{\rm TDB}$ $-$ 2,450,000]	4236^{+20}_{-23}	4146^{+100}_{-170}
Orbital eccentricity e	0.295 $\pm$ 0.021	$0.39^{+0.23}_{-0.17}$
Argument of periastron [deg] ω	183.3 $\pm$ 5.1	$181.5^{+5.3}_{-6.7}$
Radial velocity semi-amplitude K [km s^{-1}]	42.95 $\pm$ 0.77	$48.8^{+9.9}_{-6.4}$
Minimum mass $M \sin i$ [M$_{\rm Jup}$]	2.88 $\pm$ 0.10	$3.4^{+1.1}_{-0.7}$
Orbital semi-major axis a [au]	4.67 $\pm$ 0.14	$5.6^{+3.5}_{-1.4}$

found values in good agreement with previous findings with the exception of HAT-P-56 and WASP-99 for which our analysis indicates the presence of unreported drifts with a significance of 4.0σ and 4.6σ, respectively (see Table 8). However, more data are certainly required to establish whether these drifts are caused by outer companions or have instrumental origin. The trend of WASP-99 is mainly driven by the first datapoint, which is $\sim$ 50 m s^{-1} below the other 19 measurements collected by Hellier et al. (2014).

With our HARPS-N data we could detect and/or characterise better the two long-period companions HAT-P-17c and KELT-6c of the inner giant planets HAT-P-17b and KELT-6b, respectively. We derived the orbital parameters of KELT-6c previously in Damasso et al. (2015b) and we report in Table 4 the improved parameters of HAT-P-17c. The precision on its orbital period, eccentricity, and mass is at least two times better than Fulton et al. (2013) thanks to the extended orbital coverage. In Fig. 6 we show the Keplerian models of both HAT-P-17b and HAT-P-17c overplotted on the HIRES (red triangles) and HARPS-N (blue circles) radial velocities.

The derived orbital parameters of the outer companions with a complete (or nearly complete) RV orbital coverage such as HAT-P-13c, Kepler-424c, Kepler-432c, and WASP-8c are fully consistent with the published values. As in Knutson et al. (2014), we had to fit a circular orbit for WASP-8c to reach convergence of the DE-MCMC chains. We tried to do the same for WASP-34, but failed to reach convergence and proper mixing of the DE-MCMC chains given the poor orbital coverage of the outer companion (see Fig. 9 in Knutson et al. 2014) and thus, unlike these authors, we fitted a curvature.

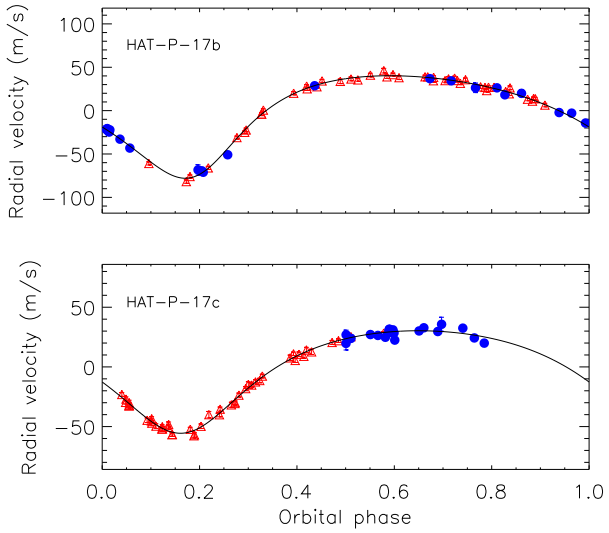


Fig. 6. Keplerian best fits to the RV curves of the inner giant planet HAT-P-17b (top) and its outer long-period ($P \sim 4000$ d) companion HAT-P-17c (bottom). HIRES and HARPS-N data are shown with red triangles and blue circles. Formal error bars of the RVs are usually smaller than symbol sizes.

5.3. Updated stellar and planetary parameters

The derived masses, densities, and surface gravities, of the 231 TGPs are listed in Table 9. Our uncertainties on planetary masses are comparable with the literature error bars, with differences typically less than 10% for 37% of the considered TGPs, while they are lower (higher) by > 10% in 35% (28%) of the remaining cases. Lower error bars come from the fact that different RV datasets have been combined for the first time to obtain a more precise orbital solution and hence a more precise planetary mass from the improved RV semi-amplitude. Higher uncertainties may be due to i) the inclusion of RV jitter terms in the orbital fit when not previously taken into account and/or ii) the choice of letting the eccentricity vary in the orbital fit instead of adopting a circular orbit, as often done when the eccentricity is not well constrained but is compatible with zero. However, in general, the uncertainty on the eccentricity must be propagated to that of the other orbital parameters. Therefore, both i) and ii) provide more realistic uncertainties on the orbital hence planetary parameters. Nonetheless, the absence of any significant eccentricity for $M_{\rm p}/M_{\rm s} \lesssim 0.002$ and $a/R_{\rm p} \lesssim 100$ (see Sect. 5.5 and Fig. 8) would indicate that assuming a circular orbit for this range of parameters is reasonable when RV data do not allow us to constrain well the orbital eccentricity.

As discussed in Sect. 4, we used updated values of the radius and mass of four planet-hosting stars, namely CoRoT-1,

WASP-63, WASP-78, and WASP-79 (see Table 7). The new stellar radius and mass imply revised planetary parameters for the hosted planets, although only those of CoRoT-1b, and in particular its radius, significantly differ from the literature values. Indeed, CoRoT-1b is larger, hence more inflated, than originally found by Barge et al. (2008). Its radius, mass, and density are found to be $R_p = 1.715 \pm 0.03$ R_{Jup}, $M_p = 1.23 \pm 0.10$ M_{Jup}, and $\rho_p = 0.302^{+0.031}_{-0.028}$ g cm^{-3}, which can be compared with the previous parameters: $R_p = 1.49 \pm 0.08$ R_{Jup}, $M_p = 1.03 \pm 0.12$ M_{Jup}, and $\rho_p = 0.38 \pm 0.05$ g cm^{-3} (Barge et al. 2008). The reason for the larger R_p lies in the fact that we used a hotter stellar T_{eff} than Barge et al. (2008) (see Sect. 4); this implies a slightly higher stellar mass and a significantly larger stellar radius hence planetary radius from the transit depth.

5.4. Semi-major axes and Roche limits

We find that only 4% of the TGPs in our sample do not fulfil the condition $a \geq 2a_R$, as predicted by HEM in the absence of mass and angular momentum loss. Indeed, only 9 planets out of 231 have semi-major axes that are significantly lower than $2a_R$, after taking the uncertainties on both a and a_R into account: CoRoT-1b, HAT-P-32b, Kepler-41b, TrES-4b, WASP-12b, WASP-19b, WASP-52b, WASP-103b, and WTS-2b. However, four of them, Kepler-41b, WASP-52b, WASP-103b, and WTS-2b, have undetermined eccentricities, although their orbits may be circular. The planets in our sample with the lowest ratio $\alpha = a/a_R$ are WASP-12b ($\alpha = 1.21$), WASP-19b ($\alpha = 1.27$), and WASP-103b ($\alpha = 1.31$).

Figure 7 shows the distributions of $\alpha = a/a_R$ for well-determined circular orbits (solid line) and planets with both circular orbits and undetermined eccentricities (dotted line). Both distributions peak at 2.5. A relevant issue concerns whether and how the transit probability (R_s/a for circular orbits) affects the α distribution because the closer the planet, the higher the probability seen in transit (hence discovered). To evaluate the impact of the transit probability on the α distribution, we considered the distribution for circular orbits (solid line) and $\alpha \leq 5$ that encompasses the vast majority of the circular planets of our sample. For each bin of 0.20 in α, we weighted the frequency of giant planets in the bin by the transit probability, by adding up the inverses of the transit probabilities (R_s/a) of the planets falling in that bin. The obtained normalised distribution is statistically indistinguishable from that shown in Fig. 7 (solid line) and therefore is not displayed. This can be understood by noticing that planets with similar semi-major axes (hence transit probabilities for similar R_s) may fall in different α bins because of different a_R values depending on both R_p and $(M_s/M_p)^{1/3}$.

Planets with circular orbits and relatively large α values ($\alpha > 5$), such as CoRoT-3b ($\alpha = 13.9$), CoRoT-27b ($\alpha = 9.4$), WASP-99b ($\alpha = 7.7$), and WASP-106b ($\alpha = 9.4$), appear as possible outliers with respect to the inner distribution (see Fig. 7). These planets might have undergone a different migration history, for instance smooth disc migration instead of HEM (see Sect. 5.5).

5.5. Tidal diagrams

'Tidal diagrams' are very useful in order to understand the impact of tidal star-planet interactions on the planetary orbital parameters (see e.g. P11). They show the mass ratios M_p/M_s as a function of a/R_p because the circularisation time τ_e scales as $\tau_e \propto (M_p/M_s) \cdot (a/R_p)^5$ (e.g. Goldreich & Soter 1966). The tidal diagram containing the 231 giant planets of our sample is displayed in Fig. 8 where well-determined circular orbits, undetermined eccentricities, small but significant eccentricities $e < 0.1$ and eccentricities $e \geq 0.1$ are indicated with empty circles, crosses, orange triangles, and blue squares, respectively. The solid and dashed lines show the position of a planet with $R_p = 1.2$ R_{Jup}, which represents the median of the planetary radii of our sample, and semi-major axis $a = a_R$ and $a = 2a_R$, respectively. For comparison with P11, the dotted line displays the 1 Gyr isochrone for orbital circularisation for $P = 3$ d (corresponding to the pileup of hot Jupiters; e.g. Wright et al. 2009), $Q'_p = 10^6$, and $e = 0$, where $Q'_p = 3Q_p/2k_2$ is the planetary modified tidal quality factor, Q_p is the planet tidal quality factor, and k_2 is the Love number (e.g. Murray & Dermott 1999). Q'_p is a parameterisation of the response of the planet's interior to tidal perturbation: the higher Q'_p, the lower the dissipation rate of the kinetic energy of the tides inside the planet. A similar definition applies to the stellar modified quality factor Q'_s. The 1 Gyr isochrone for orbital circularisation displayed in Fig. 8 was computed with Eq. 6 in Matsumura et al. (2008) (hereafter M08) which also applies to the case of high eccentricities and assumes that tides in the planet are mainly responsible for circularising its orbit (e.g. Matsumura et al. 2010).

As previously noticed by P11 and H12, but with a much smaller sample than ours (by a factor of three), this diagram clearly shows that the orbital parameters of TGPs in non-compact planetary systems are shaped by tidal interactions with their host stars. Indeed, all the TGPs with $e > 0.1$ (blue squares) have large separations $a/R_p \gtrsim 100$. The two planets with $a/R_p < 100$, namely WASP-89b and XO-3b, have high mass ratios $M_p/M_s > 6 \cdot 10^{-3}$, as expected from tidal theory. Moreover, virtually all the TGPs with $e > 0.1$ are found on the right side of the dotted line, that is their circularisation time is longer than 1 Gyr. We note that the slightly eccentric planets ($e < 0.1$, orange triangles) with $a/R_p < 100$ are located at the upper edge of the circular ones.

We confirm the dearth of close-in circular planets with $M_p/M_s \gtrsim 4 \cdot 10^{-3}$. These massive planets likely raise tides in the star strong enough for angular momentum exchange and tidal decay so that they end up being engulfed by their host star

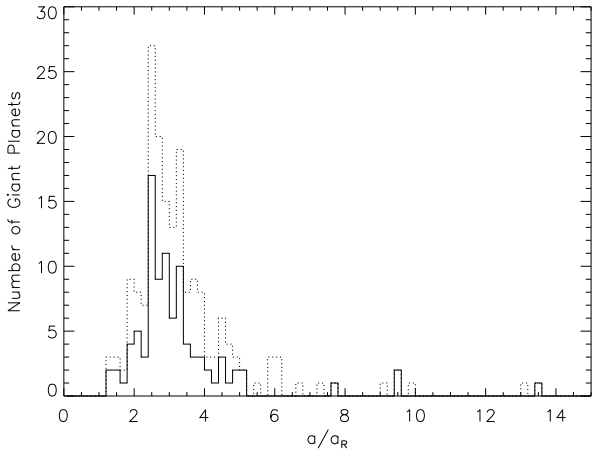


Fig. 7. Distributions of $\alpha = a/a_R$, where a_R is the Roche limit, for well-determined circular orbits (solid line) and both circular orbits and undetermined eccentricities (dashed line). The impact of transit probability on the distribution for $\alpha \leq 5$ appears to be practically negligible (see text for more details).

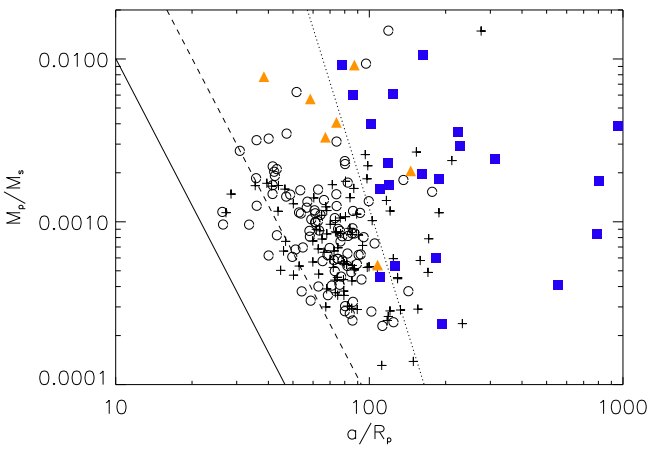


Fig. 8. Updated tidal diagram of the 231 transiting giant planets considered in this study. Empty circles show the position of giant planets with well-determined circular orbits, that is with eccentricities consistent with zero and 1σ uncertainty $\sigma_e < 0.05$ (planets designated with 'C' in the second column of Table 9); crosses indicate planets with undetermined eccentricities (indicated with 'U' in Table 9) that are usually consistent with zero (circular orbits) but have large uncertainties $\sigma_e > 0.05$; orange triangles display significant but small eccentricities, i.e. $e < 0.1$; and blue squares $e \geq 0.1$. Solid and dashed lines show the position of a planet with $R_p = 1.2\ R_{Jup}$ and semi-major axis $a = a_R$ and $a = 2a_R$, a_R being the Roche limit. The dotted line displays the 1 Gyr circularisation isochrone for $P = 3$ d, $Q'_p = 10^6$, and $e = 0$.

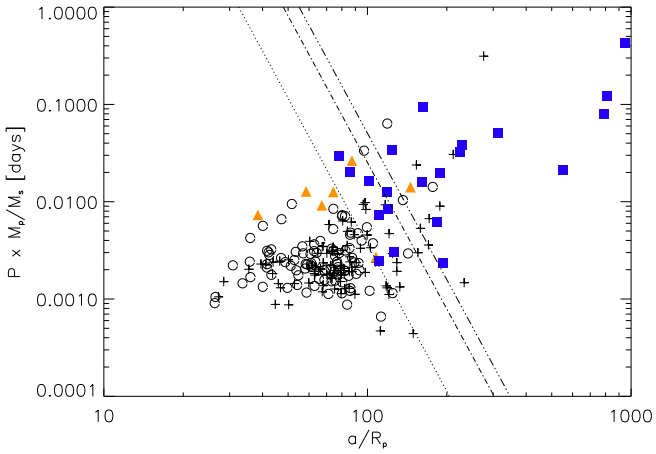


Fig. 9. 'Modified' tidal diagram of the 231 transiting giant planets considered in this study with the same symbols as in Fig. 8. The dotted, dash-dotted, and dash-three-dotted lines display the 1, 7, and 14 Gyr circularisation timescales for $Q'_p = 10^6$ and $e = 0$, respectively.

(e.g. Pätzold & Rauer 2002). However, this scarcity might also be partially explained by the higher inertia of massive planets to gravitational scattering towards inner orbits and/or a less efficient formation in discs that are not massive enough.

It is convenient to also consider a 'modified' tidal diagram where the circularisation isochrones do not depend on the orbital period P, by plotting $P \cdot M_p/M_s$ versus a/R_p. From the aforementioned Eq. 6 in M08 (see also Goldreich & Soter 1966) we find

$$P\frac{M_p}{M_s} = \tau_e \frac{63}{2\pi}\frac{1}{Q'_p}\left(\frac{a}{R_p}\right)^{-5}. \quad (1)$$

While the orbital period was fixed at $P = 3$ d for the tidal diagram in Fig. 8, we show for comparison $P \cdot M_p/M_s$ as a function of a/R_p in Fig. 9 along with the 1, 7, and 14 Gyr circularisation timescales for $Q'_p = 10^6$ and $e = 0$. This 'modified' tidal diagram reveals even more evidently the same trends discussed above for the 'classical' tidal diagram thanks to the independence of the isochrones on the adopted orbital period. Like in Fig. 8, all the eccentric planets in Fig. 9 with $e \geq 0.1$ (blue squares) are found beyond the 1 Gyr circularisation isochrone. The four TGPs with well-determined circular orbits, $a/R_p \gtrsim 100$, and $P \cdot (M_p/M_s) \gtrsim 0.01$ d are CoRoT-3b, CoRoT-27b, WASP-99b, and WASP-106b, all having $\alpha > 5$ (Sect. 5.4 and Fig. 7). Their circular orbits might be primordial since they lie in a region of the 'modified' tidal diagram where tidal circularisation is not expected to occur within 7 Gyr (or even 14 Gyr). We note that this part of the diagram is otherwise populated by eccentric planets (cf. Fig. 9). Therefore planets with $\alpha > 5$ may have undergone disc migration instead of HEM.

5.6. Constraints on planetary and stellar modified tidal quality factors

After identifying circular and eccentric orbits, we can estimate the upper and lower limits of Q'_p by considering a tidal constant Q' model (e.g. Souchay et al. 2013; Ogilvie 2014). Indeed, following M08, an upper limit on Q'_p can be derived from their Eq. 7, that is from the constraint that the circularisation time must be shorter than the system (or stellar) age for circular planets ($\sigma_e < 0.05$), on the assumption that their orbits were initially eccentric. On the contrary, lower limits on both Q'_p and Q'_s can be derived with Eqs. 8 and 9 in M08, by imposing that the circularisation time must be longer than the system age for eccentric orbits, if we assume that the eccentricity is not presently excited by a third body in the system.

These equations require the knowledge of both the stellar and planetary rotation periods. Stellar rotation periods as derived from ground-based or space-based photometry, which are reported in the seventh column of Table 7 when available, are used for approximately thirty systems. For the other systems they were estimated from the $V \sin i$ and R_s assuming a stellar inclination of 90 deg, which thus provides upper limits for the true P_{rot} when the stellar equator is not seen edge-on. This may lead to slightly overestimated lower limits of Q'_s, but this effect is negligible in the vast majority of cases. Concerning the planetary spin, we assume i) perfect synchronisation for the circular planets, which is reasonable given that synchronisation times are much lower than the circularisation times (e.g. Rasio et al. 1996), and ii) pseudo-synchronisation for the eccentric systems (Hut 1981).

Figures 10, 11, and 12 show the upper and lower limits of Q'_p, and the lower limits of Q'_s, as a function of the semi-major axis. The large error bars are due to the propagation of the uncertainties on system ages; unconstrained values of Q'_p and Q'_s due to unconstrained ages in Table 7 (e.g. those spanning 0-14 Gyr at 1σ) are not shown. The lower limits of Q'_p also depend on the Q'_s values (see Eq. 8 in M08) and we adopted values of Q'_s that are ten times their lower limits: $Q'_s = 10 \cdot Q'_{s,min}$. This explains why the variations seen in Figs. 11 and 12 are evidently correlated.

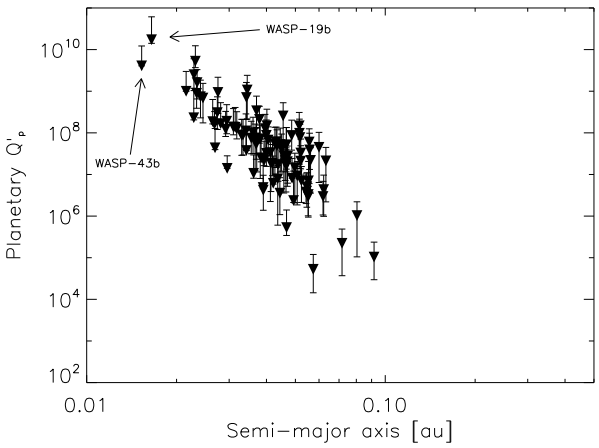


Fig. 10. Upper limits of the planetary modified tidal quality factor $Q'_{\rm p}$ for clearly circular orbits ($\sigma_e < 0.05$).

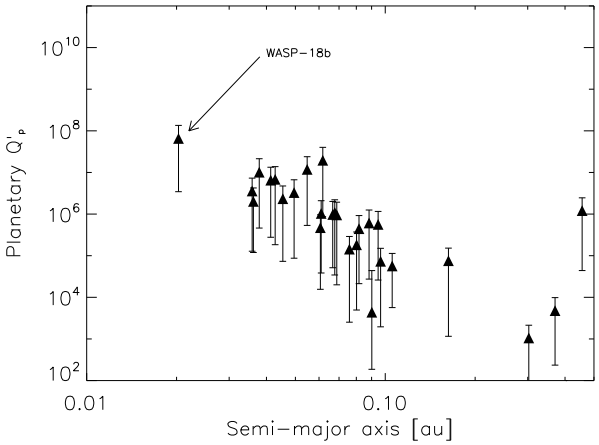


Fig. 11. Lower limits of the planetary modified tidal quality factor $Q'_{\rm p}$ for eccentric orbits.

Hot Jupiters with orbital distances typically lower than 0.05 au have $10^5 \lesssim Q'_{\rm p} \lesssim 10^9$, but estimates of the $Q'_{\rm p}$ lower and upper limits are inevitably affected by the large uncertainties on stellar ages. The main trends in Figs. 10 and 11 seem to indicate that the closer the planet, the higher its $Q'_{\rm p}$ hence its lower internal dissipation. This is also related to the differences in tidal frequencies as a function of the orbital distance. Little can be said for planets at semi-major axis $a \gtrsim 0.1$ au, given the small number of systems.

Modified tidal quality factors of stars hosting hot Jupiters with $a < 0.05$ au are generally $Q'_{\rm s} \gtrsim 10^6 - 10^7$ (Fig. 12). The highest value $Q'_{\rm s} > 10^8$ in Fig. 12 is that of the star WASP-18 whose hot Jupiter at $a = 0.02$ au ($P = 0.94$ d) has a small but significant eccentricity: $e = 0.0076 \pm 0.0010$. This is consistent with estimates relying on the timescales of the orbital decay of very hot Jupiters with $P \lesssim 1$ d (e.g. Ogilvie 2014).

6. Summary, discussion, and conclusions

We carried out a homogeneous determination of the orbital parameters of 231 TGPs by analysing with our Bayesian DE-MCMC tool both the literature RVs and the new high-accuracy

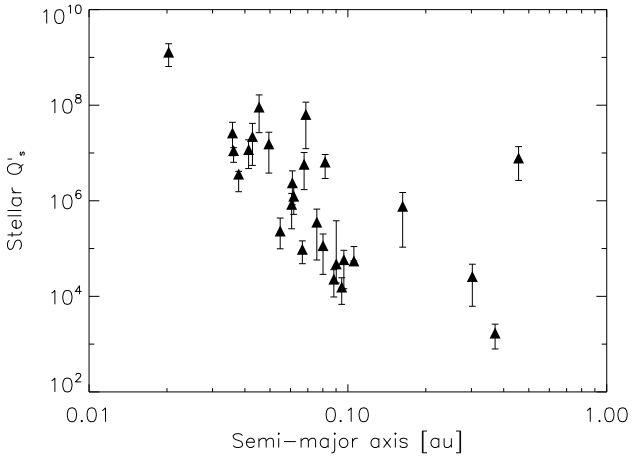


Fig. 12. Lower limits of the modified tidal quality factor $Q'_{\rm s}$ of stars hosting eccentric planets.

and high-precision HARPS-N data we acquired for 45 TGPs orbiting relatively bright stars over ∼3 years. We thus produced the largest uniform catalogue of giant planet orbital and physical parameters. For several systems we combined for the first time RV datasets collected with different spectrographs by different groups thus improving the orbital solution. In general, we fitted a separate jitter term for each dataset by allowing for different values of extra noise caused by instrumental effects and/or changing levels of stellar activity in different observing seasons.

This way, we uniformly derived the orbital eccentricities of TGPs that represent a fundamental imprint of their migration history. We detected for the first time a significant eccentricity for HAT-P-29b. On the contrary, our results do not confirm any significant eccentricity for five planets that were previously regarded to be eccentric or to have hints of non-zero eccentricity, namely CoRoT-2b, CoRoT-23b, TrES-3b, HAT-P-23b, and WASP-54b. In particular, our results favour a circular orbit for CoRoT-2b and TrES-3b.

Limiting ourselves to the 45 systems we monitored with HARPS-N, we confirm the RV long-term linear trends for three of them, HAT-P-4, HAT-P-7, and WASP-11, with the same slope as previously found (Knutson et al. 2014). We report the first evidence of a curvature in the RV residuals of HAT-P-2, HAT-P-22, and HAT-P-29, and derived constraints on their long-period companions from RV data only. Moreover, our HARPS-N measurements allowed us to refine significantly the orbital solution of HAT-P-17c, the outer planetary companion of HAT-P-17b, thanks to the extended orbital coverage.

Our tidal diagrams clearly show how the orbital parameters of TGPs in non-compact planetary systems are shaped by tides raised by their host stars. Indeed, the most eccentric planets have either relatively large orbital separations and/or high mass ratios, as expected from the equilibrium tide theory. This feature would be the outcome of planetary migration from highly eccentric orbits that were originally produced by planet-planet scattering, Kozai-Lidov perturbations, or secular chaos.

The $\alpha = a/a_{\rm R}$ distribution showing that only ∼ 4% of circular TGPs have $a < 2a_{\rm R}$ agrees with the theoretical prediction by the HEM that the final distances of circularised orbits must be $a \geq 2a_{\rm R}$ (e.g. Faber et al. 2005). The handful of TGPs with $a < 2a_{\rm R}$ may also be explained in the framework of the HEM by considering the effect of tidal decay driven by tidal dissipation

inside the star, which may account for even the lowest observed $\alpha \sim 1.2$ value (Valsecchi & Rasio 2014). The condition $a > 2a_R$, however, may not be a peculiar imprint of the HEM and, for instance, could also be reproduced by migration in the disc that was stopped because of truncation of the inner disc by magnetic fields (e.g. Lin et al. 1996). The derived α distribution peaking at 2.5 represents an important observational constraint that theoretical models of planet migration must be able to reproduce. The planets of our sample with circular orbits and relatively large α (> 5) values, namely CoRoT-3b, CoRoT-27b, WASP-99b, and WASP-106b, seem to deviate from the inner α distribution. They have circular orbits although their circularisation timescale (in case of a non-zero eccentricity) is longer than $\sim 7 - 14$ Gyr. This would indicate that their circular orbits are likely primordial, that is they presumably migrated through disc-planet interactions, which tend to damp any small eccentricity, instead of HEM.

As previously discussed, strong evidence for disc migration is mainly provided by the discovery of giant planets around very young stars and in compact systems. In addition, Dawson et al. (2015) found a paucity of super-eccentric proto-hot Jupiters[3] among the *Kepler* sample that seems to be inconsistent with the theoretical predictions of HEM by Socrates et al. (2012b). However, alternative explanations of this dearth are also possible in the context of HEM, for instance if gravitational scattering of giant planets occurs during migration of type II inside the water-ice line (see, e.g. Marzari et al. 2010; Guillochon et al. 2011, and Sect. 4 in Dawson et al. 2015). This may also reconcile the HEM with the apparently inconsistent occurrence of planetary companions of hot Jupiters inside the water-ice line (Schlaufman & Winn 2016). In any case, it is difficult to explain the general properties of the tidal diagrams shown in Figs. 8 and 9 and discussed in Sect. 5.5, in terms of migration in the disc alone given that disc-planet interactions may only excite modest eccentricities $e < 0.1$ (Duffell & Chiang 2015).

We estimated upper and lower limits of the planetary modified tidal quality factors Q'_p and found that high values (up to $10^7 - 10^9$) are required to explain the presence of the closest giant planets with $a < 0.05$ au. These high values of Q'_p are in agreement with the predicted very low internal dissipation in massive planets with a small core (Goodman & Lackner 2009). On the other hand, currently large Q'_p are not necessarily at variance with the values required for the circularisation of very eccentric initial orbits as assumed by HEM ($10^5 \lesssim Q'_p \lesssim 5 \times 10^6$, cf. Naoz et al. 2011; Socrates et al. 2012a). This happens because Q'_p is a function of the tidal frequency and it is ill-defined in the case of highly eccentric orbits. In such a case, tidal dissipation is a highly non-sinusoidal function of the time strongly peaked around periastron so that an impulse approximation is much more adequate for its description (cf. Nagasawa et al. 2008; Ogilvie 2014). Moreover, we lack observational constraints on the initial orbital and planetary parameters and on the duration of the circularisation process because young hot Jupiters are very difficult to discover and confirm owing to the high level of stellar activity. This inevitably makes any estimate of the tidal dissipation rate during HEM uncertain.

Stellar modified tidal quality factors $Q'_s \gtrsim 10^6 - 10^7$ were found for stars with eccentric planets at short orbital distances $a < 0.05$ au. This range is consistent with that estimated from tidal evolution calculations for a few individual systems such as OGLE-TR-56b (Carone & Pätzold 2007) and CoRoT-11b (Lanza et al. 2011b), and with the results by Hansen (2012). Tidal evolution models for the population of hot Jupiters as computed by Jackson et al. (2008, 2009) are also in general agreement with $10^6 \lesssim Q'_s \lesssim 10^7$, but our ignorance of the initial conditions of the close giant planet population ultimately hampers any possibility of precisely estimating Q'_s. We note that our values are also in general agreement with those theoretically expected in the case of stars hosting hot Jupiters according to the dynamic tide theory in Ogilvie & Lin (2007) that may account for the differences in the estimated Q'_s between close stellar binary systems and star-planet systems.

Our catalogue will be updated at the end of our survey by including new HARPS-N data, additional constraints from future secondary eclipse observations, and newly discovered giant planets, among which those announced in 2016, as these are detected by ground-based and space-based transit surveys. To this end, we stress the importance of collecting for each new system not only the RV data that are required for the confirmation of its planetary nature, but also – when possible – sufficient and precise enough RV measurements that permit an accurate determination of its orbital parameters and, specifically, its eccentricity. Indeed, almost half of the TGPs in our sample have undetermined eccentricities.

We point out that different methods are currently used to determine stellar, hence planetary, parameters (mass, radius, and age) such as stellar evolutionary tracks, empirical relations, or gyrochronology relations for stellar ages; sometimes, the last are then used as priors in stellar models. Although we used system ages estimated from evolutionary tracks (and recomputed them when only gyrochronologic estimates were available from the literature; see Sect. 4), a homogeneous determination of stellar parameters may also be very useful to get a uniform catalogue of stellar and planetary parameters. However, this goes beyond the scope of the present work. In some cases, more accurate stellar parameters are also expected from absolute luminosities as derived with Gaia parallaxes released in April 2018.

Long-term RV monitoring is also essential in order to discover long-period companions, derive their orbital parameters, and thus investigate their possible influence on the eccentricity and obliquity of the orbits of the close-in giant planets (e.g. Matsumura et al. 2010; Knutson et al. 2014). Future work will thus focus on detailed studies of the statistical properties and frequencies of close-in giant planets in connection with the presence of distant companions, taking advantage of the full temporal baseline ($\gtrsim 5 - 6$ years) of the HARPS-N observations upon conclusion of our survey.

[3] Super-eccentric proto-hot Jupiters are defined as highly eccentric ($e > 0.9$) giant planets that could become hot Jupiters through the mechanism of HEM.

References

Adams, E. R., López-Morales, M., Elliot, J. L., Seager, S., & Osip, D. J. 2010, ApJ, 721, 1829
Adams, E. R., López-Morales, M., Elliot, J. L., Seager, S., & Osip, D. J. 2011a, ApJ, 728, 125
Adams, E. R., López-Morales, M., Elliot, J. L., et al. 2011b, ApJ, 741, 102
Agol, E., Cowan, N. B., Knutson, H. A., et al. 2010, ApJ, 721, 1861
Aigrain, S., Collier Cameron, A., Ollivier, M., et al. 2008, A&A, 488, L43
Albrecht, S., Winn, J. N., Butler, R. P., et al. 2012, ApJ, 744, 189
Almenara, J. M., Bouchy, F., Gaulme, P., et al. 2013, A&A, 555, A118
Almenara, J. M., Damiani, C., Bouchy, F., et al. 2015, A&A, 575, A71
Alonso, R., Auvergne, M., Baglin, A., et al. 2008, A&A, 482, L21
Alonso, R., Brown, T. M., Torres, G., et al. 2004, ApJ, 613, L153
Alsubai, K. A., Parley, N. R., Bramich, D. M., et al. 2011, MNRAS, 417, 709
Anderson, D. R., Barros, S. C. C., Boisse, I., et al. 2011a, PASP, 123, 555
Anderson, D. R., Collier Cameron, A., Delrez, L., et al. 2014, MNRAS, 445, 1114
Anderson, D. R., Collier Cameron, A., Gillon, M., et al. 2012, MNRAS, 422, 1988
Anderson, D. R., Collier Cameron, A., Gillon, M., et al. 2011b, A&A, 534, A16
Anderson, D. R., Collier Cameron, A., Hellier, C., et al. 2015, A&A, 575, A61
Anderson, D. R., Collier Cameron, A., Hellier, C., et al. 2011c, A&A, 531, A60
Anderson, D. R., Collier Cameron, A., Hellier, C., et al. 2011d, ApJ, 726, L19
Anderson, D. R., Gillon, M., Hellier, C., et al. 2008, MNRAS, 387, L4
Anderson, D. R., Hellier, C., Gillon, M., et al. 2010, ApJ, 709, 159
Anderson, D. R., Smith, A. M. S., Lanotte, A. A., et al. 2011e, MNRAS, 416, 2108
Angus, R., Aigrain, S., Foreman-Mackey, D., & McQuillan, A. 2015, MNRAS, 450, 1787
Bakos, G. Á., Hartman, J., Torres, G., et al. 2011, ApJ, 742, 116
Bakos, G. Á., Hartman, J. D., Bhatti, W., et al. 2015a, AJ, 149, 149
Bakos, G. Á., Hartman, J. D., Torres, G., et al. 2012, AJ, 144, 19
Bakos, G. Á., Howard, A. W., Noyes, R. W., et al. 2009, ApJ, 707, 446
Bakos, G. Á., Kovács, G., Torres, G., et al. 2007a, ApJ, 670, 826
Bakos, G. Á., Noyes, R. W., Kovács, G., et al. 2007b, ApJ, 656, 552
Bakos, G. Á., Penev, K., Bayliss, D., et al. 2015b, ApJ, 813, 111
Bakos, G. Á., Shporer, A., Pál, A., et al. 2007c, ApJ, 671, L173
Baluev, R. V., Sokov, E. N., Shaidulin, V. S., et al. 2015, MNRAS, 450, 3101
Barge, P., Baglin, A., Auvergne, M., et al. 2008, A&A, 482, L17
Barros, S. C. C., Boué, G., Gibson, N. P., et al. 2013, MNRAS, 430, 3032
Barros, S. C. C., Faedi, F., Collier Cameron, A., et al. 2011, A&A, 525, A54
Barros, S. C. C., Pollacco, D. L., Gibson, N. P., et al. 2012, MNRAS, 419, 1248
Bate, M. R., Lodato, G., & Pringle, J. E. 2010, MNRAS, 401, 1505
Batygin, K. 2012, Nature, 491, 418
Batygin, K., Bodenheimer, P. H., & Laughlin, G. P. 2016, ApJ, 829, 114
Bayliss, D., Hartman, J. D., Bakos, G. Á., et al. 2015, AJ, 150, 49
Bayliss, D., Zhou, G., Penev, K., et al. 2013, AJ, 146, 113
Bean, J. L., Désert, J.-M., Seifahrt, A., et al. 2013, ApJ, 771, 108
Beatty, T. G., Pepper, J., Siverd, R. J., et al. 2012, ApJ, 756, L39
Becker, J. C., Vanderburg, A., Adams, F. C., Rappaport, S. A., & Schwengeler, H. M. 2015, ApJ, 812, L18
Beerer, I. M., Knutson, H. A., Burrows, A., et al. 2011, ApJ, 727, 23
Bentley, S. J., Hellier, C., Maxted, P. F. L., et al. 2009, A&A, 505, 901
Bieryla, A., Hartman, J. D., Bakos, G. Á., et al. 2014, AJ, 147, 84
Birkby, J. L., Cappetta, M., Cruz, P., et al. 2014, MNRAS, 440, 1470
Blecic, J., Harrington, J., Madhusudhan, N., et al. 2014, ApJ, 781, 116
Blecic, J., Harrington, J., Madhusudhan, N., et al. 2013, ApJ, 779, 5
Bodenheimer, P., Hubickyj, O., & Lissauer, J. J. 2000, Icarus, 143, 2
Boisse, I., Hartman, J. D., Bakos, G. Á., et al. 2013, A&A, 558, A86
Boisse, I., Moutou, C., Vidal-Madjar, A., et al. 2009, A&A, 495, 959
Bonomo, A. S., Hébrard, G., Raymond, S. N., et al. 2017, ArXiv e-prints arXiv:1703.06477
Bonomo, A. S., Hébrard, G., Santerne, A., et al. 2012, A&A, 538, A96
Bonomo, A. S. & Lanza, A. F. 2012, A&A, 547, A37
Bonomo, A. S., Santerne, A., Alonso, R., et al. 2010, A&A, 520, A65
Bonomo, A. S., Sozzetti, A., Lovis, C., et al. 2014, A&A, 572, A2
Bonomo, A. S., Sozzetti, A., Santerne, A., et al. 2015, A&A, 575, A85
Bordé, P., Bouchy, F., Deleuil, M., et al. 2010, A&A, 520, A66
Borsa, F., Scandariato, G., Rainer, M., et al. 2015, A&A, 578, A64
Borsato, L., Marzari, F., Nascimbeni, V., et al. 2014, A&A, 571, A38
Bouchy, F., Bonomo, A. S., Santerne, A., et al. 2011, A&A, 533, A83
Bouchy, F., Hebb, L., Skillen, I., et al. 2010, A&A, 519, A98
Bouchy, F., Hébrard, G., Udry, S., et al. 2009, A&A, 505, 853
Bouchy, F., Pont, F., Melo, C., et al. 2005a, A&A, 431, 1105
Bouchy, F., Pont, F., Santos, N. C., et al. 2004, A&A, 421, L13
Bouchy, F., Queloz, D., Deleuil, M., et al. 2008, A&A, 482, L25
Bouchy, F., Udry, S., Mayor, M., et al. 2005b, A&A, 444, L15
Brahm, R., Jordán, A., Hartman, J. D., et al. 2015, AJ, 150, 33
Brothwell, R. D., Watson, C. A., Hébrard, G., et al. 2014, MNRAS, 440, 3392
Brown, D. J. A., Cameron, A. C., Anderson, D. R., et al. 2012a, MNRAS, 423, 1503
Brown, D. J. A., Collier Cameron, A., Díaz, R. F., et al. 2012b, ApJ, 760, 139
Bryan, M. L., Alsubai, K. A., Latham, D. W., et al. 2012, ApJ, 750, 84
Bryan, M. L., Alsubai, K. A., Latham, D. W., et al. 2014, ApJ, 782, 121
Bryan, M. L., Knutson, H. A., Howard, A. W., et al. 2016, ApJ, 821, 89
Buchhave, L. A., Bakos, G. Á., Hartman, J. D., et al. 2010, ApJ, 720, 1118
Buchhave, L. A., Bakos, G. Á., Hartman, J. D., et al. 2011a, ApJ, 733, 116
Buchhave, L. A., Latham, D. W., Carter, J. A., et al. 2011b, ApJS, 197, 3
Burke, C. J., McCullough, P. R., Bergeron, L. E., et al. 2010, ApJ, 719, 1796
Burke, C. J., McCullough, P. R., Valenti, J. A., et al. 2007, ApJ, 671, 2115
Burke, C. J., McCullough, P. R., Valenti, J. A., et al. 2008, ApJ, 686, 1331
Butler, R. P., Wright, J. T., Marcy, G. W., et al. 2006, ApJ, 646, 505
Cabrera, J., Bruntt, H., Ollivier, M., et al. 2010, A&A, 522, A110
Cabrera, J., Csizmadia, S., Montagnier, G., et al. 2015, A&A, 579, A36
Cáceres, C., Ivanov, V. D., Minniti, D., et al. 2011, A&A, 530, A5
Campo, C. J., Harrington, J., Hardy, R. A., et al. 2011, ApJ, 727, 125
Cappetta, M., Saglia, R. P., Birkby, J. L., et al. 2012, MNRAS, 427, 1877
Carone, L. & Pätzold, M. 2007, Planet. Space Sci., 55, 643
Carter, J. A., Winn, J. N., Gilliland, R., & Holman, M. J. 2009, ApJ, 696, 241
Chan, T., Ingemyr, M., Winn, J. N., et al. 2011, AJ, 141, 179
Charbonneau, D., Allen, L. E., Megeath, S. T., et al. 2005, ApJ, 626, 523
Charbonneau, D., Knutson, H. A., Barman, T., et al. 2008, ApJ, 686, 1341
Chatterjee, S., Ford, E. B., Matsumura, S., & Rasio, F. A. 2008, ApJ, 686, 580
Chen, G., van Boekel, R., Madhusudhan, N., et al. 2014a, A&A, 564, A6
Chen, G., van Boekel, R., Wang, H., et al. 2014b, A&A, 563, A40
Chen, G., van Boekel, R., Wang, H., et al. 2014c, A&A, 567, A8
Christian, D. J., Gibson, N. P., Simpson, E. K., et al. 2009, MNRAS, 392, 1585
Christiansen, J. L., Ballard, S., Charbonneau, D., et al. 2010, ApJ, 710, 97
Ciceri, S., Lillo-Box, J., Southworth, J., et al. 2015, A&A, 573, L5
Ciceri, S., Mancini, L., Southworth, J., et al. 2016, MNRAS, 456, 990
Ciceri, S., Mancini, L., Southworth, J., et al. 2013, A&A, 557, A30
Collier Cameron, A., Bouchy, F., Hébrard, G., et al. 2007, MNRAS, 375, 951
Collins, K. A., Eastman, J. D., Beatty, T. G., et al. 2014, AJ, 147, 39
Cosentino, R., Lovis, C., Pepe, F., et al. 2014, in Society of Photo-Optical Instrumentation Engineers (SPIE) Conference Series, Vol. 9147, Society of Photo-Optical Instrumentation Engineers (SPIE) Conference Series, 8
Cosentino, R., Lovis, C., Pepe, F., et al. 2012, in Society of Photo-Optical Instrumentation Engineers (SPIE) Conference Series, Vol. 8446, Society of Photo-Optical Instrumentation Engineers (SPIE) Conference Series, 1
Covino, E., Esposito, M., Barbieri, M., et al. 2013, A&A, 554, A28
Croll, B., Albert, L., Jayawardhana, R., et al. 2015, ApJ, 802, 28
Croll, B., Albert, L., Lafreniere, D., Jayawardhana, R., & Fortney, J. J. 2010a, ApJ, 717, 1084
Croll, B., Jayawardhana, R., Fortney, J. J., Lafrenière, D., & Albert, L. 2010b, ApJ, 718, 920
Csizmadia, S., Moutou, C., Deleuil, M., et al. 2011, A&A, 531, A41
Cubillos, P., Harrington, J., Madhusudhan, N., et al. 2014, ApJ, 797, 42
Cubillos, P., Harrington, J., Madhusudhan, N., et al. 2013, ApJ, 768, 42
Damasso, M., Biazzo, K., Bonomo, A. S., et al. 2015a, A&A, 575, A111
Damasso, M., Esposito, M., Nascimbeni, V., et al. 2015b, A&A, 581, L6
Damiani, C. & Lanza, A. F. 2015, A&A, 574, A39
Dawson, R. I., Johnson, J. A., Fabrycky, D. C., et al. 2014, ApJ, 791, 89
Dawson, R. I., Johnson, J. A., Morton, T. D., et al. 2012, ApJ, 761, 163
Dawson, R. I. & Murray-Clay, R. A. 2013, ApJ, 767, L24
Dawson, R. I., Murray-Clay, R. A., & Johnson, J. A. 2015, ApJ, 798, 66
Deeg, H. J., Moutou, C., Erikson, A., et al. 2010, Nature, 464, 384
Deleuil, M., Almenara, J.-M., Santerne, A., et al. 2014, A&A, 564, A56
Deleuil, M., Bonomo, A. S., Ferraz-Mello, S., et al. 2012, A&A, 538, A145
Deleuil, M., Deeg, H. J., Alonso, R., et al. 2008, A&A, 491, 889
Delrez, L., Van Grootel, V., Anderson, D. R., et al. 2014, A&A, 563, A143
Demarque, P., Woo, J.-H., Kim, Y.-C., & Yi, S. K. 2004, ApJS, 155, 667
Deming, D., Knutson, H., Agol, E., et al. 2011, ApJ, 726, 95
Deming, D., Knutson, H., Kammer, J., et al. 2015, ApJ, 805, 132
Demory, B.-O., Seager, S., Madhusudhan, N., et al. 2011, ApJ, 735, L12
Désert, J.-M., Charbonneau, D., Demory, B.-O., et al. 2011, ApJS, 197, 14
Díaz, R. F., Ségransan, D., Udry, S., et al. 2016, A&A, 585, A134
Dittmann, J. A., Close, L. M., Scuderi, L. J., Turner, J., & Stephenson, P. C. 2012, New A, 17, 438
Donati, J. F., Moutou, C., Malo, L., et al. 2016, Nature, 534, 662
Duffell, P. C. & Chiang, E. 2015, ApJ, 812, 94
Dumusque, X., Santos, N. C., Udry, S., Lovis, C., & Bonfils, X. 2011, A&A, 527, A82
Dunham, E. W., Borucki, W. J., Koch, D. G., et al. 2010, ApJ, 713, L136
Dunhill, A. C., Alexander, R. D., & Armitage, P. J. 2013, MNRAS, 428, 3072
Eastman, J., Gaudi, B. S., & Agol, E. 2013, PASP, 125, 83

Endl, M., Caldwell, D. A., Barclay, T., et al. 2014, ApJ, 795, 151
Endl, M., MacQueen, P. J., Cochran, W. D., et al. 2011, ApJS, 197, 13
Enoch, B., Anderson, D. R., Barros, S. C. C., et al. 2011a, AJ, 142, 86
Enoch, B., Cameron, A. C., Anderson, D. R., et al. 2011b, MNRAS, 410, 1631
Enoch, B., Collier Cameron, A., Parley, N. R., & Hebb, L. 2010, A&A, 516, A33
Esposito, M., Covino, E., Mancini, L., et al. 2014, A&A, 564, L13
Faber, J. A., Rasio, F. A., & Willems, B. 2005, Icarus, 175, 248
Fabrycky, D. & Tremaine, S. 2007, ApJ, 669, 1298
Faedi, F., Barros, S. C. C., Anderson, D. R., et al. 2011, A&A, 531, A40
Faedi, F., Pollacco, D., Barros, S. C. C., et al. 2013, A&A, 551, A73
Faigler, S., Tal-Or, L., Mazeh, T., Latham, D. W., & Buchhave, L. A. 2013, ApJ, 771, 26
Fischer, D. A., Vogt, S. S., Marcy, G. W., et al. 2007, ApJ, 669, 1336
Ford, E. B. 2006, ApJ, 642, 505
Ford, E. B. & Rasio, F. A. 2006, ApJ, 638, L45
Fortney, J. J., Demory, B.-O., Désert, J.-M., et al. 2011, ApJS, 197, 9
Fressin, F., Knutson, H. A., Charbonneau, D., et al. 2010, ApJ, 711, 374
Fridlund, M., Hébrard, G., Alonso, R., et al. 2010, A&A, 512, A14
Fukui, A., Kawashima, Y., Ikoma, M., et al. 2014, ApJ, 790, 108
Fulton, B. J., Collins, K. A., Gaudi, B. S., et al. 2015, ApJ, 810, 30
Fulton, B. J., Howard, A. W., Winn, J. N., et al. 2013, ApJ, 772, 80
Gandolfi, D., Collier Cameron, A., Endl, M., et al. 2012, A&A, 543, L5
Gandolfi, D., Hébrard, G., Alonso, R., et al. 2010, A&A, 524, A55
Gandolfi, D., Parviainen, H., Deeg, H. J., et al. 2015, A&A, 576, A11
Gandolfi, D., Parviainen, H., Fridlund, M., et al. 2013, A&A, 557, A74
Gibson, N. P., Aigrain, S., Barstow, J. K., et al. 2013, MNRAS, 428, 3680
Gibson, N. P., Aigrain, S., Pollacco, D. L., et al. 2010, MNRAS, 404, L114
Gillon, M., Anderson, D. R., Collier-Cameron, A., et al. 2014, A&A, 562, L3
Gillon, M., Anderson, D. R., Collier-Cameron, A., et al. 2013, A&A, 552, A82
Gillon, M., Anderson, D. R., Triaud, A. H. M. J., et al. 2009, A&A, 501, 785
Gillon, M., Doyle, A. P., Lendl, M., et al. 2011, A&A, 533, A88
Gillon, M., Hatzes, A., Csizmadia, S., et al. 2010a, A&A, 520, A97
Gillon, M., Lanotte, A. A., Barman, T., et al. 2010b, A&A, 511, A3
Gillon, M., Triaud, A. H. M. J., Fortney, J. J., et al. 2012, A&A, 542, A4
Goldreich, P. & Soter, S. 1966, Icarus, 5, 375
Goldreich, P. & Tremaine, S. 1980, ApJ, 241, 425
Gómez Maqueo Chew, Y., Faedi, F., Pollacco, D., et al. 2013, A&A, 559, A36
Goodman, J. & Lackner, C. 2009, ApJ, 696, 2054
Granata, V., Nascimbeni, V., Piotto, G., et al. 2014, Astronomische Nachrichten, 335, 797
Gregory, P. C. 2005, ApJ, 631, 1198
Guenther, E. W., Díaz, R. F., Gazzano, J.-C., et al. 2012, A&A, 537, A136
Guillochon, J., Ramirez-Ruiz, E., & Lin, D. 2011, ApJ, 732, 74
Hamers, A. S., Antonini, F., Lithwick, Y., Perets, H. B., & Portegies Zwart, S. F. 2017, MNRAS, 464, 688
Hansen, B. M. S. 2012, ApJ, 757, 6
Hartman, J. D., Bakos, G. Á., Béky, B., et al. 2012, AJ, 144, 139
Hartman, J. D., Bakos, G. Á., Sato, B., et al. 2011a, ApJ, 726, 52
Hartman, J. D., Bakos, G. Á., Torres, G., et al. 2014, AJ, 147, 128
Hartman, J. D., Bakos, G. Á., Torres, G., et al. 2009, ApJ, 706, 785
Hartman, J. D., Bakos, G. Á., Torres, G., et al. 2011b, ApJ, 742, 59
Hartman, J. D., Bhatti, W., Bakos, G. Á., et al. 2015, AJ, 150, 168
Hatzes, A. P. & Rauer, H. 2015, ApJ, 810, L25
Hebb, L., Collier-Cameron, A., Triaud, A. H. M. J., et al. 2010, ApJ, 708, 224
Hébrard, G., Almenara, J.-M., Santerne, A., et al. 2013a, A&A, 554, A114
Hébrard, G., Bouchy, F., Pont, F., et al. 2008, A&A, 488, 763
Hébrard, G., Collier Cameron, A., Brown, D. J. A., et al. 2013b, A&A, 549, A134
Hébrard, G., Désert, J.-M., Díaz, R. F., et al. 2010, A&A, 516, A95
Hébrard, G., Evans, T. M., Alonso, R., et al. 2011, A&A, 533, A130
Hébrard, G., Santerne, A., Montagnier, G., et al. 2014, A&A, 572, A93
Hellier, C., Anderson, D. R., Cameron, A. C., et al. 2014, MNRAS, 440, 1982
Hellier, C., Anderson, D. R., Collier Cameron, A., et al. 2015, AJ, 150, 18
Hellier, C., Anderson, D. R., Collier Cameron, A., et al. 2012, MNRAS, 426, 739
Hellier, C., Anderson, D. R., Collier Cameron, A., et al. 2009a, Nature, 460, 1098
Hellier, C., Anderson, D. R., Collier Cameron, A., et al. 2011a, A&A, 535, L7
Hellier, C., Anderson, D. R., Collier Cameron, A., et al. 2010, ApJ, 723, L60
Hellier, C., Anderson, D. R., Collier-Cameron, A., et al. 2011b, ApJ, 730, L31
Hellier, C., Anderson, D. R., Gillon, M., et al. 2009b, ApJ, 690, L89
Henry, G. W. & Winn, J. N. 2008, AJ, 135, 68
Hirano, T., Narita, N., Sato, B., et al. 2011, PASJ, 63, L57
Holman, M. J., Fabrycky, D. C., Ragozzine, D., et al. 2010, Science, 330, 51
Howard, A. W., Bakos, G. Á., Hartman, J., et al. 2012, ApJ, 749, 134
Hoyer, S., Rojo, P., López-Morales, M., et al. 2011, ApJ, 733, 53
Huang, C., Wu, Y., & Triaud, A. H. M. J. 2016, ApJ, 825, 98
Huang, C. X., Hartman, J. D., Bakos, G. Á., et al. 2015, AJ, 150, 85
Husnoo, N., Pont, F., Hébrard, G., et al. 2011, MNRAS, 413, 2500
Husnoo, N., Pont, F., Mazeh, T., et al. 2012, MNRAS, 422, 3151
Hut, P. 1981, A&A, 99, 126
Jackson, B., Barnes, R., & Greenberg, R. 2009, ApJ, 698, 1357
Jackson, B., Greenberg, R., & Barnes, R. 2008, ApJ, 678, 1396
Jenkins, J. M., Borucki, W. J., Koch, D. G., et al. 2010, ApJ, 724, 1108
Johnson, J. A., Gazak, J. Z., Apps, K., et al. 2012, AJ, 143, 111
Johnson, J. A., Winn, J. N., Bakos, G. Á., et al. 2011, ApJ, 735, 24
Johnson, J. A., Winn, J. N., Narita, N., et al. 2008, ApJ, 686, 649
Jordán, A. & Bakos, G. Á. 2008, ApJ, 685, 543
Jordán, A., Brahm, R., Bakos, G. Á., et al. 2014, AJ, 148, 29
Joshi, Y. C., Pollacco, D., Collier Cameron, A., et al. 2009, MNRAS, 392, 1532
Juncher, D., Buchhave, L. A., Hartman, J. D., et al. 2015, PASP, 127, 851
Kammer, J. A., Knutson, H. A., Line, M. R., et al. 2015, ApJ, 810, 118
Kass, R. E. & Raftery, A. E. 1995, Journal of the American Statistical Association, 90, 773
Kipping, D. M., Bakos, G. Á., Hartman, J., et al. 2010, ApJ, 725, 2017
Kipping, D. M., Hartman, J., Bakos, G. Á., et al. 2011, AJ, 142, 95
Kley, W. & Nelson, R. P. 2012, ARA&A, 50, 211
Knutson, H. A., Charbonneau, D., Allen, L. E., Burrows, A., & Megeath, S. T. 2008, ApJ, 673, 526
Knutson, H. A., Charbonneau, D., Burrows, A., O'Donovan, F. T., & Mandushev, G. 2009a, ApJ, 691, 866
Knutson, H. A., Charbonneau, D., Cowan, N. B., et al. 2009b, ApJ, 703, 769
Knutson, H. A., Charbonneau, D., Cowan, N. B., et al. 2009c, ApJ, 690, 822
Knutson, H. A., Charbonneau, D., Noyes, R. W., Brown, T. M., & Gilliland, R. L. 2007, ApJ, 655, 564
Knutson, H. A., Fulton, B. J., Montet, B. T., et al. 2014, ApJ, 785, 126
Koch, D. G., Borucki, W. J., Rowe, J. F., et al. 2010, ApJ, 713, L131
Konacki, M., Torres, G., Sasselov, D. D., & Jha, S. 2005, ApJ, 624, 372
Konacki, M., Torres, G., Sasselov, D. D., et al. 2004, ApJ, 609, L37
Kovács, G., Bakos, G. Á., Hartman, J. D., et al. 2010, ApJ, 724, 866
Kovács, G., Bakos, G. Á., Torres, G., et al. 2007, ApJ, 670, L41
Kundurthy, P., Becker, A. C., Agol, E., Barnes, R., & Williams, B. 2013, ApJ, 764, 8
Lai, D. 2012, MNRAS, 423, 486
Lanza, A. F., Boisse, I., Bouchy, F., Bonomo, A. S., & Moutou, C. 2011a, A&A, 533, A44
Lanza, A. F., Damiani, C., & Gandolfi, D. 2011b, A&A, 529, A50
Lanza, A. F., Pagano, I., Leto, G., et al. 2009, A&A, 493, 193
Latham, D. W., Bakos, G. Á., Torres, G., et al. 2009, ApJ, 704, 1107
Latham, D. W., Borucki, W. J., Koch, D. G., et al. 2010, ApJ, 713, L140
Latham, D. W., Rowe, J. F., Quinn, S. N., et al. 2011, ApJ, 732, L24
Laughlin, G., Deming, D., Langton, J., et al. 2009, Nature, 457, 562
Lendl, M., Anderson, D. R., Collier-Cameron, A., et al. 2012, A&A, 544, A72
Lendl, M., Triaud, A. H. M. J., Anderson, D. R., et al. 2014, A&A, 568, A81
Lewis, N. K., Knutson, H. A., Showman, A. P., et al. 2013, ApJ, 766, 95
Liddle, A. R. 2007, MNRAS, 377, L74
Lin, D. N. C., Bodenheimer, P., & Richardson, D. C. 1996, Nature, 380, 606
Lister, T. A., Anderson, D. R., Gillon, M., et al. 2009, ApJ, 703, 752
Loeillet, B., Shporer, A., Bouchy, F., et al. 2008, A&A, 481, 529
Lucy, L. B. & Sweeney, M. A. 1971, AJ, 76, 544
Lund, M. N., Lundkvist, M., Silva Aguirre, V., et al. 2014, A&A, 570, A54
Machalek, P., McCullough, P. R., Burke, C. J., et al. 2008, ApJ, 684, 1427
Machalek, P., McCullough, P. R., Burrows, A., et al. 2009, ApJ, 701, 514
Maciejewski, G., Dimitrov, D., Seeliger, M., et al. 2013a, A&A, 551, A108
Maciejewski, G., Niedzielski, A., Wolszczan, A., et al. 2013b, AJ, 146, 147
Maggio, A., Pillitteri, I., Scandariato, G., et al. 2015, ApJ, 811, L2
Mahtani, D. P., Maxted, P. F. L., Anderson, D. R., et al. 2013, MNRAS, 432, 693
Mallonn, M., von Essen, C., Weingrill, J., et al. 2015, A&A, 580, A60
Mancini, L., Ciceri, S., Chen, G., et al. 2013a, MNRAS, 436, 2
Mancini, L., Esposito, M., Covino, E., et al. 2015a, A&A, 579, A136
Mancini, L., Hartman, J. D., Penev, K., et al. 2015b, A&A, 580, A63
Mancini, L., Nikolov, N., Southworth, J., et al. 2013b, MNRAS, 430, 2932
Mancini, L., Southworth, J., Ciceri, S., et al. 2013c, A&A, 551, A11
Mancini, L., Southworth, J., Ciceri, S., et al. 2014, MNRAS, 443, 2391
Mandushev, G., O'Donovan, F. T., Charbonneau, D., et al. 2007, ApJ, 667, L195
Mandushev, G., Quinn, S. N., Buchhave, L. A., et al. 2011, ApJ, 741, 114
Marzari, F., Baruteau, C., & Scholl, H. 2010, A&A, 514, L4
Matsakos, T. & Königl, A. 2016, ApJ, 820, L8
Matsumura, S., Peale, S. J., & Rasio, F. A. 2010, ApJ, 725, 1995
Matsumura, S., Takeda, G., & Rasio, F. A. 2008, ApJ, 686, L29
Maxted, P. F. L., Anderson, D. R., Collier Cameron, A., et al. 2013a, PASP, 125, 48
Maxted, P. F. L., Anderson, D. R., Collier Cameron, A., et al. 2010a, PASP, 122, 1465
Maxted, P. F. L., Anderson, D. R., Collier Cameron, A., et al. 2011, PASP, 123, 547

Maxted, P. F. L., Anderson, D. R., Doyle, A. P., et al. 2013b, MNRAS, 428, 2645
Maxted, P. F. L., Anderson, D. R., Gillon, M., et al. 2010b, AJ, 140, 2007
Maxted, P. F. L., Serenelli, A. M., & Southworth, J. 2015, A&A, 577, A90
Mazeh, T., Holczer, T., & Faigler, S. 2016, A&A, 589, A75
McCullough, P. R., Burke, C. J., Valenti, J. A., et al. 2008, ArXiv e-prints arXiv:0805.2921
McCullough, P. R., Stys, J. E., Valenti, J. A., et al. 2006, ApJ, 648, 1228
McQuillan, A., Mazeh, T., & Aigrain, S. 2013, ApJ, 775, L11
Mislis, D., Mancini, L., Tregloan-Reed, J., et al. 2015, MNRAS, 448, 2617
Mohler-Fischer, M., Mancini, L., Hartman, J. D., et al. 2013, A&A, 558, A55
Morris, B. M., Mandell, A. M., & Deming, D. 2013, ApJ, 764, L22
Mortier, A., Santos, N. C., Sousa, S. G., et al. 2013, A&A, 558, A106
Moutou, C., Bruntt, H., Guillot, T., et al. 2008, A&A, 488, L47
Moutou, C., Díaz, R. F., Udry, S., et al. 2011, A&A, 533, A113
Moutou, C., Hébrard, G., Bouchy, F., et al. 2009, A&A, 498, L5
Müller, H. M., Huber, K. F., Czesla, S., Wolter, U., & Schmitt, J. H. M. M. 2013, A&A, 560, A112
Murray, C. D. & Dermott, S. F. 1999, Solar system dynamics
Naef, D., Latham, D. W., Mayor, M., et al. 2001, A&A, 375, L27
Naef, D., Mayor, M., Beuzit, J. L., et al. 2004, A&A, 414, 351
Nagasawa, M., Ida, S., & Bessho, T. 2008, ApJ, 678, 498
Naoz, S., Farr, W. M., Lithwick, Y., Rasio, F. A., & Teyssandier, J. 2011, Nature, 473, 187
Narita, N., Hirano, T., Sanchis-Ojeda, R., et al. 2010, PASJ, 62, L61
Nascimbeni, V., Piotto, G., Bedin, L. R., & Damasso, M. 2011, A&A, 527, A85
Neveu-VanMalle, M., Queloz, D., Anderson, D. R., et al. 2016, A&A, 586, A93
Neveu-VanMalle, M., Queloz, D., Anderson, D. R., et al. 2014, A&A, 572, A49
Nikolov, N., Chen, G., Fortney, J. J., et al. 2013, A&A, 553, A26
Nikolov, N., Sing, D. K., Burrows, A. S., et al. 2015, MNRAS, 447, 463
Nikolov, N., Sing, D. K., Pont, F., et al. 2014, MNRAS, 437, 46
Noyes, R. W., Bakos, G. Á., Torres, G., et al. 2008, ApJ, 673, L79
Nutzman, P., Gilliland, R. L., McCullough, P. R., et al. 2011, ApJ, 726, 3
Nymeyer, S., Harrington, J., Hardy, R. A., et al. 2011, ApJ, 742, 35
O'Donovan, F. T., Charbonneau, D., Harrington, J., et al. 2010, ApJ, 710, 1551
Ogilvie, G. I. 2014, ARA&A, 52, 171
Ogilvie, G. I. & Lin, D. N. C. 2007, ApJ, 661, 1180
Ollivier, M., Gillon, M., Santerne, A., et al. 2012, A&A, 541, A149
O'Rourke, J. G., Knutson, H. A., Zhao, M., et al. 2014, ApJ, 781, 109
Ortiz, M., Gandolfi, D., Reffert, S., et al. 2015, A&A, 573, L6
Pál, A., Bakos, G. Á., Fernandez, J., et al. 2009, ApJ, 700, 783
Pál, A., Bakos, G. Á., Torres, G., et al. 2010, MNRAS, 401, 2665
Pál, A., Bakos, G. Á., Torres, G., et al. 2008, ApJ, 680, 1450
Papaloizou, J. C. B. & Larwood, J. D. 2000, MNRAS, 315, 823
Parviainen, H., Gandolfi, D., Deleuil, M., et al. 2014, A&A, 562, A140
Pätzold, M., Endl, M., Csizmadia, S., et al. 2012, A&A, 545, A6
Pätzold, M. & Rauer, H. 2002, ApJ, 568, L117
Penev, K., Bakos, G. Á., Bayliss, D., et al. 2013, AJ, 145, 5
Pepe, F., Mayor, M., Galland, F., et al. 2002, A&A, 388, 632
Pepper, J., Siverd, R. J., Beatty, T. G., et al. 2013, ApJ, 773, 64
Perrakis, K., Ntzoufras, I., & Tsionas, E. G. 2014, Computational Statistics & Data Analysis, 77, 54
Petrovich, C. 2015, ApJ, 799, 27
Petrovich, C. & Tremaine, S. 2016, ApJ, 829, 132
Petrucci, R., Jofré, E., Schwartz, M., et al. 2013, ApJ, 779, L23
Pollacco, D., Skillen, I., Collier Cameron, A., et al. 2008, MNRAS, 385, 1576
Pont, F. 2009, MNRAS, 396, 1789
Pont, F., Bouchy, F., Melo, C., et al. 2005, A&A, 438, 1123
Pont, F., Husnoo, N., Mazeh, T., & Fabrycky, D. 2011, MNRAS, 414, 1278
Pont, F., Tamuz, O., Udalski, A., et al. 2008, A&A, 487, 749
Poretti, E., Boccato, C., Claudi, R., et al. 2015, ArXiv e-prints arXiv:1509.03661
Queloz, D., Anderson, D. R., Collier Cameron, A., et al. 2010, A&A, 517, L1
Quinn, S. N., Bakos, G. Á., Hartman, J., et al. 2012, ApJ, 745, 80
Quinn, S. N., White, T. R., Latham, D. W., et al. 2015, ApJ, 803, 49
Raetz, S., Maciejewski, G., Ginski, C., et al. 2014, MNRAS, 444, 1351
Rafikov, R. R. 2006, ApJ, 648, 666
Ramón-Fox, F. G. & Sada, P. V. 2013, Rev. Mexicana Astron. Astrofis., 49, 71
Rasio, F. A. & Ford, E. B. 1996, Science, 274, 954
Rasio, F. A., Tout, C. A., Lubow, S. H., & Livio, M. 1996, ApJ, 470, 1187
Rauer, H., Queloz, D., Csizmadia, S., et al. 2009, A&A, 506, 281
Rostron, J. W., Wheatley, P. J., Anderson, D. R., et al. 2014, MNRAS, 441, 3666
Rouan, D., Parviainen, H., Moutou, C., et al. 2012, A&A, 537, A54
Sada, P. V., Deming, D., Jennings, D. E., et al. 2012, PASP, 124, 212
Sanchis-Ojeda, R., Winn, J. N., Holman, M. J., et al. 2011, ApJ, 733, 127
Santerne, A., Bonomo, A. S., Hébrard, G., et al. 2011a, A&A, 536, A70
Santerne, A., Díaz, R. F., Bouchy, F., et al. 2011b, A&A, 528, A63
Sato, B., Fischer, D. A., Henry, G. W., et al. 2005, ApJ, 633, 465
Sato, B., Hartman, J. D., Bakos, G. Á., et al. 2012, PASJ, 64, 97
Schlaufman, K. C. & Winn, J. N. 2016, ApJ, 825, 62
Schneider, J., Dedieu, C., Le Sidaner, P., Savalle, R., & Zolotukhin, I. 2011, A&A, 532, A79
Shporer, A., Bakos, G. Á., Bouchy, F., et al. 2009, ApJ, 690, 1393
Silva-Valio, A. 2008, ApJ, 683, L179
Simpson, E. K., Barros, S. C. C., Brown, D. J. A., et al. 2011a, AJ, 141, 161
Simpson, E. K., Faedi, F., Barros, S. C. C., et al. 2011b, AJ, 141, 8
Simpson, E. K., Pollacco, D., Cameron, A. C., et al. 2011c, MNRAS, 414, 3023
Sing, D. K., Wakeford, H. R., Showman, A. P., et al. 2015, MNRAS, 446, 2428
Skillen, I., Pollacco, D., Collier Cameron, A., et al. 2009, A&A, 502, 391
Smalley, B., Anderson, D. R., Collier-Cameron, A., et al. 2012, A&A, 547, A61
Smalley, B., Anderson, D. R., Collier Cameron, A., et al. 2010, A&A, 520, A56
Smalley, B., Anderson, D. R., Collier Cameron, A., et al. 2011, A&A, 526, A130
Smith, A. M. S. 2014, ArXiv e-prints arXiv:1412.0451
Smith, A. M. S., Anderson, D. R., Armstrong, D. J., et al. 2014, A&A, 570, A64
Smith, A. M. S., Anderson, D. R., Bouchy, F., et al. 2013, A&A, 552, A120
Smith, A. M. S., Anderson, D. R., Collier Cameron, A., et al. 2012a, AJ, 143, 81
Smith, A. M. S., Anderson, D. R., Madhusudhan, N., et al. 2012b, A&A, 545, A93
Smith, A. M. S., Hebb, L., Collier Cameron, A., et al. 2009, MNRAS, 398, 1827
Socrates, A., Katz, B., & Dong, S. 2012a, ArXiv e-prints arXiv:1209.5724
Socrates, A., Katz, B., Dong, S., & Tremaine, S. 2012b, ApJ, 750, 106
Souchay, J., Mathis, S., & Tokieda, T., eds. 2013, Lecture Notes in Physics, Berlin Springer Verlag, Vol. 861, Tides in Astronomy and Astrophysics
Southworth, J. 2010, MNRAS, 408, 1689
Southworth, J. 2011, MNRAS, 417, 2166
Southworth, J. 2012, MNRAS, 426, 1291
Southworth, J., Bruni, I., Mancini, L., & Gregorio, J. 2012a, MNRAS, 420, 2580
Southworth, J., Hinse, T. C., Burgdorf, M., et al. 2014, MNRAS, 444, 776
Southworth, J., Hinse, T. C., Dominik, M., et al. 2012b, MNRAS, 426, 1338
Southworth, J., Mancini, L., Browne, P., et al. 2013, MNRAS, 434, 1300
Southworth, J., Mancini, L., Ciceri, S., et al. 2015a, MNRAS, 447, 711
Southworth, J., Mancini, L., Maxted, P. F. L., et al. 2012c, MNRAS, 422, 3099
Southworth, J., Mancini, L., Tregloan-Reed, J., et al. 2015b, MNRAS, 454, 3094
Sozzetti, A., Bonomo, A. S., Biazzo, K., et al. 2015, A&A, 575, L15
Sozzetti, A., Torres, G., Charbonneau, D., et al. 2007, ApJ, 664, 1190
Sozzetti, A., Torres, G., Charbonneau, D., et al. 2009, ApJ, 691, 1145
Steffen, J. H., Ragozzine, D., Fabrycky, D. C., et al. 2012, Proceedings of the National Academy of Science, 109, 7982
Stevenson, K. B., Harrington, J., Fortney, J. J., et al. 2012, ApJ, 754, 136
Street, R. A., Simpson, E., Barros, S. C. C., et al. 2010, ApJ, 720, 337
ter Braak, C. J. F. 2006, Statistics and Computing, 16, 239
Tingley, B., Endl, M., Gazzano, J.-C., et al. 2011, A&A, 528, A97
Todorov, K., Deming, D., Harrington, J., et al. 2010, ApJ, 708, 498
Todorov, K. O., Deming, D., Knutson, H. A., et al. 2013, ApJ, 770, 102
Todorov, K. O., Deming, D., Knutson, H. A., et al. 2012, ApJ, 746, 111
Torres, G., Andersen, J., & Giménez, A. 2010a, A&A Rev., 18, 67
Torres, G., Bakos, G. Á., Hartman, J., et al. 2010b, ApJ, 715, 458
Torres, G., Bakos, G. Á., Kovács, G., et al. 2007, ApJ, 666, L121
Torres, G., Fischer, D. A., Sozzetti, A., et al. 2012, ApJ, 757, 161
Torres, G., Konacki, M., Sasselov, D. D., & Jha, S. 2004, ApJ, 609, 1071
Torres, G., Winn, J. N., & Holman, M. J. 2008, ApJ, 677, 1324
Tregloan-Reed, J. & Southworth, J. 2013, MNRAS, 431, 966
Tregloan-Reed, J., Southworth, J., Burgdorf, M., et al. 2015, MNRAS, 450, 1760
Triaud, A. H. M. J., Anderson, D. R., Collier Cameron, A., et al. 2013, A&A, 551, A80
Triaud, A. H. M. J., Collier Cameron, A., Queloz, D., et al. 2010, A&A, 524, A25
Triaud, A. H. M. J., Queloz, D., Bouchy, F., et al. 2009, A&A, 506, 377
Triaud, A. H. M. J., Queloz, D., Hellier, C., et al. 2011, A&A, 531, A24
Udalski, A., Pont, F., Naef, D., et al. 2008, A&A, 482, 299
Valsecchi, F. & Rasio, F. A. 2014, ApJ, 787, L9
Van Eylen, V., Lindholm Nielsen, M., Hinrup, B., Tingley, B., & Kjeldsen, H. 2013, ApJ, 774, L19
Wang, X.-B., Gu, S.-H., Collier Cameron, A., et al. 2013, Research in Astronomy and Astrophysics, 13, 593
Weiss, L. M., Marcy, G. W., Rowe, J. F., et al. 2013, ApJ, 768, 14
West, R. G., Anderson, D. R., Gillon, M., et al. 2009a, AJ, 137, 4834
West, R. G., Collier Cameron, A., Hebb, L., et al. 2009b, A&A, 502, 395
Wheatley, P. J., Collier Cameron, A., Harrington, J., et al. 2010, ArXiv e-prints arXiv:1004.0836
Wilson, D. M., Gillon, M., Hellier, C., et al. 2008, ApJ, 675, L113
Winn, J. N., Holman, M. J., Henry, G. W., et al. 2009a, ApJ, 693, 794
Winn, J. N., Holman, M. J., Torres, G., et al. 2008, ApJ, 683, 1076
Winn, J. N., Howard, A. W., Johnson, J. A., et al. 2009b, ApJ, 703, 2091
Winn, J. N., Johnson, J. A., Albrecht, S., et al. 2009c, ApJ, 703, L99
Winn, J. N., Johnson, J. A., Marcy, G. W., et al. 2006, ApJ, 653, L69
Wong, I., Knutson, H. A., Cowan, N. B., et al. 2014, ApJ, 794, 134
Wong, I., Knutson, H. A., Lewis, N. K., et al. 2015, ApJ, 811, 122

Wright, J. T., Upadhyay, S., Marcy, G. W., et al. 2009, ApJ, 693, 1084
Wu, Y. & Lithwick, Y. 2011, ApJ, 735, 109
Zellem, R. T., Griffith, C. A., Pearson, K. A., et al. 2015, ApJ, 810, 11
Zellem, R. T., Lewis, N. K., Knutson, H. A., et al. 2014, ApJ, 790, 53
Zhao, M., O'Rourke, J. G., Wright, J. T., et al. 2014, ApJ, 796, 115
Zhou, G., Bayliss, D., Penev, K., et al. 2014, AJ, 147, 144

Acknowledgements. We thank the two anonymous referees for their comments that allowed us to improve the present manuscript. We are grateful to C. A. Latham and D. Latham for providing us with the corrected and new radial-velocity measurements of Qatar-2 that were gathered with the TRES spectrograph on the 1.5 m Tillinghast Reflector at the Fred L. Whipple Observatory, Arizona. GAPS acknowledges support from INAF (Italian National Institute of Astrophysics) through the 'Progetti Premiali' funding scheme of the Italian Ministry of Education, University, and Research. A.S.B., L.A., and L.M. acknowledge funding from the European Union Seventh Framework programme (FP7/2007-2013) under grant agreement No. 313014 (ETAEARTH). G.S. acknowledges financial support from "Accordo ASI–INAF" n. 2013-016-R.0 July 9, 2013. We acknowledge the use of e-infrastructure and support provided by IA2 (Italian Center for Astronomical Archives) of INAF - http://ia2.inaf.it.

Table 5. Summary of the radial-velocity data used in the present work. The number of the HARPS-N RVs in the third column, N_{RV} H-N, only refers to the 45 systems that we monitored. N_{Dat} is the number of different RV datasets per object.

Star	N_{RV} tot	N_{RV} H-N	Duration days	N_{Dat}	Ref.
CoRoT-1	9	-	197	1	1
CoRoT-2	23	-	54	2	2
CoRoT-3	22	-	334	3	3
CoRoT-4	20	-	102	2	4
CoRoT-5	19	-	342	2	5
CoRoT-6	14	-	73	1	6
CoRoT-8	19	-	371	1	7
CoRoT-9	28	-	1785	1	8,9
CoRoT-10	19	-	438	1	10
CoRoT-11	12	-	338	2	11
CoRoT-12	20	-	488	3	12
CoRoT-13	15	-	85	1	13
CoRoT-14	14	-	90	2	14
CoRoT-16	31	-	418	3	15
CoRoT-17	17	-	101	1	16
CoRoT-18	22	-	106	3	17
CoRoT-19	22	-	114	3	18
CoRoT-20	15	-	59	3	19
CoRoT-21	19	-	455	2	20
CoRoT-23	10	-	59	1	21
CoRoT-25	34	-	814	2	22
CoRoT-26	24	-	805	1	22
CoRoT-27	13	-	69	1	23
CoRoT-28	42	-	713	3	24
CoRoT-29	20	-	417	1	24
HAT-P-1	61	11	3416	3	25,26
HAT-P-2	85	18	3226	3	27,28,29,30
HAT-P-3	33	24	2927	2	31
HAT-P-4	49	13	2722	3	32,33,30
HAT-P-5	8	-	28	1	34
HAT-P-6	36	10	3251	2	35,30
HAT-P-7	101	11	2873	4	36,37,33,30
HAT-P-8	43	12	2955	3	38,39,30
HAT-P-9	15	-	358	1	40
HAT-P-12	23	-	2158	1	41,30
HAT-P-13	66	-	2126	1	42,30
HAT-P-14	59	11	2514	4	43,44,30
HAT-P-15	29	-	1859	1	45,30
HAT-P-16	20	10	2256	2	46,30
HAT-P-17	72	25	2957	2	47,30
HAT-P-18	48	17	2747	2	48,30
HAT-P-19	39	-	200	2	48
HAT-P-20	42	27	2077	2	49,30
HAT-P-21	39	24	2224	2	49
HAT-P-22	58	39	2620	2	49
HAT-P-23	13	-	556	1	49
HAT-P-24	36	13	2185	2	50,30
HAT-P-25	8	-	63	1	51
HAT-P-27	27	-	503	3	52,53
HAT-P-28	17	-	145	2	54
HAT-P-29	37	25	1805	2	54,30
HAT-P-30	52	13	1685	4	55,56,30
HAT-P-31	25	14	1925	2	57,30
HAT-P-32	30	-	1828	1	58,30
HAT-P-33	26	-	1538	1	58,30
HAT-P-34	33	-	814	3	59,30
HAT-P-35	12	-	79	2	59

Table 5. continued.

Star	N_{RV} tot	N_{RV} H-N	Duration days	N_{Dat}	Ref.
HAT-P-36	12	-	34	1	59
HAT-P-37	13	-	52	1	59
HAT-P-38	14	-	3	1	60
HAT-P-39	28	-	745	1	61
HAT-P-40	13	-	662	1	61
HAT-P-41	22	-	439	2	61
HAT-P-42	14	-	51	1	62
HAT-P-43	6	-	7	1	62
HAT-P-45	10	-	323	1	63
HAT-P-49	22	-	127	2	64
HAT-P-50	30	-	289	3	65
HAT-P-51	26	-	114	2	65
HAT-P-52	7	-	527	1	65
HAT-P-53	6	-	95	1	65
HAT-P-54	17	-	410	2	66
HAT-P-55	16	-	104	2	67
HAT-P-56	18	-	44	1	68
HATS-1	33	-	334	3	69
HATS-2	14	-	334	2	70
HATS-3	29	-	67	3	71
HATS-4	41	-	204	4	72
HATS-5	21	-	164	2	73
HATS-7	10	-	4	1	74
HATS-8	9	-	85	1	75
HATS-9	22	-	258	3	76
HATS-10	21	-	331	3	76
HATS-13	40	-	162	3	77
HATS-14	17	-	543	2	77
HD 149026	46	-	3325	2	78,79,30
HD 17156	97	54	3610	3	80,81
HD 189733	126	-	1504	3	82,83,84
HD 209458	251	-	2923	3	85,86
HD 80606	139	-	3480	3	87,88,89
KELT-2A	17	-	93	1	90
KELT-3	24	-	332	3	91
KELT-6	107	45	1178	3	92,93
KELT-8	12	-	86	1	94
Kepler-5	8	-	124	1	95
Kepler-6	9	-	58	1	96
Kepler-7	9	-	9	1	97
Kepler-8	16	-	152	1	98
Kepler-12	16	-	747	1	99
Kepler-15	30	-	225	2	100
Kepler-17	21	-	275	2	101,102
Kepler-39	13	-	47	1	103
Kepler-40	11	-	61	1	104
Kepler-41	12	-	126	1	105
Kepler-43	22	-	425	2	102,106
Kepler-44	7	-	13	1	102
Kepler-45	14	-	93	1	107
Kepler-74	17	-	170	2	108
Kepler-75	9	-	32	1	108
Kepler-76	18	-	131	2	109
Kepler-77	30	-	835	3	110,106
Kepler-412	6	-	245	1	111
Kepler-419	20	-	506	1	112
Kepler-422	15	-	778	1	106
Kepler-423	27	-	1146	2	113,106
Kepler-424	26	-	653	1	106
Kepler-425	10	-	339	1	114

Table 5. continued.

Star	N_{RV} tot	N_{RV} H-N	Duration days	N_{Dat}	Ref.
Kepler-426	10	-	338	1	114
Kepler-427	9	-	338	1	114
Kepler-428	6	-	337	1	114
Kepler-432	139	-	1292	3	115,116,117
Kepler-433	12	-	161	1	118
Kepler-434	11	-	333	1	118
Kepler-435	12	-	787	1	118
OGLE-TR-10	16	-	728	2	119,120
OGLE-TR-56	11	-	384	1	121
OGLE-TR-111	8	-	7	1	122
OGLE-TR-113	14	-	395	2	123,124
OGLE-TR-132	4	-	3	1	125
OGLE-TR-182	24	-	418	1	126
OGLE-TR-211	19	-	416	1	127
Qatar-1	15	15	1002	2[1]	128
Qatar-2	69	-	470	1	129
TrES-1	23	15	4311	2	130
TrES-2	40	12	3041	3	33,30
TrES-3	17	-	1947	2	131,30
TrES-4	24	18	2778	2	132,30
TrES-5	8	-	217	1	133
WASP-1	41	10	3291	4	134,135,30
WASP-2	22	-	2198	3	136,33,134,30
WASP-3	21	-	1861	2	137,30
WASP-4	32	-	2172	3	138,33,30
WASP-5	22	-	414	2	139,33
WASP-6	59	-	396	2	140
WASP-7	40	-	1879	3	141,33,30
WASP-8	63	-	2099	3	142,30
WASP-10	23	-	2192	3	143,30
WASP-11	58	32	2797	4	144,145,30
WASP-12	59	15	2180	3	146,30
WASP-13	28	17	2662	2	147
WASP-14	59	12	2685	5	148,146,30
WASP-15	21	-	133	1	149,30
WASP-16	84	-	1574	3	150,151,30
WASP-17	84	-	1850	3	152,30
WASP-18	53	-	1849	3	153,154,30
WASP-19	59	-	660	2	155,156,30
WASP-20	89	-	1918	2	157
WASP-21	47	8	2551	4	158
WASP-22	54	-	1934	3	159,30
WASP-23	38	-	585	1	160
WASP-24	74	11	2318	4	161,135,30
WASP-25	28	-	181	1	162
WASP-26	41	9	2341	3	163,164
WASP-28	42	-	1267	2	157
WASP-29	13	-	97	1	165
WASP-31	74	12	2192	3	166,151
WASP-32	46	9	2268	3	167,52
WASP-34	32	-	1472	2	168,30
WASP-35	19	10	2091	2	56
WASP-36	19	-	306	1	169
WASP-37	13	-	72	2	170
WASP-38	67	16	1910	4	52,135,30
WASP-39	17	-	76	2	171
WASP-41	22	-	214	1	172
WASP-42	53	-	401	2	173
WASP-43	42	27	1940	2	174
WASP-44	15	-	104	1	175

Table 5. continued.

Star	N_{RV} tot	N_{RV} H-N	Duration days	N_{Dat}	Ref.
WASP-45	13	-	94	1	175
WASP-46	16	-	120	1	175
WASP-48	25	11	1954	2	56
WASP-49	32	7	2045	2	173
WASP-50	25	10	1738	2	176
WASP-52	41	-	445	3	177
WASP-54	36	13	1657	3	178
WASP-55	20	-	173	1	179
WASP-56	13	-	40	1	178
WASP-57	25	-	140	2	178
WASP-58	15	-	33	1	177
WASP-59	12	-	32	1	177
WASP-60	31	-	474	2	177
WASP-61	15	-	298	1	179
WASP-62	25	-	370	1	179
WASP-63	23	-	423	1	179
WASP-64	16	-	250	1	180
WASP-65	18	-	321	1	181
WASP-66	30	-	428	1	179
WASP-67	19	-	86	1	179
WASP-68	43	-	824	1	182
WASP-69	22	-	736	1	183
WASP-70A	26	-	1072	2	183
WASP-71	22	-	87	2	184
WASP-72	18	-	354	1	180
WASP-73	20	-	712	1	182
WASP-74	20	-	417	1	185
WASP-75	15	-	350	1	181
WASP-77A	19	-	849	2	186
WASP-78	17	-	82	1	187
WASP-79	21	-	422	1	187
WASP-80	44	-	419	2	188
WASP-83	28	-	710	1	185
WASP-84	20	-	87	1	183
WASP-88	23	-	733	1	182
WASP-89	20	-	734	1	185
WASP-94A	32	-	734	1	189
WASP-95	14	-	297	1	190
WASP-96	21	-	379	1	190
WASP-97	12	-	64	1	190
WASP-98	14	-	365	1	190
WASP-99	20	-	356	1	190
WASP-100	19	-	170	1	190
WASP-101	19	-	796	1	190
WASP-103	18	-	101	1	191
WASP-104	21	-	169	2	192
WASP-106	29	-	398	2	192
WASP-117	95	-	681	2	193
WTS-2	7	-	86	1	194
XO-1	18	12	3338	2	195
XO-2N	72	32	2401	3	196,197,30
XO-3	75	19	2833	4	198,199,30
XO-4	41	14	1699	3	200,30
XO-5	34	-	2021	2	201,202,30

[1]The two datasets refer to HARPS-N data taken before and after the replacement of the HARPS-N CCD in September 2012 because of the failure of the CCD red side readout. Owing to different RV zero points, these data were considered as independent datasets.

References. (1) Barge et al. 2008; (2) Alonso et al. 2008; (3) Deleuil et al. 2008; (4) Moutou et al. 2008; (5) Rauer et al. 2009; (6) Fridlund et al. 2010; (7) Bordé et al. 2010; (8) Deeg et al. 2010;(9) Bonomo et al. 2017; (10) Bonomo et al. 2010; (11) Gandolfi et al. 2010; (12) Gillon et al. 2010a; (13) Cabrera et al. 2010; (14) Tingley et al. 2011; (15) Ollivier et al. 2012; (16) Csizmadia et al. 2011; (17) Hébrard et al. 2011; (18) Guenther et al. 2012; (19) Deleuil et al. 2012; (20) Pätzold et al. 2012; (21) Rouan et al. 2012; (22) Almenara et al. 2013; (23) Parviainen et al. 2014; (24) Cabrera et al. 2015; (25) Bakos et al. 2007b; (26) Johnson et al. 2008; (27) Pál et al. 2010; (28) Loeillet et al. 2008; (29) Bakos et al. 2007a; (30) Knutson et al. 2014; (31) Torres et al. 2007; (32) Kovács et al. 2007; (33) Husnoo et al. 2012; (34) Bakos et al. 2007c; (35) Noyes et al. 2008; (36) Pál et al. 2008; (37) Winn et al. 2009c; (38) Latham et al. 2009; (39) Moutou et al. 2011; (40) Shporer et al. 2009; (41) Hartman et al. 2009; (42) Bakos et al. 2009; (43) Torres et al. 2010b; (44) Simpson et al. 2011a; (45) Kovács et al. 2010; (46) Buchhave et al. 2010; (47) Howard et al. 2012; (48) Hartman et al. 2011a; (49) Bakos et al. 2011; (50) Kipping et al. 2010; (51) Quinn et al. 2012; (52) Brown et al. 2012b; (53) Anderson et al. 2011a; (54) Buchhave et al. 2011a; (55) Johnson et al. 2011; (56) Enoch et al. 2011a; (57) Kipping et al. 2011; (58) Hartman et al. 2011b; (59) Bakos et al. 2012; (60) Sato et al. 2012; (61) Hartman et al. 2012; (62) Boisse et al. 2013; (63) Hartman et al. 2014; (64) Bieryla et al. 2014; (65) Hartman et al. 2015; (66) Bakos et al. 2015a; (67) Juncher et al. 2015; (68) Huang et al. 2015; (69) Penev et al. 2013;(70) Mohler-Fischer et al. 2013; (71) Bayliss et al. 2013; (72) Jordán et al. 2014; (73) Zhou et al. 2014; (74) Bakos et al. 2015b;(75) Bayliss et al. 2015; (76) Brahm et al. 2015; (77) Mancini et al. 2015b;(78) Sato et al. 2005; (79) Butler et al. 2006; (80) Fischer et al. 2007; (81) Winn et al. 2009a; (82) Bouchy et al. 2005b; (83) Winn et al. 2006; (84) Boisse et al. 2009; (85) Naef et al. 2004; (86) Butler et al. 2006; (87) Naef et al. 2001; (88) Winn et al. 2009b; (89) Moutou et al. 2009; (90) Beatty et al. 2012; (91) Pepper et al. 2013; (92) Collins et al. 2014; (93) Damasso et al. 2015b; (94) Fulton et al. 2015; (95) Koch et al. 2010; (96) Dunham et al. 2010; (97) Latham et al. 2010; (98) Jenkins et al. 2010; (99) Fortney et al. 2011; (100) Endl et al. 2011; (101) Désert et al. 2011; (102) Bonomo et al. 2012; (103) Bouchy et al. 2011; (104) Santerne et al. 2011b; (105) Santerne et al. 2011a; (106) Endl et al. 2014; (107) Johnson et al. 2012; (108) Hébrard et al. 2013a; (109) Faigler et al. 2013; (110) Gandolfi et al. 2013; (111) Deleuil et al. 2014; (112) Dawson et al. 2014; (113) Gandolfi et al. 2015; (114) Hébrard et al. 2014; (115) Quinn et al. 2015; (116) Ortiz et al. 2015; (117) Ciceri et al. 2015; (118) Almenara et al. 2015; (119) Bouchy et al. 2005a; (120) Konacki et al. 2005; (121) Torres et al. 2004; (122) Pont et al. 2005; (123) Konacki et al. 2004; (124) Pont et al. 2005; (125) Bouchy et al. 2004; (126) Pont et al. 2008; (127) Udalski et al. 2008; (128) Covino et al. 2013; (129) Bryan et al. 2012; (130) Alonso et al. 2004; (131) Sozzetti et al. 2009; (132) Sozzetti et al. 2015; (133) Mandushev et al. 2011; (134) Collier Cameron et al. 2007; (135) Simpson et al. 2011c; (136) Mandushev et al. 2011; (137) Pollacco et al. 2008; (138) Wilson et al. 2008; (139) Anderson et al. 2008; (140) Gillon et al. 2009; (141) Hellier et al. 2009b; (142) Queloz et al. 2010; (143) Christian et al. 2009; (144) West et al. 2009b; (145) Mancini et al. 2015a; (146) Husnoo et al. 2011; (147) Skillen et al. 2009; (148) Joshi et al. 2009; (149) West et al. 2009a; (150) Lister et al. 2009; (151) Brown et al. 2012a; (152) Anderson et al. 2010; (153) Hellier et al. 2009a; (154) Triaud et al. 2010; (155) Hebb et al. 2010; (156) Hellier et al. 2011b; (157) Anderson et al. 2015; (158) Bouchy et al. 2010; (159) Maxted et al. 2010b; (160) Triaud et al. 2011; (161) Street et al. 2010; (162) Enoch et al. 2011b; (163) Smalley et al. 2010; (164) Anderson et al. 2011b; (165) Hellier et al. 2010; (166) Anderson et al. 2011c; (167) Maxted et al. 2010a; (168) Smalley et al. 2011; (169) Smith et al. 2012a; (170) Simpson et al. 2011b; (171) Faedi et al. 2011; (172) Maxted et al. 2011; (173) Lendl et al. 2012; (174) Hellier et al. 2011a; (175) Anderson et al. 2012; (176) Gillon et al. 2011; (177) Hébrard et al. 2013b; (178) Faedi et al. 2013; (179) Hellier et al. 2012; (180) Gillon et al. 2013; (181) Gómez Maqueo Chew et al. 2013; (182) Delrez et al. 2014; (183) Anderson et al. 2014; (184) Smith et al. 2013; (185) Hellier et al. 2015; (186) Maxted et al. 2013a; (187) Smalley et al. 2012; (188) Triaud et al. 2013; (189) Neveu-VanMalle et al. 2014; (190) Hellier et al. 2014; (191) Gillon et al. 2014; (192) Smith et al. 2014; (193) Lendl et al. 2014; (194) Birkby et al. 2014; (195) McCullough et al. 2006; (196) Burke et al. 2007; (197) Damasso et al. 2015a; (198) Hébrard et al. 2008; (199) Hirano et al. 2011; (200) Narita et al. 2010; (201) Burke et al. 2008; (202) Pál et al. 2009;

Table 6. Priors on orbital periods, and transit and occultation midtimes from ground-based and/or space-based photometry.

Planet	Period days	Transit Midtime $BJD_{TDB} - 2,450,000$	Ephemeris Reference	Occultation Midtime $BJD_{TDB} - 2,450,000$	Occultation Reference
CoRoT-1b	1.50896820 ± 5.0E-07	4138.328070 ± 6.0E-05	1	5162.1651 ± 0.0036	2
				5159.1441 ± 0.0021	2
CoRoT-2b	1.74299673 ± 3.1E-07	5628.44758 ± 0.00014	3	5160.4504 ± 0.0012	2
				4771.76060 ± 0.00070	2
				4771.7641 ± 0.0019	2
CoRoT-3b	4.2567994 ± 3.5E-06	4283.13388 ± 0.00024	4		
CoRoT-4b	9.20205 ± 0.00037	4141.36493 ± 0.00089	5		
CoRoT-5b	4.0378962 ± 1.9E-06	4400.199630 ± 2.0E-05	6		
CoRoT-6b	8.886593 ± 4.0E-05	4595.61515 ± 0.00020	7		
CoRoT-8b	6.212381 ± 5.7E-05	4239.03384 ± 0.00078	8		
CoRoT-9b	95.272656 ± 6.8E-05	5365.52723 ± 0.00037	9		
CoRoT-10b	13.24060 ± 0.00020	4273.3443 ± 0.0012	10		
CoRoT-11b	2.994325 ± 2.1E-05	4690.49911 ± 0.00016	11		
CoRoT-12b	2.828042 ± 1.3E-05	4398.62785 ± 0.00036	12		
CoRoT-13b	4.035190 ± 3.0E-05	4790.80990 ± 0.00060	13		
CoRoT-14b	1.51214 ± 0.00013	4787.6702 ± 0.0053	14		
CoRoT-16b	5.35227 ± 0.00020	4923.9145 ± 0.0022	15		
CoRoT-17b	3.76810 ± 0.00030	4923.3100 ± 0.0036	16		
CoRoT-18b	1.9000693 ± 2.8E-06	5321.72490 ± 0.00018	17		
CoRoT-19b	3.897130 ± 2.0E-05	5257.44180 ± 0.00060	18		
CoRoT-20b	9.24285 ± 0.00030	5266.0009 ± 0.0014	19		
CoRoT-21b	2.72474 ± 0.00014	4399.02900 ± 0.00090	20		
CoRoT-23b	3.63130 ± 1.0E-04	5308.9400 ± 0.0010	21		
CoRoT-25b	4.860690 ± 6.0E-05	4576.21630 ± 0.00080	22		
CoRoT-26b	4.204740 ± 5.0E-05	4573.63060 ± 0.00080	22		
CoRoT-27b	3.575320 ± 6.0E-05	5748.6850 ± 0.0010	23		
CoRoT-28b	5.20851 ± 0.00038	5755.8474 ± 0.0029	24		
CoRoT-29b	2.8505700 ± 6.0E-06	5753.1158 ± 0.0010	24		
HAT-P-1b	4.46529976 ± 5.5E-07	3979.93202 ± 0.00024	25	4464.4182 ± 0.0032	26
				4102.7225 ± 0.0029	26
HAT-P-2b	5.6334754 ± 2.6E-06	5288.84910 ± 0.00037	27	5284.2974 ± 0.0014	27
				5751.8802 ± 0.0011	27
				4354.7765 ± 0.0022	27
HAT-P-3b	2.8997360 ± 2.0E-06	4856.70195 ± 1.0E-04	28	5272.8294 ± 0.0032	29
				5275.7166 ± 0.0030	29
HAT-P-4b	3.0565254 ± 1.2E-06	4245.81521 ± 0.00020	1	5298.7865 ± 0.0027	29
				5442.4437 ± 0.0033	29
HAT-P-5b	2.78847360 ± 5.2E-07	5432.45510 ± 1.0E-04	30		
HAT-P-6b	3.8530030 ± 1.2E-06	4035.67616 ± 0.00025	31	5451.6520 ± 0.0040	32
				5459.3565 ± 0.0017	32
HAT-P-7b	2.204737 ± 1.7E-05	4954.3574620 ± 5.0E-06	33	4768.0528 ± 0.0035	34
				4770.2649 ± 0.0039	34
HAT-P-8b	3.0763458 ± 2.4E-06	4437.6749 ± 0.0014	35	5211.3751 ± 0.0016	32
				5208.3011 ± 0.0024	32
HAT-P-9b	3.9228140 ± 2.0E-06	4417.90840 ± 0.00060	36		
HAT-P-12b	3.21305929 ± 3.5E-07	4187.85559 ± 0.00011	29		
HAT-P-13b	2.9162383 ± 2.2E-06	5176.53878 ± 0.00027	37		
HAT-P-14b	4.6276820 ± 3.0E-06	5268.64237 ± 0.00031	38		
HAT-P-15b	10.863502 ± 3.7E-05	4638.56094 ± 0.00048	39		
HAT-P-16b	2.7759712 ± 1.5E-06	5027.59281 ± 0.00040	40		
HAT-P-17b	10.3385230 ± 9.0E-06	4801.17018 ± 0.00020	41		
HAT-P-18b	5.5080230 ± 6.0E-06	4715.02249 ± 0.00020	42		
HAT-P-19b	4.0087780 ± 6.0E-06	5091.53492 ± 0.00034	42	5999.5301 ± 0.0074	43
				6933.5705 ± 0.0071	43
HAT-P-20b	2.87531860 ± 2.0E-07	5598.48482 ± 0.00032	44	6810.4541 ± 0.0024	45
				6085.8754 ± 0.0013	45
				6816.2079 ± 0.0024	45
HAT-P-21b	4.1244810 ± 7.0E-06	4996.41389 ± 0.00069	46		
HAT-P-22b	3.2122200 ± 9.0E-06	4930.22077 ± 0.00025	46		

Table 6. continued.

Planet	Period days	Transit Midtime $BJD_{TDB} - 2,450,000$	Ephemeris Reference	Occultation Midtime $BJD_{TDB} - 2,450,000$	Occultation Reference
HAT-P-23b	1.21288287 ± 1.7E-07	4852.26542 ± 0.00020	47	5895.9542 ± 0.0018	48
				5897.1687 ± 0.0015	48
				6117.9129 ± 0.0027	48
HAT-P-24b	3.3552479 ± 6.2E-06	5629.67130 ± 0.00034	49		
HAT-P-25b	3.652836 ± 1.9E-05	5176.85233 ± 0.00047	50		
HAT-P-27b	3.0395824 ± 3.5E-06	5186.01982 ± 0.00032	1		
HAT-P-28b	3.2572150 ± 7.0E-06	5417.59908 ± 0.00053	51		
HAT-P-29b	5.7233900 ± 1.0E-06	6210.615360 ± 5.0E-05	52		
HAT-P-30b	2.8105950 ± 5.0E-06	5456.46637 ± 0.00037	53		
HAT-P-31b	5.005425 ± 9.2E-05	4320.8866 ± 0.0052	54		
HAT-P-32b	2.15000825 ± 1.2E-07	4420.446450 ± 9.0E-05	55	5855.57877 ± 0.00095	56
				5864.1770 ± 0.0012	56
HAT-P-33b	3.4744740 ± 1.0E-06	5110.92672 ± 0.00022	55		
HAT-P-34b	5.452654 ± 1.6E-05	5431.59706 ± 0.00055	57		
HAT-P-35b	3.646706 ± 2.1E-05	5578.66158 ± 0.00050	57		
HAT-P-36b	1.3273470 ± 3.0E-06	5565.18221 ± 0.00020	57		
HAT-P-37b	2.7974360 ± 7.0E-06	5642.14395 ± 0.00029	57		
HAT-P-38b	4.640382 ± 3.2E-05	5863.12034 ± 0.00035	58		
HAT-P-39b	3.5438700 ± 5.0E-06	5208.75126 ± 0.00041	59		
HAT-P-40b	4.457243 ± 1.0E-05	5813.17661 ± 0.00054	59		
HAT-P-41b	2.6940470 ± 4.0E-06	4983.8624 ± 0.0011	59		
HAT-P-42b	4.641878 ± 3.2E-05	5952.52679 ± 0.00075	60		
HAT-P-43b	3.332687 ± 1.5E-05	5997.37183 ± 0.00032	60		
HAT-P-45b	3.128992 ± 2.1E-05	5729.98689 ± 0.00041	61		
HAT-P-49b	2.6915480 ± 6.0E-06	6399.62484 ± 0.00063	62		
HAT-P-50b	3.1220109 ± 6.5E-06	6285.91071 ± 0.00036	63		
HAT-P-51b	4.2180278 ± 5.9E-06	6194.12282 ± 0.00040	63		
HAT-P-52b	2.7535953 ± 9.4E-06	5852.104026 ± 0.000410	63		
HAT-P-53b	1.9616241 ± 3.9E-06	5829.448576 ± 0.000440	63		
HAT-P-54b	3.799847 ± 1.4E-05	6299.304478 ± 0.000240	64		
HAT-P-55b	3.5852467 ± 6.4E-06	6730.83468 ± 0.00027	65		
HAT-P-56b	2.7908327 ± 4.7E-06	6553.61723 ± 0.00042	66		
HATS-1b	3.4464590 ± 4.0E-06	5241.28799 ± 0.00071	67		
HATS-2b	1.3541330 ± 1.0E-06	5954.586530 ± 9.0E-05	68		
HATS-3b	3.5478510 ± 5.0E-06	6155.96812 ± 0.00014	69		
HATS-4b	2.5167290 ± 2.0E-06	5808.34172 ± 0.00036	70		
HATS-5b	4.763387 ± 1.0E-05	6273.791460 ± 10.0E-05	71		
HATS-7b	3.1853150 ± 5.4E-06	6528.29697 ± 0.00058	72		
HATS-8b	3.583893 ± 1.0E-05	6672.11098 ± 0.0012	73		
HATS-9b	1.9153073 ± 5.2E-06	6124.25974 ± 0.00086	74		
HATS-10b	3.3128460 ± 5.8E-06	6457.88271 ± 0.00022	74		
HATS-13b	3.0440499 ± 2.7E-06	6340.31783 ± 0.00026	75		
HATS-14b	2.7667641 ± 2.7E-06	6408.765398 ± 0.000210	75		
HD 149026b	2.8758916 ± 1.4E-06	4597.70713 ± 0.00016	76	4535.8764 ± 0.0010	77
				4596.2676 ± 0.0019	77
				4912.6140 ± 0.0020	77
HD 17156b	21.216398 ± 1.6E-05	4884.028940 ± 7.3E-05	78		
HD 189733b	2.218575200 ± 7.7E-08	3955.5255510 ± 9.0E-06	3	3699.2823 ± 0.0052	79
				4280.5472 ± 0.0026	80
				4038.7237 ± 0.0027	81
HD 209458b	3.52474859 ± 3.8E-07	2826.629283 ± 8.7E-05	82	3702.5256 ± 0.0024	83
				5214.6470 ± 0.0012	84
				5218.1702 ± 0.0011	84
HD 80606b	111.43670 ± 0.00040	5210.64280 ± 0.00100	85	4424.737 ± 0.030	86
KELT-2Ab	4.113791 ± 1.0E-05	5974.60338 ± 0.00082	87		
KELT-3b	2.703390 ± 1.0E-05	6023.459 ± 0.017	88		
KELT-6b	7.845582 ± 7.0E-06	7124.50954 ± 0.00057	89		
KELT-8b	3.24406 ± 0.00016	6883.48030 ± 0.00070	90		
Kepler-5b	3.5484625 ± 1.0E-06	5005.579469 ± 7.5E-05	91		
Kepler-6b	3.23469940 ± 3.5E-07	5003.006282 ± 2.9E-05	91		

Table 6. continued.

Planet	Period days	Transit Midtime $BJD_{TDB} - 2,450,000$	Ephemeris Reference	Occultation Midtime $BJD_{TDB} - 2,450,000$	Occultation Reference
Kepler-7b	4.8854886 ± 1.3E-06	5094.298833 ± 5.6E-05	91	4974.6094 ± 0.0034	92
Kepler-8b	3.52249905 ± 8.3E-07	5003.433596 ± 6.4E-05	91		
Kepler-12b	4.43796370 ± 2.0E-07	5004.009107 ± 2.0E-05	93	5010.6668 ± 0.0040	93
Kepler-15b	4.9427809 ± 1.4E-06	5097.841168 ± 6.0E-05	91		
Kepler-17b	1.48571091 ± 2.1E-07	5185.678033 ± 2.3E-05	91		
Kepler-39b	21.087210 ± 3.7E-05	5942.60708 ± 0.00024	94		
Kepler-40b	6.8731697 ± 9.6E-06	5204.83996 ± 0.00020	95		
Kepler-41b	1.85555820 ± 5.2E-07	5187.280482 ± 5.1E-05	94	$e\cos\omega = -0.002^{+0.006}_{-0.017}$	96
Kepler-43b	3.02409309 ± 2.0E-07	5095.452270 ± 5.0E-05	94		
Kepler-44b	3.2467293 ± 3.0E-06	5187.15640 ± 0.00021	94		
Kepler-45b	2.4552339 ± 4.8E-06	5374.562419 ± 9.2E-05	91		
Kepler-74b	7.3407110 ± 6.0E-06	5187.56737 ± 0.00014	94		
Kepler-75b	8.8849116 ± 3.4E-06	5740.44030 ± 0.00012	94		
Kepler-76b	1.54492870 ± 2.7E-07	4966.548110 ± 7.0E-05	97		
Kepler-77b	3.57878087 ± 2.3E-07	5095.866516 ± 2.9E-05	98		
Kepler-412b	1.720861200 ± 4.7E-08	4966.021033 ± 2.3E-05	99	$e\cos\omega = -9$E-04 ± 0.0045	99
Kepler-419b	69.75470 ± 0.00090	5238.3154 ± 0.00060	100		
Kepler-422b	7.89144830 ± 5.0E-07	5010.25005 ± 0.00011	101		
Kepler-423b	2.684328500 ± 7.0E-08	4966.354810 ± 2.1E-05	102		
Kepler-424b	3.3118644 ± 3.9E-06	4964.74270 ± 0.00023	100		
Kepler-425b	3.79701816 ± 1.9E-07	4966.508785 ± 3.9E-05	103		
Kepler-426b	3.21751883 ± 1.9E-07	4966.631964 ± 4.7E-05	103		
Kepler-427b	10.2909940 ± 1.1E-06	4970.02207 ± 9.0E-05	103		
Kepler-428b	3.52563254 ± 1.5E-07	5003.048008 ± 3.2E-05	103		
Kepler-432b	52.50113 ± 0.00011	5949.5374 ± 0.0018	104		
Kepler-433b	5.3340838 ± 1.1E-06	4964.98152 ± 0.00015	105		
Kepler-434b	12.8747099 ± 1.0E-06	5003.02283 ± 0.00042	105		
Kepler-435b	8.6001536 ± 1.8E-06	5010.64241 ± 0.00040	105		
OGLE-TR-10b	3.1012780 ± 4.0E-06	4262.818228 ± 0.00030	106		
OGLE-TR-56b	1.21191096 ± 6.5E-07	3936.60070 ± 0.00044	107		
OGLE-TR-111b	4.0144477 ± 1.9E-06	4092.80691 ± 0.00025	108		
OGLE-TR-113b	1.43247425 ± 3.4E-07	3464.61755 ± 0.00022	109		
OGLE-TR-132b	1.68986531 ± 6.4E-07	3142.59199 ± 0.00053	110		
OGLE-TR-182b	3.979100 ± 1.0E-05	4270.5744 ± 0.0020	111		
OGLE-TR-211b	3.677240 ± 3.0E-05	3428.3347 ± 0.0030	112		
Qatar-1b	1.42002504 ± 7.1E-07	5518.41075 ± 0.00028	113	6136.8322 ± 0.0018	114
Qatar-2b	1.33711647 ± 2.6E-07	5624.267096 ± 8.7E-05	115		
TrES-1b	3.03006973 ± 1.8E-07	5016.969937 ± 7.0E-05	3	3309.5302 ± 0.0036	116
				3630.7159 ± 0.0016	117
				3309.5290 ± 0.0016	117
TrES-2b	2.470613374 ± 1.9E-08	3957.635499 ± 1.3E-05	118	4070.04880 ± 0.00086	119
				4324.5227 ± 0.0026	119
				4994.0613 ± 0.0033	120
TrES-3b	1.306186483 ± 7.0E-08	4185.910993 ± 5.0E-05	121	4665.9372 ± 0.0021	122
				4668.5454 ± 0.0020	122
				4985.9550 ± 0.0019	123
TrES-4b	3.55392771 ± 4.7E-07	4230.90560 ± 0.00030	124	4392.614440 ± 0.0080	125
				4396.167240 ± 0.0039	125
TrES-5b	1.48224460 ± 7.0E-07	5443.25232 ± 0.00011	126		
WASP-1b	2.51994480 ± 5.0E-07	5530.31970 ± 0.00016	45	$e\cos\omega = 0 \pm 0.0011$	127
WASP-2b	2.15222163 ± 4.2E-07	5894.07919 ± 0.00015	3	$e\cos\omega = 0 \pm 0.0013$	127
WASP-3b	1.84683510 ± 4.0E-07	4143.85112 ± 0.00024	128	4728.3744 ± 0.0011	129
				5130.9846 ± 0.0013	129
				4998.0150 ± 0.0022	114
WASP-4b	1.338231624 ± 6.8E-08	4966.782814 ± 2.1E-05	3	5102.61236 ± 0.00074	130
				5172.2019 ± 0.0013	131
				5174.87801 ± 0.00087	131
WASP-5b	1.62842953 ± 5.2E-07	6446.98868 ± 0.00017	3	5812.7249 ± 0.0031	132
WASP-6b	3.36100239 ± 3.7E-07	5278.716260 ± 8.5E-05	133	5196.3614 ± 0.0106	43
				5219.9015 ± 0.0044	43

Table 6. continued.

Planet	Period days	Transit Midtime $BJD_{TDB} - 2,450,000$	Ephemeris Reference	Occultation Midtime $BJD_{TDB} - 2,450,000$	Occultation Reference
WASP-7b	4.9546416 ± 3.5E-06	5446.63493 ± 0.00030	134		
WASP-8b	8.158715 ± 1.6E-05	4679.33473 ± 0.00047	135	4822.2309 ± 0.0031	136
				5401.4989 ± 0.0028	136
				5409.6663 ± 0.0023	136
WASP-10b	3.09272932 ± 3.2E-07	4664.038090 ± 4.8E-05	137	5580.9234 ± 0.0025	43
				6910.79248 ± 0.00270	43
				6923.17008 ± 0.00200	43
WASP-11b	3.72247930 ± 7.0E-07	4759.68753 ± 0.00011	1		
WASP-12b	1.09142090 ± 2.0E-07	4508.97718 ± 0.00022	138	4769.28269 ± 0.00080	139
				4773.64889 ± 0.00060	139
				5576.93200 ± 0.00090	140
WASP-13b	4.353011 ± 1.3E-05	5575.5144 ± 0.0016	141		
WASP-14b	2.2437661 ± 1.1E-06	4827.06666 ± 0.00024	142	5274.66170 ± 0.00060	142
				6035.30024 ± 0.00051	143
				6044.27476 ± 0.00078	143
WASP-15b	3.75209748 ± 8.1E-07	4584.69859 ± 0.00029	144		
WASP-16b	3.1186068 ± 1.2E-06	4584.42898 ± 0.00038	144		
WASP-17b	3.7354845 ± 1.9E-06	4592.801540 ± 5.0E-05	145	$\phi_{mid-occ} = 0.50224 \pm 0.00050$	146
WASP-18b	0.94145230 ± 3.0E-07	5265.55250 ± 1.0E-04	147	4820.71680 ± 0.00070	148
				4824.48150 ± 0.00050	148
				5431.71910 ± 0.00030	147
WASP-19b	0.7888396 ± 1.0E-06	4775.33745 ± 0.00035	149	5997.6440 ± 0.0010	150
				6023.6763 ± 0.0010	150
				4921.6687 ± 0.0019	151
WASP-20b	4.8996284 ± 3.3E-06	5715.65640 ± 0.00029	152		
WASP-21b	4.3225126 ± 2.2E-06	4743.04054 ± 0.00065	40		
WASP-22b	3.5327313 ± 5.8E-06	5497.40043 ± 0.00025	153		
WASP-23b	2.9444300 ± 1.1E-06	4813.68159 ± 0.00042	154		
WASP-24b	2.34122170 ± 8.0E-07	5687.75616 ± 0.00016	155	$\phi_{mid-occ} = 0.50028 \pm 0.00055$	156
WASP-25b	3.76483270 ± 9.0E-07	5888.66484 ± 0.00013	155		
WASP-26b	2.7565972 ± 1.9E-06	5837.59821 ± 0.00044	156	$\phi_{mid-occ} = 0.4998 \pm 0.0005$	157
WASP-28b	3.4088300 ± 6.0E-06	5290.40597 ± 0.00031	152		
WASP-29b	3.9227186 ± 6.8E-06	5830.18886 ± 0.00016	158		
WASP-31b	3.40588600 ± 7.8E-07	5873.86662 ± 0.00011	159		
WASP-32b	2.7186591 ± 2.4E-06	5849.75000 ± 0.00037	1		
WASP-34b	4.3176782 ± 4.5E-06	4647.55434 ± 0.00064	160		
WASP-35b	3.1615750 ± 2.0E-06	5531.47984 ± 0.00015	161		
WASP-36b	1.5373653 ± 2.6E-06	5569.838094 ± 9.5E-05	162		
WASP-37b	3.577469 ± 1.1E-05	5338.61958 ± 0.00060	163		
WASP-38b	6.871815 ± 4.5E-05	5335.92127 ± 0.00074	164		
WASP-39b	4.05529470 ± 9.7E-07	5342.97036 ± 0.00020	165	6022.23636 ± 0.00660	43
				6026.28857 ± 0.00580	43
WASP-41b	3.0524010 ± 4.0E-06	5343.46378 ± 0.00100	166		
WASP-42b	4.9816872 ± 7.3E-06	5650.56798 ± 0.00023	167		
WASP-43b	0.81347437 ± 1.3E-07	5934.792239 ± 4.0E-05	168	5726.95069 ± 0.00084	169
				5772.50450 ± 0.00030	170
				5773.31790 ± 0.00030	170
WASP-44b	2.4238133 ± 2.3E-06	5434.37642 ± 0.00037	171		
WASP-45b	3.1260876 ± 3.5E-06	5441.26999 ± 0.00058	172		
WASP-46b	1.4303700 ± 2.3E-06	5392.31628 ± 0.00020	172	5843.6050 ± 0.0021	173
WASP-48b	2.1436340 ± 3.0E-06	5364.55119 ± 0.00042	161	5811.5018 ± 0.0029	48
				5783.6319 ± 0.0054	48
WASP-49b	2.7817387 ± 5.6E-06	5580.59513 ± 0.00029	167		
WASP-50b	1.9550938 ± 1.3E-06	5558.61237 ± 0.00020	174		
WASP-52b	1.7497835 ± 1.1E-06	6673.82149 ± 0.00013	3		
WASP-54b	3.6936411 ± 5.9E-06	5518.35087 ± 0.00053	175		
WASP-55b	4.4656330 ± 4.0E-06	5737.94024 ± 0.00030	176		
WASP-56b	4.6171010 ± 3.0E-06	5730.79900 ± 0.00100	175		
WASP-57b	2.83891856 ± 8.1E-07	6058.54910 ± 0.00016	177		
WASP-58b	5.017180 ± 1.1E-05	5183.93434 ± 0.00100	178		

Table 6. continued.

Planet	Period days	Transit Midtime $BJD_{TDB} - 2,450,000$	Ephemeris Reference	Occultation Midtime $BJD_{TDB} - 2,450,000$	Occultation Reference
WASP-59b	7.919585 ± 1.0E-05	5830.95631 ± 0.00053	178		
WASP-60b	4.3050011 ± 6.2E-06	5747.0300 ± 0.0022	178		
WASP-61b	3.8559000 ± 3.0E-06	5859.52908 ± 0.00023	176		
WASP-62b	4.4119530 ± 3.0E-06	5855.39285 ± 0.00027	176		
WASP-63b	4.3780900 ± 6.0E-06	5921.65359 ± 0.00050	176		
WASP-64b	1.5732918 ± 1.5E-06	5582.60157 ± 0.00027	179		
WASP-65b	2.3114243 ± 1.5E-06	6110.68772 ± 0.00015	180		
WASP-66b	4.0860520 ± 7.0E-06	5929.09697 ± 0.00035	176		
WASP-67b	4.6144109 ± 2.7E-06	5824.374962 ± 0.00022	176	6846.46968 ± 0.00350	43
				6869.5398 ± 0.0064	43
WASP-68b	5.084298 ± 1.5E-05	6064.86356 ± 0.00061	181		
WASP-69b	3.8681382 ± 1.7E-06	5748.83422 ± 0.00018	182		
WASP-70Ab	3.7130203 ± 4.7E-06	5736.50426 ± 0.00027	182		
WASP-71b	2.9036747 ± 6.8E-06	5738.85035 ± 0.00070	183		
WASP-72b	2.2167421 ± 8.1E-06	5583.6528 ± 0.0021	179		
WASP-73b	4.08722 ± 0.00022	6128.7063 ± 0.0011	181		
WASP-74b	2.1377500 ± 1.0E-06	6506.892589 ± 0.00020	184		
WASP-75b	2.4841930 ± 3.0E-06	6016.26690 ± 0.00030	180		
WASP-77Ab	1.3600309 ± 2.0E-06	5870.45054 ± 0.00014	185		
WASP-78b	2.1751763 ± 4.7E-06	5882.35964 ± 0.00053	186		
WASP-79b	3.6623866 ± 8.5E-06	5545.2361 ± 0.0015	186		
WASP-80b	3.06785952 ± 7.7E-07	6125.417574 ± 8.6E-05	187		
WASP-83b	4.971252 ± 1.5E-05	5928.88608 ± 0.00040	184		
WASP-84b	8.5234865 ± 7.0E-06	6286.106610 ± 9.0E-05	182		
WASP-88b	4.954000 ± 1.9E-05	6474.73154 ± 0.00086	181		
WASP-89b	3.3564227 ± 2.5E-06	6207.021921 ± 0.00012	184		
WASP-94Ab	3.9501907 ± 3.7E-06	6416.40215 ± 0.00026	188		
WASP-95b	2.1846730 ± 1.4E-06	6338.45927 ± 0.00024	189		
WASP-96b	3.4252602 ± 2.7E-06	6258.06278 ± 0.00020	189		
WASP-97b	2.0727600 ± 1.0E-06	6438.18778 ± 0.00018	189		
WASP-98b	2.9626400 ± 1.3E-06	6333.39188 ± 1.0E-04	189		
WASP-99b	5.752510 ± 4.0E-05	6224.9832 ± 0.0014	189		
WASP-100b	2.8493750 ± 8.0E-06	6272.34012 ± 0.00090	189		
WASP-101b	3.5857220 ± 4.0E-06	6164.69413 ± 0.00020	189		
WASP-103b	0.9255456 ± 1.3E-06	6836.296445 ± 5.5E-05	190		
WASP-104b	1.7554137 ± 3.0E-06	6406.11210 ± 0.00012	191		
WASP-106b	9.2897150 ± 10.0E-06	6649.55057 ± 0.00033	191		
WASP-117b	10.02165 ± 0.00055	6533.82401 ± 0.00093	192		
WTS-2b	1.01870680 ± 6.5E-07	4317.81338 ± 0.00065	193		
XO-1b	3.94150685 ± 1.8E-07	3887.74774 ± 0.00022	194	4193.2170 ± 0.0039	195
				4323.2878 ± 0.0039	195
XO-2Nb	2.61585922 ± 2.8E-07	5565.546480 ± 5.4E-05	196	4421.105 ± 0.021	197
				4423.723 ± 0.018	197
XO-3b	3.19153285 ± 5.8E-07	5292.43266 ± 0.00015	198	5294.5736 ± 0.0015	198
				6248.8405 ± 0.0010	198
				6433.9484 ± 0.0010	198
XO-4b	4.1250823 ± 3.9E-06	4485.93307 ± 0.00036	33	5181.0176 ± 0.0062	33
				5172.7595 ± 0.0016	33
XO-5b	4.18775581 ± 5.8E-07	6864.31366 ± 0.00023	199		

References. (1) Sada et al. 2012; (2) Deming et al. 2011; (3) Baluev et al. 2015; (4) Triaud et al. 2009; (5) Aigrain et al. 2008; (6) Rauer et al. 2009; (7) Fridlund et al. 2010; (8) Southworth 2011; (9) Bonomo et al. 2017; (10) Bonomo et al. 2010; (11) Gandolfi et al. 2012; (12) Gillon et al. 2010a; (13) Cabrera et al. 2010; (14) Tingley et al. 2011; (15) Ollivier et al. 2012; (16) Csizmadia et al. 2011; (17) Hébrard et al. 2011; (18) Guenther et al. 2012; (19) Deleuil et al. 2012; (20) Pätzold et al. 2012; (21) Rouan et al. 2012; (22) Almenara et al. 2013; (23) Parviainen et al. 2014; (24) Cabrera et al. 2015; (25) Nikolov et al. 2014; (26) Todorov et al. 2010; (27) Lewis et al. 2013; (28) Chan et al. 2011; (29) Todorov et al. 2013; (30) Southworth et al. 2012c; (31) Noyes et al. 2008; (32) Todorov et al. 2012; (33) Morris et al. 2013; (34) Christiansen et al. 2010; (35) Mancini et al. 2013c; (36) Dittmann et al. 2012; (37) Southworth et al. 2012a; (38) Nascimbeni et al. 2011; (39) Kovács et al. 2010; (40) Ciceri et al. 2013; (41) Howard et al. 2012; (42) Hartman et al. 2011a; (43) Kammer et al. 2015; (44) Granata et al. 2014; (45) Deming et al. 2015; (46) Bakos et al. 2011; (47) Ramón-Fox & Sada 2013; (48) O'Rourke et al. 2014; (49) Wang et al. 2013; (50) Quinn et al. 2012; (51) Buchhave et al. 2011a; (52) Esposito et al., in prep.; (53) Johnson et al. 2011; (54) Kipping et al. 2011; (55) Hartman et al. 2011b; (56) Zhao et al. 2014; (57) Bakos et al. 2012; (58) Sato et al. 2012; (59) Hartman et al. 2012; (60) Boisse et al. 2013; (61) Hartman et al. 2014; (62) Bieryla et al. 2014; (63) Hartman et al. 2015; (64) Bakos et al. 2015a; (65) Juncher et al. 2015; (66) Huang et al. 2015; (67) Penev et al. 2013; (68) Mohler-Fischer et al. 2013; (69) Bayliss et al. 2013; (70) Jordán et al. 2014; (71) Zhou et al. 2014; (72) Bakos et al. 2015b; (73) Bayliss et al. 2015; (74) Brahm et al. 2015; (75) Mancini et al. 2015b; (76) Knutson et al. 2009b; (77) Stevenson et al. 2012; (78) Nutzman et al. 2011; (79) Charbonneau et al. 2008; (80) Agol et al. 2010; (81) Knutson et al. 2009c; (82) Knutson et al. 2007; (83) Knutson et al. 2008; (84) Zellem et al. 2014; (85) Hébrard et al. 2010; (86) Laughlin et al. 2009; (87) Beatty et al. 2012; (88) Pepper et al. 2013; (89) Damasso et al. 2015b; (90) Fulton et al. 2015; (91) Müller et al. 2013; (92) Demory et al. 2011; (93) Fortney et al. 2011; (94) Bonomo et al. 2015; (95) Southworth 2012; (96) Santerne et al. 2011a; (97) Faigler et al. 2013; (98) Gandolfi et al. 2013; (99) Deleuil et al. 2014; (100) Dawson et al. 2014; (101) Endl et al. 2014; (102) Gandolfi et al. 2015; (103) Hébrard et al. 2014; (104) Quinn et al. 2015; (105) Almenara et al. 2015; (106) Bentley et al. 2009; (107) Adams et al. 2011b; (108) Hoyer et al. 2011; (109) Adams et al. 2010; (110) Adams et al. 2011a; (111) Pont et al. 2008; (112) Udalski et al. 2008; (113) Covino et al. 2013; (114) Croll et al. 2015; (115) Mancini et al. 2014; (116) Charbonneau et al. 2005; (117) Cubillos et al. 2014; (118) Raetz et al. 2014; (119) O'Donovan et al. 2010; (120) Croll et al. 2010a; (121) Kundurthy et al. 2013; (122) Fressin et al. 2010; (123) Croll et al. 2010b; (124) Sozzetti et al. 2015; (125) Knutson et al. 2009a; (126) Mandushev et al. 2011; (127) Wheatley et al. 2010; (128) Maciejewski et al. 2013b; (129) Rostron et al. 2014; (130) Cáceres et al. 2011; (131) Beerer et al. 2011; (132) Chen et al. 2014a; (133) Nikolov et al. 2015; (134) Albrecht et al. 2012; (135) Queloz et al. 2010; (136) Cubillos et al. 2013; (137) Barros et al. 2013; (138) Maciejewski et al. 2013a; (139) Campo et al. 2011; (140) Croll et al. 2015; (141) Barros et al. 2012; (142) Blecic et al. 2013; (143) Wong et al. 2015; (144) Southworth et al. 2013; (145) Southworth et al. 2012b; (146) Anderson et al. 2011e; (147) Maxted et al. 2013b; (148) Nymeyer et al. 2011; (149) Mancini et al. 2013a; (150) Bean et al. 2013; (151) Gibson et al. 2010; (152) Anderson et al. 2015; (153) Anderson et al. 2011b; (154) Nikolov et al. 2013; (155) Southworth et al. 2014; (156) Smith et al. 2012b; (157) Mahtani et al. 2013; (158) Gibson et al. 2013; (159) Sing et al. 2015; (160) Smalley et al. 2011; (161) Enoch et al. 2011a; (162) Smith et al. 2012a; (163) Simpson et al. 2011b; (164) Barros et al. 2011; (165) Faedi et al. 2011; (166) Maxted et al. 2011; (167) Lendl et al. 2012; (168) Chen et al. 2014b; (169) Gillon et al. 2012; (170) Blecic et al. 2014; (171) Mancini et al. 2013b; (172) Anderson et al. 2012; (173) Chen et al. 2014c; (174) Tregloan-Reed & Southworth 2013; (175) Faedi et al. 2013; (176) Hellier et al. 2012; (177) Southworth et al. 2015b; (178) Hébrard et al. 2013b; (179) Gillon et al. 2013; (180) Gómez Maqueo Chew et al. 2013; (181) Delrez et al. 2014; (182) Anderson et al. 2014; (183) Smith et al. 2013; (184) Hellier et al. 2015; (185) Maxted et al. 2013a; (186) Smalley et al. 2012; (187) Fukui et al. 2014; (188) Neveu-VanMalle et al. 2014; (189) Hellier et al. 2014; (190) Southworth et al. 2015a; (191) Smith et al. 2014; (192) Lendl et al. 2014; (193) Birkby et al. 2014; (194) Burke et al. 2010; (195) Machalek et al. 2008; (196) Damasso et al. 2015a; (197) Machalek et al. 2009; (198) Wong et al. 2014; (199) Smith 2014.

Table 7. System parameters that were used, along with the orbital parameters in Table 8, to update the mass, density, and surface gravity of the 231 transiting giant planets in our sample (see Table 9). The vast majority of them are taken from the literature, although estimates of ages for 37 systems with stellar evolutionary tracks are provided here for the first time (Sect. 4). In a very few cases, namely CoRoT-1, WASP-63, WASP-78, and WASP-79, we adopted our values of stellar mass and stellar/planetary radii (see Sect. 4).

System	M_s [$M_\odot$]	R_s [$R_\odot$]	T_{eff} [K]	[Fe/H] [dex]	$V \sin i$ [km s^{-1}]	P_{rot} [days]	Age [Gyr]	i_p [deg]	R_p [R_{Jup}]	System Reference
CoRoT-1	1.220 ± 0.030	1.230 ± 0.020	6298 ± 66	0.060 ± 0.070	5.2 ± 1.0	-	1.60 ± 0.50	85.10 ± 0.50	1.715 ± 0.030	1, this work[1]
CoRoT-2	0.970 ± 0.060	0.902 ± 0.018	5625 ± 120	0.0 ± 0.1	11.85 ± 0.50	4.522 ± 0.024	$2.7^{+3.2}_{-2.7}$	$88.08^{+0.18}_{-0.16}$	$1.466^{+0.042}_{-0.044}$	2, 3, 4, 5
CoRoT-3	1.370 ± 0.090	1.560 ± 0.090	6740 ± 140	-0.020 ± 0.060	17.0 ± 1.0	-	2.20 ± 0.60	85.90 ± 0.80	1.010 ± 0.070	6
CoRoT-4	$1.160^{+0.030}_{-0.020}$	$1.1700^{+0.0100}_{-0.030}$	6190 ± 60	0.050 ± 0.070	6.4 ± 1.0	8.9 ± 1.1	$1.00^{+1.0}_{-0.30}$	$90.000^{+0.00}_{-0.085}$	1.190 ± 0.055	7
CoRoT-5	1.000 ± 0.020	1.186 ± 0.040	6100 ± 65	-0.250 ± 0.060	1.0 ± 1.0	-	6.9 ± 1.4	$85.83^{+0.99}_{-1.4}$	$1.388^{+0.046}_{-0.047}$	8
CoRoT-6	1.050 ± 0.050	1.025 ± 0.026	6090 ± 50	-0.200 ± 0.100	7.5 ± 1.0	6.40 ± 0.50	$2.5^{+2.1}_{-1.7}$	89.07 ± 0.30	1.166 ± 0.035	9, 10
CoRoT-8	0.880 ± 0.040	0.770 ± 0.020	5080 ± 80	0.300 ± 0.100	2.0 ± 1.0	-	$3.00^{+0.00}_{-3.0}$	88.400 ± 0.100	0.570 ± 0.020	11
CoRoT-9	0.960 ± 0.040	0.960 ± 0.060	5625 ± 80	-0.010 ± 0.060	$3.50^{+0.00}_{-3.5}$	-	6.0 ± 3.0	$89.900^{+0.066}_{-0.084}$	$1.066^{+0.075}_{-0.063}$	12
CoRoT-10	0.890 ± 0.050	0.790 ± 0.050	5075 ± 75	0.260 ± 0.070	2.00 ± 0.50	-	$3.00^{+0.00}_{-3.0}$	88.55 ± 0.20	0.970 ± 0.070	13
CoRoT-11	1.270 ± 0.050	1.370 ± 0.030	6440 ± 120	-0.030 ± 0.080	40.0 ± 5.0	-	2.0 ± 1.0	83.17 ± 0.15	1.430 ± 0.030	14
CoRoT-12	$1.078^{+0.077}_{-0.072}$	$1.116^{+0.096}_{-0.092}$	5675 ± 80	0.160 ± 0.100	1.0 ± 1.0	-	6.3 ± 3.1	$85.48^{+0.72}_{-0.77}$	1.44 ± 0.13	15
CoRoT-13	1.090 ± 0.020	1.010 ± 0.030	5945 ± 90	0.010 ± 0.070	4.0 ± 1.0	-	1.6 ± 1.5	$88.02^{+0.34}_{-0.36}$	0.885 ± 0.014	16
CoRoT-14	1.130 ± 0.090	1.210 ± 0.080	6040 ± 100	0.05 ± 0.15	9.00 ± 0.50	-	4.2 ± 3.8	79.60 ± 0.80	1.090 ± 0.070	17
CoRoT-16	$1.098^{+0.082}_{-0.078}$	$1.19^{+0.14}_{-0.13}$	5650 ± 100	0.190 ± 0.060	0.50 ± 0.50	-	6.7 ± 2.8	$85.01^{+0.94}_{-1.2}$	$1.17^{+0.14}_{-0.16}$	18
CoRoT-17	1.040 ± 0.100	1.590 ± 0.070	5740 ± 80	0.000 ± 0.100	4.50 ± 0.50	-	10.7 ± 1.0	88.3 ± 1.5	1.020 ± 0.070	19
CoRoT-18	0.95 ± 0.15	1.00 ± 0.13	5440 ± 100	-0.100 ± 0.100	8.0 ± 1.0	5.40 ± 0.40	$0.60^{+0.00}_{-0.60}$	$86.50^{+1.4}_{-0.90}$	1.31 ± 0.18	20
CoRoT-19	1.210 ± 0.050	1.650 ± 0.040	6090 ± 70	-0.020 ± 0.100	6.0 ± 1.0	-	5.0 ± 1.0	88.00 ± 0.70	1.290 ± 0.030	21
CoRoT-20	1.140 ± 0.080	1.020 ± 0.050	5880 ± 90	0.14 ± 0.12	4.5 ± 1.0	-	$0.100^{+0.80}_{-0.040}$	88.21 ± 0.53	0.840 ± 0.040	22
CoRoT-21	1.290 ± 0.090	1.95 ± 0.21	6200 ± 100	0.000 ± 0.100	11.0 ± 1.0	-	$4.10^{+0.50}_{-0.30}$	86.8 ± 2.1	1.30 ± 0.14	23
CoRoT-23	1.140 ± 0.080	1.61 ± 0.18	5900 ± 100	0.050 ± 0.100	9.0 ± 1.0	-	$7.2^{+1.5}_{-1.0}$	$85.7^{+2.6}_{-1.5}$	1.05 ± 0.13	24
CoRoT-25	$1.090^{+0.11}_{-0.050}$	$1.190^{+0.14}_{-0.030}$	6040 ± 90	-0.01 ± 0.13	4.30 ± 0.50	-	$4.5^{+1.8}_{-2.0}$	$84.50^{+0.80}_{-0.30}$	$1.080^{+0.30}_{-0.100}$	25
CoRoT-26	1.090 ± 0.060	$1.790^{+0.18}_{-0.090}$	5590 ± 100	0.01 ± 0.13	2.0 ± 1.0	-	$8.60^{+1.8}_{-0.90}$	$86.8^{+2.2}_{-1.4}$	$1.260^{+0.13}_{-0.070}$	25
CoRoT-27	1.05 ± 0.11	$1.080^{+0.18}_{-0.060}$	5900 ± 120	-0.100 ± 0.100	4.0 ± 1.0	-	4.2 ± 2.7	$86.70^{+1.2}_{-0.87}$	1.007 ± 0.044	26
CoRoT-28	1.01 ± 0.14	1.78 ± 0.11	5150 ± 100	0.150 ± 0.100	3.00 ± 0.50	-	12.0 ± 1.5	88.10 ± 0.80	0.955 ± 0.066	27
CoRoT-29	0.97 ± 0.14	0.90 ± 0.12	5260 ± 100	0.200 ± 0.100	3.50 ± 0.50	-	$4.0^{+4.0}_{-3.0}$	87.3 ± 2.7	0.90 ± 0.16	27
HAT-P-1	$1.133^{+0.075}_{-0.079}$	1.135 ± 0.048	5980 ± 120	0.130 ± 0.080	2.20 ± 0.20	-	$2.7^{+2.5}_{-2.0}$	86.11 ± 0.18	1.242 ± 0.053	28
HAT-P-2	1.360 ± 0.040	$1.640^{+0.090}_{-0.080}$	6290 ± 60	0.140 ± 0.080	20.80 ± 0.30	-	2.60 ± 0.50	$86.72^{+1.1}_{-0.87}$	$1.157^{+0.073}_{-0.063}$	29
HAT-P-3	$0.928^{+0.044}_{-0.054}$	$0.833^{+0.034}_{-0.044}$	5185 ± 80	0.270 ± 0.080	0.50 ± 0.50	-	$1.5^{+5.4}_{-1.4}$	87.24 ± 0.69	$0.899^{+0.043}_{-0.049}$	28
HAT-P-4	$1.248^{+0.070}_{-0.11}$	$1.596^{+0.060}_{-0.075}$	5860 ± 80	0.240 ± 0.080	5.50 ± 0.50	-	$4.6^{+2.2}_{-1.0}$	$89.910^{+0.090}_{-2.2}$	$1.274^{+0.049}_{-0.060}$	28
HAT-P-5	$1.157^{+0.043}_{-0.081}$	$1.165^{+0.046}_{-0.052}$	5960 ± 100	0.24 ± 0.15	2.6 ± 1.5	-	$2.6^{+2.1}_{-1.4}$	86.75 ± 0.44	$1.254^{+0.051}_{-0.056}$	28
HAT-P-6	1.290 ± 0.060	1.460 ± 0.060	6570 ± 80	-0.130 ± 0.080	8.7 ± 1.0	-	$2.30^{+0.50}_{-0.70}$	85.51 ± 0.35	1.330 ± 0.061	30
HAT-P-7	$1.510^{+0.040}_{-0.050}$	$2.00^{+0.01}_{-0.02}$	6350 ± 80	0.260 ± 0.080	3.80 ± 0.50	-	$2.07^{+0.28}_{-0.23}$	$83.151^{+0.030}_{-0.033}$	1.510 ± 0.020	31, 32, 33
HAT-P-8	1.280 ± 0.040	$1.580^{+0.080}_{-0.060}$	6200 ± 80	0.010 ± 0.080	11.50 ± 0.50	-	3.4 ± 1.0	$87.50^{+1.9}_{-0.90}$	1.500 ± 0.070	34
HAT-P-9	1.28 ± 0.13	1.320 ± 0.070	6350 ± 150	0.12 ± 0.20	11.9 ± 1.0	-	$1.6^{+1.8}_{-1.4}$	86.50 ± 0.20	1.400 ± 0.060	35
HAT-P-12	0.730 ± 0.018	$0.701^{+0.017}_{-0.012}$	4650 ± 60	-0.290 ± 0.050	0.50 ± 0.40	-	2.5 ± 2.0	89.00 ± 0.40	$0.959^{+0.029}_{-0.021}$	36
HAT-P-13	$1.220^{+0.050}_{-0.100}$	1.560 ± 0.080	5653 ± 90	0.410 ± 0.080	2.9 ± 1.0	-	$5.00^{+2.5}_{-0.70}$	83.40 ± 0.60	1.281 ± 0.079	37
HAT-P-14	1.386 ± 0.045	1.468 ± 0.054	6600 ± 90	0.110 ± 0.080	8.40 ± 0.50	-	1.30 ± 0.40	83.50 ± 0.30	1.150 ± 0.052	38
HAT-P-15	1.013 ± 0.043	1.080 ± 0.039	5568 ± 90	0.220 ± 0.080	2.00 ± 0.50	-	$6.5^{+2.8}_{-1.6}$	89.10 ± 0.20	1.072 ± 0.043	39
HAT-P-16	1.218 ± 0.039	1.237 ± 0.054	6158 ± 80	0.170 ± 0.080	3.50 ± 0.50	-	2.00 ± 0.80	86.60 ± 0.70	1.289 ± 0.066	40
HAT-P-17	0.857 ± 0.039	0.837 ± 0.021	5246 ± 80	0.000 ± 0.080	0.30 ± 0.50	-	7.8 ± 3.3	$89.20^{+0.20}_{-0.10}$	1.010 ± 0.029	41
HAT-P-18	0.770 ± 0.031	0.749 ± 0.037	4803 ± 80	0.100 ± 0.080	0.50 ± 0.50	-	$12.4^{+1.4}_{-6.4}$	88.80 ± 0.30	0.995 ± 0.052	42
HAT-P-19	0.842 ± 0.042	0.820 ± 0.048	4990 ± 130	0.230 ± 0.080	0.70 ± 0.50	35.5 ± 2.5	8.8 ± 5.2	88.20 ± 0.40	1.132 ± 0.072	42, 43
HAT-P-20	0.756 ± 0.028	0.694 ± 0.021	4595 ± 80	0.350 ± 0.080	2.10 ± 0.50	-	$6.7^{+5.7}_{-3.8}$	86.80 ± 0.20	0.867 ± 0.033	44

Table 7. continued.

System	M_s [$M_\odot$]	R_s [$R_\odot$]	T_{eff} [K]	[Fe/H] dex	$V \sin i$ [km s^{-1}]	P_{rot} [days]	Age [Gyr]	i_p [deg]	R_p [R_{Jup}]	System Reference
HAT-P-21	0.947 ± 0.042	1.105 ± 0.083	5588 ± 80	0.010 ± 0.080	3.50 ± 0.50	15.90 ± 0.80	10.2 ± 2.5	87.20 ± 0.70	1.024 ± 0.092	44, 45
HAT-P-22	0.916 ± 0.035	1.040 ± 0.044	5302 ± 80	0.240 ± 0.080	0.50 ± 0.50	-	$12.4^{+1.6}_{-2.6}$	$86.90^{+0.60}_{-0.50}$	1.080 ± 0.058	44
HAT-P-23	1.130 ± 0.035	1.203 ± 0.074	5905 ± 80	0.150 ± 0.040	8.10 ± 0.50	-	4.0 ± 1.0	85.1 ± 1.5	1.368 ± 0.090	44
HAT-P-24	1.191 ± 0.042	1.317 ± 0.068	6373 ± 80	−0.160 ± 0.080	10.00 ± 0.50	-	2.80 ± 0.60	88.60 ± 0.70	1.242 ± 0.067	46
HAT-P-25	1.010 ± 0.032	$0.959^{+0.054}_{-0.037}$	5500 ± 80	0.310 ± 0.080	0.50 ± 0.50	-	3.2 ± 2.3	87.60 ± 0.50	$1.190^{+0.081}_{-0.056}$	47
HAT-P-27	0.920 ± 0.060	0.870 ± 0.040	5190^{+160}_{-170}	0.14 ± 0.11	$0.60^{+0.70}_{-0.40}$	-	$6.4^{+5.9}_{-3.1}$	85.00 ± 0.20	$1.020^{+0.070}_{-0.060}$	48
HAT-P-28	1.025 ± 0.047	$1.103^{+0.091}_{-0.069}$	5680 ± 90	0.120 ± 0.080	$0.20^{+0.50}_{-0.20}$	-	$6.1^{+2.6}_{-1.9}$	88.00 ± 0.90	$1.212^{+0.11}_{-0.082}$	49
HAT-P-29	1.207 ± 0.046	$1.224^{+0.13}_{-0.075}$	6087 ± 88	0.210 ± 0.080	3.90 ± 0.50	-	2.2 ± 1.1	$87.10^{+0.50}_{-0.70}$	$1.107^{+0.14}_{-0.082}$	49
HAT-P-30	1.242 ± 0.041	1.215 ± 0.051	6304 ± 88	0.130 ± 0.080	2.20 ± 0.50	-	$1.00^{+0.80}_{-0.50}$	83.600 ± 0.040	1.340 ± 0.065	50
HAT-P-31	$1.218^{+0.089}_{-0.063}$	$1.36^{+0.27}_{-0.18}$	6070 ± 100	0.150 ± 0.080	0.50 ± 0.60	-	$3.17^{+0.70}_{-1.1}$	$87.1^{+1.8}_{-2.7}$	$1.07^{+0.24}_{-0.16}$	51
HAT-P-32	1.160 ± 0.041	1.219 ± 0.016	6207 ± 88	−0.040 ± 0.080	20.70 ± 0.50	-	2.70 ± 0.80	88.90 ± 0.40	1.789 ± 0.025	52
HAT-P-33	1.375 ± 0.040	1.637 ± 0.034	6446 ± 88	0.050 ± 0.080	13.70 ± 0.50	-	2.30 ± 0.30	$87.200^{+0.00}_{-0.100}$	1.686 ± 0.045	52
HAT-P-34	1.392 ± 0.047	$1.53^{+0.14}_{-0.10}$	6442 ± 88	0.220 ± 0.040	24.00 ± 0.50	-	$1.70^{+0.40}_{-0.50}$	87.1 ± 1.2	$1.197^{+0.13}_{-0.092}$	53
HAT-P-35	1.236 ± 0.048	1.435 ± 0.084	6096 ± 88	0.110 ± 0.080	0.50 ± 0.50	-	$3.50^{+0.80}_{-0.50}$	87.3 ± 1.0	1.332 ± 0.098	53
HAT-P-36	1.022 ± 0.049	1.096 ± 0.056	5560 ± 100	0.260 ± 0.100	3.58 ± 0.50	-	$6.6^{+2.9}_{-1.8}$	86.0 ± 1.3	1.264 ± 0.071	53
HAT-P-37	0.929 ± 0.043	$0.877^{+0.059}_{-0.044}$	5500 ± 100	0.030 ± 0.100	3.07 ± 0.50	-	$3.6^{+4.1}_{-2.2}$	$86.90^{+0.40}_{-0.50}$	1.178 ± 0.077	53
HAT-P-38	0.886 ± 0.044	$0.923^{+0.096}_{-0.067}$	5330 ± 100	0.060 ± 0.100	0.40 ± 0.50	-	$10.1^{+3.9}_{-4.8}$	88.30 ± 0.70	$0.825^{+0.092}_{-0.063}$	54
HAT-P-39	1.404 ± 0.051	$1.625^{+0.081}_{-0.062}$	6430 ± 100	0.190 ± 0.100	12.70 ± 0.50	-	2.00 ± 0.40	87.0 ± 1.0	$1.571^{+0.11}_{-0.081}$	55
HAT-P-40	$1.512^{+0.045}_{-0.110}$	2.206 ± 0.061	6080 ± 100	0.220 ± 0.100	6.90 ± 0.50	-	$2.70^{+0.90}_{-0.30}$	88.30 ± 0.90	1.730 ± 0.062	55
HAT-P-41	1.418 ± 0.047	$1.683^{+0.058}_{-0.036}$	6390 ± 100	0.210 ± 0.100	19.60 ± 0.50	-	2.20 ± 0.40	87.7 ± 1.0	$1.685^{+0.076}_{-0.051}$	55
HAT-P-42	1.178 ± 0.068	1.53 ± 0.14	5743 ± 50	0.270 ± 0.080	3.50 ± 0.50	-	$5.20^{+1.8}_{-0.70}$	$85.90^{+1.3}_{-0.80}$	1.28 ± 0.15	56
HAT-P-43	$1.048^{+0.031}_{-0.042}$	$1.103^{+0.041}_{-0.021}$	5645 ± 74	0.230 ± 0.080	2.40 ± 0.50	-	$5.7^{+1.9}_{-1.1}$	88.70 ± 0.70	$1.281^{+0.062}_{-0.033}$	56
HAT-P-45	1.259 ± 0.058	$1.319^{+0.16}_{-0.072}$	6330 ± 100	0.070 ± 0.100	9.30 ± 0.50	-	2.00 ± 0.80	87.80 ± 0.90	$1.426^{+0.18}_{-0.087}$	57
HAT-P-49	1.543 ± 0.051	$1.833^{+0.14}_{-0.076}$	6820 ± 52	0.074 ± 0.080	16.00 ± 0.50	-	1.50 ± 0.20	86.2 ± 1.7	$1.413^{+0.13}_{-0.077}$	58
HAT-P-50	$1.273^{+0.049}_{-0.120}$	1.698 ± 0.071	6280 ± 49	−0.180 ± 0.080	8.90 ± 0.50	-	$3.37^{+1.4}_{-0.27}$	83.65 ± 0.57	1.288 ± 0.064	59
HAT-P-51	0.976 ± 0.028	$1.041^{+0.038}_{-0.029}$	5449 ± 50	0.270 ± 0.080	1.70 ± 0.50	-	8.2 ± 1.7	88.48 ± 0.57	1.293 ± 0.054	59
HAT-P-52	0.887 ± 0.027	0.893 ± 0.047	5131 ± 50	0.280 ± 0.080	0.60 ± 0.50	-	9.4 ± 4.1	87.02 ± 0.86	1.009 ± 0.072	59
HAT-P-53	1.093 ± 0.043	$1.209^{+0.081}_{-0.062}$	5956 ± 50	0.000 ± 0.080	4.10 ± 0.50	-	$4.67^{+1.4}_{-0.83}$	86.2 ± 1.5	1.318 ± 0.091	59
HAT-P-54	0.645 ± 0.020	0.617 ± 0.013	4390 ± 50	−0.127 ± 0.080	2.35 ± 0.50	-	$3.9^{+4.3}_{-2.1}$	87.040 ± 0.084	0.944 ± 0.028	60
HAT-P-55	1.013 ± 0.037	1.011 ± 0.036	5808 ± 50	−0.030 ± 0.080	1.80 ± 0.50	-	4.2 ± 1.7	87.70 ± 0.56	1.182 ± 0.055	61
HAT-P-56	1.296 ± 0.036	1.428 ± 0.030	6566 ± 50	−0.077 ± 0.080	40.06 ± 0.50	-	2.01 ± 0.35	82.13 ± 0.18	1.466 ± 0.040	62
HATS-1	0.986 ± 0.054	$1.038^{+0.13}_{-0.075}$	5870 ± 100	−0.06 ± 0.12	2.52 ± 0.50	-	6.0 ± 2.8	$85.60^{+0.60}_{-1.40}$	$1.302^{+0.160}_{-0.098}$	63
HATS-2	0.882 ± 0.037	0.898 ± 0.019	5227 ± 95	0.150 ± 0.050	1.50 ± 0.50	24.98 ± 0.04	9.7 ± 2.9	87.20 ± 0.70	1.168 ± 0.030	64
HATS-3	1.210 ± 0.040	1.400 ± 0.030	6351 ± 76	−0.157 ± 0.070	9.1 ± 1.3	-	$3.20^{+0.60}_{-0.40}$	86.20 ± 0.30	1.381 ± 0.035	65
HATS-4	1.000 ± 0.020	0.930 ± 0.020	5403 ± 50	0.430 ± 0.080	0.70 ± 0.50	-	2.1 ± 1.6	88.50 ± 0.60	1.020 ± 0.037	66
HATS-5	0.940 ± 0.030	0.870 ± 0.020	5304 ± 50	0.190 ± 0.080	0.80 ± 0.50	-	$3.6^{+2.6}_{-1.9}$	89.30 ± 0.30	0.912 ± 0.025	67
HATS-7	0.849 ± 0.027	$0.815^{+0.049}_{-0.035}$	4985 ± 50	0.250 ± 0.080	0.50 ± 0.50	-	7.8 ± 5.0	87.92 ± 0.75	$0.563^{+0.046}_{-0.034}$	68
HATS-8	1.056 ± 0.037	$1.086^{+0.150}_{-0.059}$	5679 ± 50	0.210 ± 0.080	2.00 ± 0.50	-	5.1 ± 1.7	$87.8^{+1.2}_{-1.8}$	$0.873^{+0.120}_{-0.075}$	69
HATS-9	1.030 ± 0.039	$1.503^{+0.100}_{-0.043}$	5366 ± 70	0.340 ± 0.050	4.58 ± 0.90	-	10.8 ± 1.5	$86.5^{+1.6}_{-2.5}$	1.065 ± 0.098	70
HATS-10	1.101 ± 0.054	$1.105^{+0.055}_{-0.040}$	5880 ± 120	0.150 ± 0.100	5.68 ± 0.70	-	3.3 ± 1.7	87.79 ± 0.72	$0.969^{+0.061}_{-0.045}$	70
HATS-13	0.962 ± 0.029	0.887 ± 0.019	5523 ± 69	0.050 ± 0.060	2.82 ± 0.30	-	2.5 ± 1.7	88.55 ± 0.43	1.212 ± 0.035	71
HATS-14	0.967 ± 0.024	$0.933^{+0.023}_{-0.015}$	5346 ± 60	0.330 ± 0.060	3.8 ± 1.2	-	4.9 ± 1.7	88.83 ± 0.66	$1.039^{+0.032}_{-0.022}$	71
HD149026	1.340 ± 0.020	$1.534^{+0.049}_{-0.047}$	6160 ± 50	0.360 ± 0.080	6.00 ± 0.50	-	2.60 ± 0.20	$84.50^{+0.60}_{-0.52}$	$0.811^{+0.029}_{-0.027}$	72
HD17156	1.275 ± 0.018	1.5007 ± 0.0076	6079 ± 80	0.240 ± 0.030	2.80 ± 0.50	-	$3.37^{+0.20}_{-0.47}$	$86.49^{+0.24}_{-0.20}$	1.0870 ± 0.0066	73
HD189733	0.806 ± 0.048	0.756 ± 0.018	5040 ± 50	−0.030 ± 0.080	3.5 ± 1.0	11.9500 ± 0.0100	$6.8^{+5.2}_{-4.4}$	85.580 ± 0.060	1.138 ± 0.027	28, 74
HD209458	1.119 ± 0.033	$1.155^{+0.014}_{-0.016}$	6065 ± 50	0.000 ± 0.050	4.49 ± 0.50	10.65 ± 0.75	$3.10^{+0.80}_{-0.70}$	86.710 ± 0.050	$1.359^{+0.016}_{-0.019}$	28, 75
HD80606	1.018 ± 0.035	1.037 ± 0.032	5574 ± 72	0.340 ± 0.050	1.80 ± 0.50	-	$5.9^{+1.6}_{-2.0}$	89.232 ± 0.029	1.003 ± 0.023	10
KELT-2A	$1.308^{+0.028}_{-0.025}$	$1.828^{+0.070}_{-0.034}$	6148 ± 48	0.034 ± 0.077	9.0 ± 2.0	-	3.97 ± 0.01	$88.6^{+1.0}_{-1.3}$	$1.290^{+0.064}_{-0.050}$	76
KELT-3	$1.278^{+0.063}_{-0.061}$	$1.472^{+0.065}_{-0.062}$	6308 ± 50	0.040 ± 0.080	10.20 ± 0.50	-	3.00 ± 0.20	$84.23^{+0.65}_{-0.58}$	1.345 ± 0.072	77

Table 7. continued.

System	M_s [$M_\odot$]	R_s [$R_\odot$]	T_{eff} [K]	[Fe/H] dex	$V \sin i$ [km s^{-1}]	P_{rot} [days]	Age [Gyr]	i_p [deg]	R_p [R_{Jup}]	System Reference
KELT-6	1.126 ± 0.058	1.53 ± 0.14	6272 ± 61	-0.270 ± 0.060	4.53 ± 0.26	-	$4.90^{+0.70}_{-0.50}$	$88.81^{+0.79}_{-0.91}$	1.18 ± 0.11	78
KELT-8	$1.211^{+0.078}_{-0.066}$	$1.67^{+0.14}_{-0.12}$	5754^{+54}_{-55}	0.272 ± 0.038	3.7 ± 1.5	-	$5.40^{+0.40}_{-0.50}$	$82.65^{+0.81}_{-1.00}$	$1.86^{+0.18}_{-0.16}$	79
Kepler-5	$1.374^{+0.040}_{-0.059}$	$1.793^{+0.043}_{-0.062}$	6297 ± 60	0.040 ± 0.060	4.8 ± 1.0	-	3.00 ± 0.60	86.30 ± 0.50	1.431 ± 0.047	80
Kepler-6	$1.114^{+0.150}_{-0.062}$	$1.261^{+0.057}_{-0.024}$	5647 ± 44	0.340 ± 0.040	3.0 ± 1.0	-	$5.70^{+0.80}_{-2.30}$	$89.90^{+0.10}_{-0.70}$	$1.169^{+0.052}_{-0.022}$	81, 10
Kepler-7	1.413 ± 0.081	2.028 ± 0.025	5933 ± 50	0.110 ± 0.050	4.20 ± 0.50	-	2.90 ± 0.30	85.32 ± 0.16	1.649 ± 0.030	82, 83
Kepler-8	$1.213^{+0.067}_{-0.063}$	$1.486^{+0.053}_{-0.062}$	6210 ± 150	-0.055 ± 0.030	10.50 ± 0.70	-	3.8 ± 1.5	84.07 ± 0.33	$1.419^{+0.056}_{-0.058}$	84
Kepler-12	$1.166^{+0.051}_{-0.054}$	$1.483^{+0.025}_{-0.029}$	5950 ± 100	0.070 ± 0.040	0.80 ± 0.50	-	$4.00^{+0.30}_{-0.40}$	88.760 ± 0.080	$1.695^{+0.028}_{-0.032}$	85
Kepler-15	$1.018^{+0.044}_{-0.032}$	$0.992^{+0.058}_{-0.070}$	5520^{+120}_{-130}	0.360 ± 0.070	2.0 ± 2.0	-	$3.7^{+1.5}_{-3.6}$	$87.44^{+0.18}_{-0.20}$	$0.960^{+0.060}_{-0.070}$	86
Kepler-17	1.160 ± 0.060	1.050 ± 0.030	5781 ± 85	0.260 ± 0.100	6.0 ± 2.0	12.10 ± 0.16	$1.80^{+0.00}_{-1.8}$	87.22 ± 0.15	1.330 ± 0.040	87, 88, 89
Kepler-39	$1.290^{+0.060}_{-0.070}$	1.400 ± 0.100	6350 ± 100	0.10 ± 0.14	16.0 ± 2.5	4.500 ± 0.070	$2.10^{+0.80}_{-0.90}$	89.07 ± 0.22	$1.240^{+0.090}_{-0.100}$	90
Kepler-40	1.46 ± 0.18	2.48 ± 0.17	6510 ± 100	$0.10^{+0.15}_{-0.10}$	9.0 ± 2.0	-	$0.8^{+3.6}_{-1.5}$	85.47 ± 0.94	1.44 ± 0.11	91, 82
Kepler-41	1.150 ± 0.040	1.290 ± 0.020	5750 ± 100	0.38 ± 0.11	4.5 ± 1.5	-	$4.4^{+1.3}_{-1.1}$	82.510 ± 0.090	1.290 ± 0.020	90
Kepler-43	1.270 ± 0.040	$1.380^{+0.050}_{-0.030}$	6050 ± 100	0.400 ± 0.100	5.5 ± 1.5	12.95 ± 0.25	$2.30^{+0.80}_{-0.70}$	$84.57^{+0.18}_{-0.37}$	$1.160^{+0.040}_{-0.030}$	90
Kepler-44	1.120 ± 0.080	1.350 ± 0.080	5800 ± 100	0.150 ± 0.100	4.0 ± 2.0	-	$5.8^{+2.4}_{-1.5}$	$84.96^{+0.50}_{-0.62}$	1.090 ± 0.070	90
Kepler-45	0.590 ± 0.060	0.55 ± 0.11	3820 ± 90	0.28 ± 0.14	–	15.80 ± 0.20	$0.80^{+0.70}_{-0.50}$	87.00 ± 0.70	0.96 ± 0.11	92
Kepler-74	1.180 ± 0.040	1.120 ± 0.040	6000 ± 100	0.42 ± 0.11	5.0 ± 1.0	-	$0.80^{+0.90}_{-0.50}$	87.460 ± 0.070	0.960 ± 0.020	90
Kepler-75	0.910 ± 0.040	0.890 ± 0.020	5200 ± 100	0.30 ± 0.12	3.5 ± 1.5	19.18 ± 0.25	$6.2^{+3.5}_{-2.8}$	$89.12^{+0.51}_{-0.64}$	1.050 ± 0.030	90
Kepler-76	1.20 ± 0.20	1.320 ± 0.080	6409 ± 95	-0.10 ± 0.20	6.5 ± 2.0	-	$3.6^{+3.7}_{-1.3}$	78.00 ± 0.20	1.250 ± 0.080	93, this work[2]
Kepler-77	0.950 ± 0.040	0.990 ± 0.020	5520 ± 60	0.200 ± 0.050	1.5 ± 1.0	-	7.5 ± 2.0	88.00 ± 0.11	0.960 ± 0.016	94
Kepler-412	1.167 ± 0.091	1.287 ± 0.035	5750 ± 90	0.27 ± 0.12	5.0 ± 1.0	-	5.1 ± 1.7	80.89 ± 0.20	1.325 ± 0.043	95
Kepler-419	$1.390^{+0.080}_{-0.070}$	$1.750^{+0.080}_{-0.070}$	6430 ± 79	0.176 ± 0.070	14.4 ± 1.3	4.492 ± 0.012	2.8 ± 1.3	$88.95^{+0.14}_{-0.17}$	0.96 ± 0.12	96, 97
Kepler-422	1.150 ± 0.060	1.24 ± 0.12	5972 ± 84	0.230 ± 0.090	2.2 ± 1.3	-	$3.40^{+0.90}_{-1.10}$	88.33 ± 0.35	1.15 ± 0.11	98, this work[2]
Kepler-423	0.850 ± 0.040	0.950 ± 0.040	5560 ± 80	-0.100 ± 0.050	2.50 ± 0.50	22.05 ± 0.12	11.0 ± 2.0	87.83 ± 0.13	1.192 ± 0.052	99, 100
Kepler-424	1.010 ± 0.054	0.940 ± 0.056	5460 ± 81	0.44 ± 0.14	0.5 ± 1.0	-	$4.9^{+3.3}_{-2.4}$	84.68 ± 0.79	$0.890^{+0.080}_{-0.060}$	98, this work[2]
Kepler-425	0.930 ± 0.050	0.860 ± 0.020	5170 ± 70	0.24 ± 0.11	3.0 ± 1.0	-	5.0 ± 4.0	87.020 ± 0.080	0.978 ± 0.022	101
Kepler-426	0.910 ± 0.060	0.920 ± 0.020	5725 ± 90	-0.210 ± 0.080	3.0 ± 1.0	-	6.0 ± 4.0	85.740 ± 0.060	1.090 ± 0.030	101
Kepler-427	0.960 ± 0.060	1.35 ± 0.20	5800 ± 70	-0.190 ± 0.070	3.0 ± 1.0	-	7.0 ± 4.0	89.50 ± 0.45	1.23 ± 0.21	101
Kepler-428	0.870 ± 0.050	0.800 ± 0.020	5150 ± 100	0.09 ± 0.17	2.0 ± 2.0	-	5.0 ± 4.0	89.36 ± 0.43	1.080 ± 0.030	101
Kepler-432	$1.350^{+0.100}_{-0.070}$	$4.12^{+0.12}_{-0.08}$	4995 ± 78	-0.070 ± 0.100	2.70 ± 0.50	77 ± 14	$4.20^{+0.80}_{-1.00}$	$88.17^{+0.61}_{-0.33}$	$1.145^{+0.036}_{-0.039}$	102
Kepler-433	1.46 ± 0.17	2.26 ± 0.25	6340 ± 140	0.06 ± 0.19	11.0 ± 1.0	-	2.67 ± 0.91	$89.21^{+0.52}_{-0.90}$	1.45 ± 0.16	103
Kepler-434	1.198 ± 0.093	1.38 ± 0.13	5970 ± 100	0.35 ± 0.15	3.0 ± 1.0	-	4.0 ± 1.7	$86.46^{+0.38}_{-0.74}$	$1.13^{+0.26}_{-0.18}$	103
Kepler-435	1.538 ± 0.088	3.21 ± 0.30	6090 ± 110	-0.170 ± 0.100	6.0 ± 1.0	-	2.25 ± 0.42	85.51 ± 0.52	1.99 ± 0.18	103
OGLE-TR-10	$1.140^{+0.100}_{-0.120}$	$1.17^{+0.13}_{-0.11}$	5950 ± 130	0.15 ± 0.15	3.0 ± 2.0	-	$3.2^{+4.0}_{-3.1}$	$90.0^{+0.0}_{-3.9}$	$1.25^{+0.14}_{-0.12}$	28
OGLE-TR-56	$1.228^{+0.072}_{-0.078}$	$1.363^{+0.089}_{-0.086}$	6050 ± 100	0.220 ± 0.100	3.2 ± 1.0	-	$3.0^{+1.0}_{-1.3}$	$77.60^{+0.91}_{-1.00}$	$1.363^{+0.092}_{-0.090}$	28
OGLE-TR-111	$0.852^{+0.058}_{-0.052}$	$0.831^{+0.045}_{-0.040}$	5040 ± 80	0.190 ± 0.070	1.0 ± 1.0	-	$8.8^{+5.2}_{-6.6}$	$88.25^{+0.83}_{-0.30}$	$1.051^{+0.057}_{-0.053}$	28
OGLE-TR-113	$0.779^{+0.017}_{-0.015}$	$0.774^{+0.020}_{-0.011}$	4790 ± 75	0.090 ± 0.080	9.0 ± 3.0	-	$13.20^{+0.80}_{-2.40}$	$87.80^{+1.60}_{-0.60}$	$1.093^{+0.028}_{-0.022}$	28
OGLE-TR-132	$1.305^{+0.075}_{-0.067}$	$1.32^{+0.17}_{-0.12}$	6210 ± 75	0.370 ± 0.100	–	-	$1.2^{+1.5}_{-1.1}$	$83.4^{+2.9}_{-1.3}$	$1.20^{+0.15}_{-0.11}$	28
OGLE-TR-182	1.187 ± 0.039	1.53 ± 0.17	5924 ± 64	0.370 ± 0.080	–	-	$4.30^{+0.50}_{-1.9}$	84.3 ± 1.2	1.47 ± 0.14	104
OGLE-TR-211	$1.312^{+0.059}_{-0.056}$	$1.560^{+0.180}_{-0.100}$	6325 ± 91	0.110 ± 0.100	–	-	$2.60^{+0.60}_{-0.70}$	88.0 ± 2.0	$1.262^{+0.160}_{-0.091}$	104
Qatar-1	0.850 ± 0.030	0.800 ± 0.050	4910 ± 100	0.200 ± 0.100	1.70 ± 0.30	23.700 ± 0.100	$11.60^{+0.60}_{-4.70}$	83.82 ± 0.25	1.180 ± 0.090	105, 106, this work[2]
Qatar-2	0.743 ± 0.020	0.776 ± 0.007	4645 ± 50	0.020 ± 0.080	2.80 ± 0.50	-	7.0 ± 7.0	86.120 ± 0.080	1.254 ± 0.012	107, this work[2]
TrES-1	$0.878^{+0.038}_{-0.040}$	$0.807^{+0.017}_{-0.016}$	5230 ± 50	0.020 ± 0.050	1.30 ± 0.30	-	$3.7^{+3.4}_{-2.8}$	$90.0^{+0.0}_{-1.1}$	$1.067^{+0.022}_{-0.021}$	28
TrES-2	$0.983^{+0.059}_{-0.063}$	1.003 ± 0.033	5850 ± 50	-0.150 ± 0.100	2.0 ± 1.5	-	$5.0^{+2.7}_{-2.1}$	83.57 ± 0.14	1.224 ± 0.041	28
TrES-3	$0.928^{+0.028}_{-0.048}$	$0.829^{+0.015}_{-0.022}$	5650 ± 75	-0.190 ± 0.080	1.5 ± 1.0	-	$0.9^{+2.8}_{-0.8}$	81.85 ± 0.16	$1.336^{+0.031}_{-0.037}$	108
TrES-4	1.450 ± 0.050	1.810 ± 0.080	6295 ± 65	0.280 ± 0.090	8.50 ± 0.50	-	2.20 ± 0.40	$83.07^{+0.51}_{-0.44}$	$1.838^{+0.081}_{-0.090}$	109
TrES-5	0.893 ± 0.024	0.866 ± 0.013	5171 ± 36	0.200 ± 0.080	3.80 ± 0.36	-	7.4 ± 1.9	84.529 ± 0.005	1.209 ± 0.021	110
WASP-1	$1.301^{+0.049}_{-0.047}$	$1.517^{+0.052}_{-0.045}$	6110 ± 75	0.260 ± 0.080	5.77 ± 0.35	-	3.00 ± 0.60	$90.0^{+0.0}_{-2.9}$	$1.514^{+0.052}_{-0.047}$	28
WASP-2	0.89 ± 0.12	$0.840^{+0.062}_{-0.065}$	5200 ± 200	0.10 ± 0.20	0.90 ± 0.50	-	7.0 ± 7.0	$84.81^{+0.35}_{-0.27}$	$1.071^{+0.080}_{-0.083}$	28
WASP-3	1.260 ± 0.100	1.366 ± 0.044	6400 ± 100	0.00 ± 0.20	13.4 ± 1.5	-	2.1 ± 1.2	83.72 ± 0.39	1.416 ± 0.047	10

Table 7. continued.

System	M_s [$M_\odot$]	R_s [$R_\odot$]	T_{eff} [K]	[Fe/H] dex	$V \sin i$ [km s^{-1}]	P_{rot} [days]	Age [Gyr]	i_p [deg]	R_p [R_{Jup}]	System Reference
WASP-4	0.89 ± 0.01	0.920 ± 0.060	5436 ± 34	-0.050 ± 0.040	$2.2^{+0.6}_{-1.0}$	22.2 ± 3.3	7.0 ± 2.9	86.8 ± 1.8	1.33 ± 0.16	111, 112
WASP-5	1.033 ± 0.045	1.088 ± 0.040	5770 ± 65	0.090 ± 0.090	3.40 ± 0.70	16.20 ± 0.40	5.6 ± 2.2	85.8 ± 1.1	1.175 ± 0.056	82, 45
WASP-6	$0.880^{+0.050}_{-0.080}$	$0.870^{+0.025}_{-0.036}$	5450 ± 100	-0.200 ± 0.090	1.4 ± 1.0	23.80 ± 0.15	$11.0^{+3.0}_{-7.0}$	$88.47^{+0.65}_{-0.47}$	$1.224^{+0.051}_{-0.052}$	113, 114
WASP-7	1.285 ± 0.063	1.466 ± 0.094	6400 ± 100	0.000 ± 0.100	17.0 ± 2.0	-	$2.50^{+0.80}_{-0.90}$	87.03 ± 0.93	1.363 ± 0.093	10
WASP-8	$1.030^{+0.054}_{-0.061}$	$0.945^{+0.051}_{-0.036}$	5600 ± 80	0.170 ± 0.070	1.590 ± 0.085	-	4.0 ± 1.0	$88.55^{+0.15}_{-0.17}$	$1.038^{+0.007}_{-0.047}$	115
WASP-10	0.752 ± 0.081	0.703 ± 0.036	4680 ± 100	0.03 ± 0.20	3.0 ± 3.0	11.910 ± 0.050	$7.0^{+6.0}_{-3.0}$	88.81 ± 0.40	1.067 ± 0.064	116, 104
WASP-11	0.806 ± 0.038	0.772 ± 0.014	4900 ± 65	0.120 ± 0.090	1.04 ± 0.15	-	$7.6^{+5.8}_{-3.0}$	89.03 ± 0.34	0.990 ± 0.022	117
WASP-12	1.38 ± 0.18	1.619 ± 0.076	6250 ± 100	0.32 ± 0.12	2.2 ± 1.5	-	$2.00^{+0.70}_{-2.00}$	83.3 ± 1.1	1.825 ± 0.091	82
WASP-13	1.22 ± 0.12	1.657 ± 0.079	5830 ± 100	0.00 ± 0.20	$4.9^{+0.0}_{-4.9}$	-	$5.0^{+2.6}_{-1.7}$	84.88 ± 0.45	1.528 ± 0.084	82
WASP-14	$1.21^{+0.13}_{-0.12}$	$1.306^{+0.066}_{-0.073}$	6480 ± 100	0.00 ± 0.20	4.9 ± 1.0	-	0.75 ± 0.25	$84.32^{+0.67}_{-0.57}$	$1.281^{+0.075}_{-0.082}$	118
WASP-15	1.18 ± 0.12	1.477 ± 0.072	6300 ± 100	-0.17 ± 0.11	4.0 ± 2.0	-	$3.9^{+2.8}_{-1.3}$	85.50 ± 0.50	1.428 ± 0.077	119
WASP-16	$1.022^{+0.074}_{-0.130}$	$0.946^{+0.057}_{-0.052}$	5700 ± 150	0.010 ± 0.100	3.0 ± 1.0	-	$2.3^{+5.8}_{-2.2}$	$85.22^{+0.27}_{-0.43}$	$1.008^{+0.083}_{-0.060}$	120
WASP-17	1.306 ± 0.026	1.572 ± 0.056	6650 ± 80	-0.190 ± 0.090	$10.05^{+0.88}_{-0.79}$	-	2.65 ± 0.25	$86.83^{+0.68}_{-0.53}$	1.991 ± 0.081	121
WASP-18	1.25 ± 0.13	$1.216^{+0.067}_{-0.054}$	6400 ± 100	0.000 ± 0.090	11.0 ± 1.5	-	1.00 ± 0.50	86.0 ± 2.5	$1.106^{+0.072}_{-0.054}$	122
WASP-19	$0.960^{+0.090}_{-0.100}$	0.940 ± 0.040	5500 ± 100	0.020 ± 0.090	4.0 ± 2.0	10.50 ± 0.20	$5.5^{+8.5}_{-4.5}$	80.50 ± 0.70	1.310 ± 0.060	123
WASP-20	1.200 ± 0.041	1.392 ± 0.044	5940 ± 100	-0.008 ± 0.060	4.75 ± 0.51	-	$7.0^{+2.0}_{-1.0}$	85.56 ± 0.22	1.462 ± 0.059	124
WASP-21	1.010 ± 0.030	1.060 ± 0.040	5800 ± 100	-0.46 ± 0.11	1.50 ± 0.60	-	$12.0^{+2.0}_{-5.0}$	$88.75^{+0.84}_{-0.70}$	1.070 ± 0.060	125
WASP-22	1.109 ± 0.026	$1.219^{+0.052}_{-0.033}$	6000 ± 100	0.050 ± 0.080	4.50 ± 0.40	-	$4.3^{+1.6}_{-1.1}$	88.26 ± 0.91	$1.158^{+0.061}_{-0.038}$	126, this work[2]
WASP-23	$0.78^{+0.13}_{-0.12}$	$0.765^{+0.033}_{-0.049}$	5150 ± 100	-0.05 ± 0.13	2.20 ± 0.30	-	$6.2^{+5.6}_{-2.5}$	$88.39^{+0.79}_{-0.45}$	$0.962^{+0.047}_{-0.056}$	127, this work[2]
WASP-24	$1.150^{+0.050}_{-0.040}$	1.331 ± 0.032	6080 ± 100	0.070 ± 0.100	7.00 ± 0.90	-	$3.8^{+1.3}_{-1.2}$	83.64 ± 0.29	$1.300^{+0.039}_{-0.038}$	128
WASP-25	1.00 ± 0.03	0.920 ± 0.040	5750 ± 100	-0.050 ± 0.100	3.0 ± 1.0	-	$0.02^{+4.00}_{-0.01}$	88.00 ± 0.50	$1.220^{+0.060}_{-0.050}$	129
WASP-26	1.120 ± 0.030	1.340 ± 0.060	5950 ± 100	-0.020 ± 0.090	2.4 ± 1.3	-	6.0 ± 2.0	82.50 ± 0.50	1.320 ± 0.080	130
WASP-28	1.021 ± 0.050	1.094 ± 0.031	6150 ± 140	-0.290 ± 0.100	3.25 ± 0.34	-	$5.0^{+3.0}_{-2.0}$	88.61 ± 0.67	1.213 ± 0.042	124
WASP-29	0.825 ± 0.033	0.808 ± 0.044	4800 ± 150	0.11 ± 0.14	1.50 ± 0.60	-	$14.0^{+0.0}_{-7.0}$	88.80 ± 0.70	$0.792^{+0.056}_{-0.035}$	131
WASP-31	1.165 ± 0.026	1.252 ± 0.033	6300 ± 100	-0.200 ± 0.090	7.90 ± 0.60	-	$1.00^{+3.0}_{-0.50}$	84.41 ± 0.22	1.549 ± 0.050	132
WASP-32	1.070 ± 0.050	1.090 ± 0.030	6140^{+90}_{-100}	-0.130 ± 0.100	$3.90^{+0.40}_{-0.50}$	11.6 ± 1.0	$2.22^{+0.62}_{-0.73}$	85.10 ± 0.20	1.100 ± 0.040	48, 133
WASP-34	1.010 ± 0.070	0.93 ± 0.12	5700 ± 100	-0.020 ± 0.100	1.40 ± 0.60	-	$7.8^{+2.7}_{-3.6}$	85.20 ± 0.20	$1.22^{+0.11}_{-0.08}$	134, this work[2]
WASP-35	1.070 ± 0.030	1.090 ± 0.020	5990 ± 90	-0.150 ± 0.090	3.90 ± 0.40	-	5.0 ± 1.2	$87.96^{+0.31}_{-0.25}$	1.320 ± 0.050	135
WASP-36	1.040 ± 0.031	0.951 ± 0.018	5900 ± 150	-0.260 ± 0.100	3.3 ± 1.2	-	$2.5^{+3.5}_{-2.2}$	83.61 ± 0.21	1.281 ± 0.029	136
WASP-37	0.93 ± 0.12	1.003 ± 0.053	5800 ± 150	-0.40 ± 0.12	2.4 ± 1.6	-	$11.0^{+3.0}_{-4.0}$	$88.82^{+0.77}_{-0.86}$	$1.160^{+0.070}_{-0.060}$	137
WASP-38	1.230 ± 0.040	1.350 ± 0.020	6180^{+40}_{-60}	-0.020 ± 0.070	$7.50^{+0.10}_{-0.20}$	-	$3.29^{+0.42}_{-0.53}$	$89.50^{+0.40}_{-0.30}$	1.090 ± 0.020	48
WASP-39	0.930 ± 0.030	0.895 ± 0.023	5400 ± 150	-0.120 ± 0.100	1.40 ± 0.60	-	$9.0^{+3.0}_{-4.0}$	$87.83^{+0.25}_{-0.22}$	1.270 ± 0.040	138
WASP-41	0.930 ± 0.030	0.900 ± 0.050	5450 ± 150	-0.080 ± 0.090	1.6 ± 1.1	18.410 ± 0.050	$9.8^{+2.3}_{-3.9}$	87.700 ± 0.080	1.200 ± 0.060	139, this work[2]
WASP-42	$0.881^{+0.086}_{-0.081}$	0.850 ± 0.035	5200 ± 150	0.05 ± 0.13	2.70 ± 0.40	-	$11.3^{+1.5}_{-4.8}$	$88.30^{+0.26}_{-0.23}$	1.063 ± 0.051	140, this work[2]
WASP-43	0.717 ± 0.025	$0.667^{+0.010}_{-0.011}$	4400 ± 200	-0.05 ± 0.17	–	15.60 ± 0.40	7.0 ± 7.0	82.33 ± 0.20	1.036 ± 0.019	141, 142
WASP-44	0.951 ± 0.034	$0.927^{+0.068}_{-0.057}$	5400 ± 150	0.060 ± 0.100	3.20 ± 0.90	-	$10.3^{+2.7}_{-5.0}$	$86.02^{+1.10}_{-0.86}$	1.14 ± 0.11	143, this work[2]
WASP-45	0.909 ± 0.060	$0.945^{+0.087}_{-0.071}$	5100 ± 200	0.36 ± 0.12	2.30 ± 0.70	-	$12.7^{+1.0}_{-5.3}$	$84.47^{+0.54}_{-0.79}$	$1.16^{+0.28}_{-0.14}$	143, this work[2]
WASP-46	0.828 ± 0.067	0.858 ± 0.024	5600 ± 150	-0.37 ± 0.13	1.9 ± 1.2	16.0 ± 1.0	$9.6^{+3.4}_{-4.2}$	82.80 ± 0.17	1.174 ± 0.033	143, 144
WASP-48	1.190 ± 0.050	1.750 ± 0.090	6000 ± 150	-0.12 ± 0.12	12.20 ± 0.70	-	$7.9^{+2.0}_{-1.6}$	$80.09^{+0.88}_{-0.79}$	1.670 ± 0.100	135
WASP-49	$0.938^{+0.080}_{-0.076}$	0.976 ± 0.034	5600 ± 150	-0.230 ± 0.070	0.90 ± 0.30	-	$11.9^{+0.8}_{-3.2}$	84.89 ± 0.19	1.115 ± 0.047	140
WASP-50	$0.892^{+0.080}_{-0.074}$	0.843 ± 0.031	5400 ± 100	-0.120 ± 0.080	2.60 ± 0.50	16.30 ± 0.50	7.0 ± 3.5	84.74 ± 0.24	1.153 ± 0.048	145
WASP-52	0.870 ± 0.030	0.790 ± 0.020	5000 ± 100	0.03 ± 0.12	3.60 ± 0.90	-	$10.7^{+1.9}_{-4.5}$	85.35 ± 0.20	1.270 ± 0.030	146, this work[2]
WASP-54	1.213 ± 0.032	$1.828^{+0.091}_{-0.081}$	6100 ± 100	-0.270 ± 0.080	4.00 ± 0.80	-	$6.9^{+1.0}_{-1.9}$	84.97 ± 0.61	$1.653^{+0.090}_{-0.083}$	147
WASP-55	1.010 ± 0.040	$1.060^{+0.030}_{-0.020}$	5900 ± 100	-0.200 ± 0.080	3.1 ± 1.0	-	$7.0^{+2.0}_{-1.9}$	89.20 ± 0.60	$1.300^{+0.050}_{-0.030}$	148, this work[2]
WASP-56	1.107 ± 0.024	$1.112^{+0.026}_{-0.022}$	5600 ± 100	0.120 ± 0.060	1.50 ± 0.90	-	$6.2^{+3.0}_{-2.1}$	$88.50^{+0.10}_{-0.20}$	$1.092^{+0.035}_{-0.033}$	147
WASP-57	0.886 ± 0.061	0.927 ± 0.031	5600 ± 100	-0.250 ± 0.100	3.7 ± 1.3	-	7.0 ± 7.0	86.05 ± 0.20	1.050 ± 0.052	147, 149
WASP-58	0.940 ± 0.100	1.17 ± 0.13	5800 ± 150	-0.450 ± 0.090	2.80 ± 0.90	-	$12.80^{+0.20}_{-2.10}$	87.4 ± 1.5	1.37 ± 0.20	146, this work[2]
WASP-59	0.719 ± 0.035	0.613 ± 0.044	4650 ± 150	-0.15 ± 0.11	2.3 ± 1.5	-	7.0 ± 7.0	89.27 ± 0.52	0.775 ± 0.068	146, this work[2]
WASP-60	1.078 ± 0.035	1.14 ± 0.13	5900 ± 100	-0.040 ± 0.090	3.40 ± 0.80	-	$6.3^{+1.7}_{-2.1}$	87.9 ± 1.6	0.86 ± 0.12	146, this work[2]

Table 7. continued.

System	M_s [$M_\odot$]	R_s [$R_\odot$]	T_{eff} [K]	[Fe/H] dex	$V \sin i$ [km s^{-1}]	P_{rot} [days]	Age [Gyr]	i_p [deg]	R_p [R_{Jup}]	System Reference
WASP-61	1.220 ± 0.070	1.360 ± 0.030	6250 ± 150	−0.10 ± 0.12	10.30 ± 0.50	-	$3.8^{+1.8}_{-0.9}$	$89.35^{+0.45}_{-0.66}$	1.240 ± 0.030	148, this work[2]
WASP-62	1.250 ± 0.050	1.280 ± 0.050	6230 ± 80	0.040 ± 0.060	8.70 ± 0.40	-	$2.60^{+0.50}_{-0.70}$	$88.30^{+0.90}_{-0.60}$	1.390 ± 0.060	148, this work[2]
WASP-63	$1.10^{+0.04}_{-0.06}$	$1.76^{+0.11}_{-0.08}$	5550 ± 100	0.080 ± 0.070	2.80 ± 0.50	-	$8.3^{+1.3}_{-1.2}$	87.8 ± 1.3	1.33 ± 0.24	148, this work[1]
WASP-64	1.004 ± 0.028	1.058 ± 0.025	5550 ± 150	−0.08 ± 0.11	3.40 ± 0.80	-	7.0 ± 3.5	$86.57^{+0.80}_{-0.60}$	1.271 ± 0.039	150
WASP-65	0.93 ± 0.14	1.010 ± 0.050	5600 ± 100	−0.070 ± 0.070	3.60 ± 0.50	-	$8.8^{+3.2}_{-2.9}$	$88.80^{+0.80}_{-0.70}$	1.112 ± 0.059	151
WASP-66	1.300 ± 0.070	1.750 ± 0.090	6600 ± 150	−0.310 ± 0.100	13.40 ± 0.90	-	$3.70^{+0.70}_{-1.2}$	85.90 ± 0.90	1.390 ± 0.090	148, this work[2]
WASP-67	0.870 ± 0.040	0.870 ± 0.040	5200 ± 100	−0.070 ± 0.090	2.10 ± 0.40	-	$12.6^{+1.0}_{-4.2}$	85.80 ± 0.35	$1.40^{+0.30}_{-0.20}$	148, this work[2]
WASP-68	1.240 ± 0.030	$1.69^{+0.11}_{-0.06}$	5910 ± 60	0.220 ± 0.080	2.30 ± 0.80	-	5.7 ± 1.3	88.1 ± 1.3	$1.24^{+0.10}_{-0.06}$	152
WASP-69	0.826 ± 0.029	0.813 ± 0.028	4700 ± 50	0.150 ± 0.080	2.20 ± 0.40	23.07 ± 0.16	7.0 ± 7.0	86.71 ± 0.20	1.057 ± 0.047	153, this work[2]
WASP-70A	1.106 ± 0.042	$1.215^{+0.064}_{-0.089}$	5700 ± 80	−0.010 ± 0.060	1.80 ± 0.40	-	9.50 ± 0.50	$87.12^{+1.20}_{-0.65}$	$1.164^{+0.073}_{-0.100}$	153
WASP-71	1.559 ± 0.070	2.26 ± 0.17	6050 ± 100	0.140 ± 0.080	9.40 ± 0.50	-	3.0 ± 1.0	84.9 ± 2.2	1.46 ± 0.13	154
WASP-72	1.386 ± 0.055	1.98 ± 0.24	6250 ± 100	−0.060 ± 0.090	6.00 ± 0.70	-	3.20 ± 0.60	$81.6^{+3.2}_{-2.6}$	1.27 ± 0.20	150
WASP-73	1.340 ± 0.050	$2.07^{+0.19}_{-0.08}$	6030 ± 120	0.14 ± 0.14	6.10 ± 0.60	-	4.3 ± 1.5	$87.4^{+1.8}_{-2.4}$	$1.16^{+0.12}_{-0.08}$	152
WASP-74	1.48 ± 0.12	1.640 ± 0.050	5990 ± 110	0.39 ± 0.13	4.10 ± 0.80	-	3.70 ± 0.90	79.81 ± 0.24	1.560 ± 0.060	155
WASP-75	1.140 ± 0.070	1.260 ± 0.040	6100 ± 100	0.070 ± 0.090	4.30 ± 0.80	-	$3.12^{+0.78}_{-0.95}$	$82.00^{+0.30}_{-0.20}$	1.270 ± 0.048	151
WASP-77A	1.002 ± 0.045	0.955 ± 0.015	5500 ± 80	0.00 ± 0.11	4.00 ± 0.20	15.40 ± 0.40	$5.8^{+2.9}_{-1.8}$	$89.40^{+0.40}_{-0.70}$	1.210 ± 0.020	156
WASP-78	$1.180^{+0.070}_{-0.090}$	$2.09^{+0.15}_{-0.12}$	6100 ± 150	−0.35 ± 0.14	7.20 ± 0.80	-	$4.^{+1.1}_{-0.9}$	$83.2^{+2.3}_{-1.6}$	1.590 ± 0.100	157, this work[1]
WASP-79	$1.420^{+0.110}_{-0.080}$	$1.69^{+0.35}_{-0.18}$	6600 ± 100	0.030 ± 0.100	19.10 ± 0.70	-	$1.92^{+0.35}_{-0.29}$	84.3 ± 1.6	$1.82^{+0.37}_{-0.23}$	157, this work[1]
WASP-80	0.570 ± 0.050	0.571 ± 0.016	4150 ± 100	−0.14 ± 0.16	3.55 ± 0.33	-	7.0 ± 7.0	$89.92^{+0.07}_{-0.12}$	$0.952^{+0.026}_{-0.027}$	158
WASP-83	1.110 ± 0.090	$1.050^{+0.060}_{-0.040}$	5480 ± 110	0.29 ± 0.12	$0.50^{+0.00}_{-0.50}$	-	7.1 ± 2.9	88.90 ± 0.70	$1.040^{+0.080}_{-0.050}$	155
WASP-84	$0.842^{+0.037}_{-0.036}$	0.748 ± 0.015	5300 ± 100	0.000 ± 0.100	4.10 ± 0.30	14.36 ± 0.35	$8.5^{+4.1}_{-5.5}$	88.368 ± 0.050	0.942 ± 0.022	153, this work[2]
WASP-88	1.450 ± 0.050	$2.08^{+0.12}_{-0.06}$	6430 ± 130	−0.08 ± 0.12	8.40 ± 0.80	-	3.0 ± 1.3	$88.0^{+1.4}_{-1.5}$	$1.70^{+0.13}_{-0.07}$	152
WASP-89	0.920 ± 0.080	0.880 ± 0.030	5000 ± 100	0.15 ± 0.14	2.50 ± 0.90	20.20 ± 0.40	$12.5^{1.5}_{-3.1}$	89.40 ± 0.50	1.040 ± 0.040	155
WASP-94A	1.450 ± 0.090	1.620 ± 0.050	6153 ± 75	0.26 ± 0.15	4.20 ± 0.50	-	2.70 ± 0.60	88.70 ± 0.70	$1.720^{+0.060}_{-0.050}$	159, this work[2]
WASP-95	1.110 ± 0.090	$1.130^{+0.080}_{-0.040}$	5830 ± 140	0.14 ± 0.16	3.10 ± 0.60	-	$5.0^{+2.8}_{-1.8}$	$88.4^{+1.2}_{-2.1}$	1.210 ± 0.060	160, this work[2]
WASP-96	1.060 ± 0.090	1.050 ± 0.050	5500 ± 150	0.14 ± 0.19	1.5 ± 1.3	-	$9.4^{+3.3}_{-2.9}$	85.60 ± 0.20	1.200 ± 0.060	160, this work[2]
WASP-97	1.120 ± 0.060	1.060 ± 0.040	5670 ± 110	0.23 ± 0.11	1.10 ± 0.50	-	$4.8^{+2.1}_{-1.6}$	$88.0^{+1.3}_{-1.0}$	1.130 ± 0.060	160, this work[2]
WASP-98	0.690 ± 0.060	0.700 ± 0.020	5550 ± 140	−0.60 ± 0.19	$0.50^{+0.00}_{-0.50}$	-	$10.5^{+2.0}_{-4.7}$	86.300 ± 0.100	1.100 ± 0.040	160, this work[2]
WASP-99	1.480 ± 0.100	1.76 ± 0.11	6150 ± 100	0.21 ± 0.15	6.80 ± 0.50	-	$3.00^{+0.60}_{-0.50}$	88.8 ± 1.1	$1.100^{+0.080}_{-0.050}$	160, this work[2]
WASP-100	1.570 ± 0.100	2.00 ± 0.30	6900 ± 120	−0.030 ± 0.100	12.80 ± 0.80	-	$1.57^{+0.30}_{-0.20}$	$82.6^{+2.6}_{-1.7}$	1.69 ± 0.29	160, this work[2]
WASP-101	1.340 ± 0.070	1.290 ± 0.040	6380 ± 120	0.20 ± 0.12	12.40 ± 0.50	-	$1.14^{+0.70}_{-0.65}$	85.00 ± 0.20	1.410 ± 0.050	160, this work[2]
WASP-103	$1.220^{+0.039}_{-0.036}$	$1.436^{+0.052}_{-0.031}$	6110 ± 160	0.06 ± 0.13	10.60 ± 0.90	-	4.0 ± 1.0	86.3 ± 2.7	$1.528^{+0.073}_{-0.047}$	161
WASP-104	1.076 ± 0.049	0.963 ± 0.027	5450 ± 130	0.320 ± 0.090	0.40 ± 0.70	-	3.0 ± 2.0	83.63 ± 0.25	1.137 ± 0.037	162
WASP-106	1.192 ± 0.054	$1.393^{+0.048}_{-0.028}$	6000 ± 150	−0.090 ± 0.090	6.30 ± 0.70	-	7.0 ± 2.0	$89.49^{+0.35}_{-0.64}$	$1.085^{+0.046}_{-0.028}$	162
WASP-117	1.126 ± 0.029	$1.170^{+0.067}_{-0.059}$	6040 ± 90	−0.11 ± 0.14	$1.67^{+0.31}_{-0.24}$	-	4.6 ± 2.0	89.14 ± 0.30	$1.021^{+0.076}_{-0.065}$	163
WTS-2	0.820 ± 0.080	0.750 ± 0.030	5000 ± 250	$0.20^{+0.30}_{-0.20}$	2.2 ± 1.0	-	$7.0^{+6.5}_{-6.4}$	83.55 ± 0.53	1.363 ± 0.061	164
XO-1	$1.027^{+0.057}_{-0.061}$	$0.934^{+0.037}_{-0.032}$	5750 ± 75	0.020 ± 0.080	1.110 ± 0.067	-	$1.0^{+3.1}_{-0.9}$	$88.81^{+0.70}_{-0.30}$	$1.206^{+0.047}_{-0.042}$	28
XO-2N	0.960 ± 0.050	0.998 ± 0.033	5332 ± 57	0.430 ± 0.050	1.070 ± 0.090	28.6 ± 1.3	$7.8^{+1.2}_{-1.3}$	$87.96^{+0.42}_{-0.34}$	1.019 ± 0.031	165, 166
XO-3	1.213 ± 0.066	1.377 ± 0.083	6430 ± 100	−0.177 ± 0.080	18.54 ± 0.17	-	$2.82^{+0.58}_{-0.82}$	84.20 ± 0.54	1.217 ± 0.073	167
XO-4	1.320 ± 0.020	1.560 ± 0.050	6400 ± 70	−0.040 ± 0.030	8.80 ± 0.50	-	2.10 ± 0.60	88.7 ± 1.1	1.340 ± 0.050	168
XO-5	0.880 ± 0.030	1.080 ± 0.040	5370 ± 70	0.050 ± 0.060	0.70 ± 0.50	-	7.0 ± 7.0	86.70 ± 0.40	1.109 ± 0.050	169

[1]The new system parameters M_s, R_s, R_p, and age were derived by using the Y2 evolutionary tracks and the published values of stellar atmospheric parameters, stellar density from the transit fitting, and R_p/R_s (as reported in the corresponding reference).
[2]The system age was estimated by using the Y2 evolutionary tracks and the published values of stellar atmospheric parameters and stellar density from the transit fitting (as reported in the corresponding reference).

References. (1) Barge et al. 2008 and Torres et al. 2012; (2) Bouchy et al. 2008; (3) Alonso et al. 2008; (4) Gillon et al. 2010b; (5) Lanza et al. 2009; (6) Deleuil et al. 2008; (7) Moutou et al. 2008; (8) Rauer et al. 2009; (9) Fridlund et al. 2010; (10) Southworth 2011;(11) Bordé et al. 2010; (12) Bonomo et al. 2017; (13) Bonomo et al. 2010; (14) Gandolfi et al. 2010; (15) Gillon et al. 2010a; (16) Cabrera et al. 2010; (17) Tingley et al. 2011; (18) Ollivier et al. 2012; (19) Csizmadia et al. 2011; (20) Hébrard et al. 2011; (21) Guenther et al. 2012; (22) Deleuil et al. 2012; (23) Pätzold et al. 2012; (24) Rouan et al. 2012; (25) Almenara et al. 2013; (26) Parviainen et al. 2014; (27) Cabrera et al. 2015; (28) Torres et al. 2008; (29) Pál et al. 2010; (30) Pál et al. 2008; (31) Noyes et al. 2008; (32) Van Eylen et al. 2013; (33) Lund et al. 2014; (34) Latham et al. 2009; (35) Shporer et al. 2009; (36) Hartman et al. 2009; (37) Bakos et al. 2009; (38) Torres et al. 2010b; (39) Kovács et al. 2010; (40) Buchhave et al. 2010; (41) Howard et al. 2012; (42) Hartman et al. 2011a; (43) Mallonn et al. 2015; (44) Bakos et al. 2011; (45) Maxted et al. 2015; (46) Kipping et al. 2010; (47) Quinn et al. 2012; (48) Brown et al. 2012b; (49) Buchhave et al. 2011a; (50) Johnson et al. 2011; (51) Kipping et al. 2011; (52) Hartman et al. 2011b; (53) Bakos et al. 2012; (54) Sato et al. 2012; (55) Hartman et al. 2012; (56) Boisse et al. 2013; (57) Hartman et al. 2014; (58) Bieryla et al. 2014; (59) Hartman et al. 2015; (60) Bakos et al. 2015a; (61) Juncher et al. 2015; (62) Huang et al. 2015; (63) Penev et al. 2013; (64) Mohler-Fischer et al. 2013; (65) Bayliss et al. 2013; (66) Jordán et al. 2014; (67) Zhou et al. 2014; (68) Bakos et al. 2015b; (69) Bayliss et al. 2015; (70) Brahm et al. 2015; (71) Mancini et al. 2015b; (72) Carter et al. 2009; (73) Nutzman et al. 2011; (74) Henry & Winn 2008; (75) Silva-Valio 2008; (76) Beatty et al. 2012; (77) Pepper et al. 2013; (78) Damasso et al. 2015b; (79) Fulton et al. 2015; (80) Koch et al. 2010; (81) Dunham et al. 2010; (82) Southworth 2012; (83) Latham et al. 2010; (84) Jenkins et al. 2010; (85) Fortney et al. 2011; (86) Endl et al. 2011; (87) Désert et al. 2011; (88) Bonomo et al. 2012; (89) Bonomo & Lanza 2012; (90) Bonomo et al. 2015; (91) Santerne et al. 2011b; (92) Johnson et al. 2012; (93) Faigler et al. 2013; (94) Gandolfi et al. 2013; (95) Deleuil et al. 2014; (96) Dawson et al. 2012; (97) Dawson et al. 2014; (98) Endl et al. 2014; (99) McQuillan et al. 2013; (100) Gandolfi et al. 2015; (101) Hébrard et al. 2014; (102) Quinn et al. 2015; (103) Almenara et al. 2015; (104) Southworth 2010; (105) Covino et al. 2013; (106) Mislis et al. 2015; (107) Mancini et al. 2014; (108) Sozzetti et al. 2009; (109) Sozzetti et al. 2015; (110) Mandushev et al. 2011; (111) Sanchis-Ojeda et al. 2011; (112) Petrucci et al. 2013; (113) Smith et al. 2009; (114) Gillon et al. 2009; (115) Queloz et al. 2010; (116) Mancini et al. 2015a; (117) Tregloan-Reed et al. 2015; (118) Joshi et al. 2009; (119) West et al. 2009a; (120) Lister et al. 2009; (121) Anderson et al. 2011e; (122) Hellier et al. 2009a; (123) Hebb et al. 2010; (124) Anderson et al. 2015; (125) Bouchy et al. 2010; (126) Anderson et al. 2011b; (127) Triaud et al. 2011; (128) Street et al. 2010; (129) Enoch et al. 2011b; (130) Smalley et al. 2010; (131) Hellier et al. 2010; (132) Anderson et al. 2011c; (133) Brothwell et al. 2014; (134) Smalley et al. 2011; (135) Enoch et al. 2011a; (136) Smith et al. 2012a; (137) Simpson et al. 2011b; (138) Faedi et al. 2011; (139) Maxted et al. 2011; (140) Lendl et al. 2012; (141) Hellier et al. 2011a; (142) Gillon et al. 2012; (143) Anderson et al. 2012; (144) Ciceri et al. 2016; (145) Gillon et al. 2011; (146) Hébrard et al. 2013b; (147) Faedi et al. 2013; (148) Hellier et al. 2012; (149) Southworth et al. 2015b; (150) Gillon et al. 2013; (151) Gómez Maqueo Chew et al. 2013; (152) Delrez et al. 2014; (153) Anderson et al. 2014; (154) Smith et al. 2013; (155) Hellier et al. 2015; (156) Maxted et al. 2013a; (157) Smalley et al. 2012; (158) Triaud et al. 2013; (159) Neveu-VanMalle et al. 2014; (160) Hellier et al. 2014; (161) Gillon et al. 2014; (162) Smith et al. 2014; (163) Lendl et al. 2014; (164) Birkby et al. 2014; (165) Damasso et al. 2015a; (166) Zellem et al. 2015; (167) Winn et al. 2008; (168) McCullough et al. 2008; (169) Pál et al. 2009;

Table 8. Derived eccentricities, RV semi-amplitudes, and trends for all the transiting giant planets considered in this study. Both the 1σ and 2σ upper limits are given for eccentricities consistent with zero. The flag letters "C", "E", and "U" stand for circular, eccentric, and unconstrained orbits (the last concern either eccentricities compatible with zero but with uncertainties $\sigma_e > 0.05$ or slightly eccentric orbits without strong enough evidence from Bayesian model comparison; see text for more details). "CURV" or "PLC" in place of the acceleration term indicates the presence of curvature regardless of its origin (distant companion, stellar activity, possible instrumental drift) or the signal of a long-period planetary companion in the RVs.

Planet	Flag	e	ω [deg]	$e\cos\omega$	$e\sin\omega$	K [m s^{-1}]	$\dot{\gamma}$ [m s^{-1} day^{-1}]	Jitter [m s^{-1}]
CoRoT-1b	C	< 0.036 (< 0.16)	-	$-0.0001^{+0.0016}_{-0.0017}$	$-0.0041^{+0.0083}_{-0.084}$	190 ± 15	$1.03^{+0.12}_{-0.11}$	< 9.1
CoRoT-2b	C	< 0.024 (< 0.069)	-	-0.00304 ± 0.00055	$0.008^{+0.034}_{-0.011}$	568^{+23}_{-22}	-	$40^{+14}_{-10.}$
CoRoT-3b	C	< 0.016 (< 0.034)	-	$-0.0057^{+0.0050}_{-0.0052}$	$0.0033^{+0.016}_{-0.0084}$	2173 ± 25	-	< 26.0
CoRoT-4b	U	< 0.14 (< 0.31)	-	$0.025^{+0.038}_{-0.032}$	$-0.064^{+0.069}_{-0.13}$	$62.4^{+6.2}_{-6.7}$	-	< 10.5
CoRoT-5b	U	< 0.087 (< 0.19)	-	$-0.024^{+0.024}_{-0.031}$	$-0.006^{+0.058}_{-0.084}$	$61.1^{+4.5}_{-4.4}$	-	< 2.7
CoRoT-6b	U	< 0.18 (< 0.37)	-	$-0.053^{+0.039}_{-0.038}$	$0.11^{+0.14}_{-0.10}$	285^{+26}_{-23}	-	< 15.8
CoRoT-8b	U	< 0.19 (< 0.47)	-	$-0.044^{+0.060}_{-0.084}$	$0.054^{+0.21}_{-0.089}$	$27.6^{+5.8}_{-4.7}$	-	< 2.9
CoRoT-9b	E	$0.134^{+0.040}_{-0.034}$	41^{+30}_{-23}	0.104 ± 0.031	0.066 ± 0.060	39.0 ± 2.4	-	< 3.4
CoRoT-10b	E	0.524 ± 0.018	$217.6^{+2.9}_{-3.2}$	-0.4144 ± 0.0067	$-0.320^{+0.034}_{-0.032}$	$297.5^{+9.8}_{-9.4}$	-	< 10.7
CoRoT-11b	U	< 0.36 (< 0.53)	-	$-0.02^{+0.11}_{-0.12}$	$0.25^{+0.16}_{-0.22}$	334^{+71}_{-66}	-	< 23.3
CoRoT-12b	C	< 0.050 (< 0.13)	-	$-0.008^{+0.015}_{-0.023}$	$0.005^{+0.054}_{-0.028}$	$125.1^{+7.6}_{-7.5}$	-	< 6.9
CoRoT-13b	U	< 0.067 (< 0.15)	-	$0.020^{+0.024}_{-0.020}$	$-0.017^{+0.033}_{-0.067}$	$160.7^{+8.6}_{-8.4}$	-	< 4.7
CoRoT-14b	C	< 0.036 (< 0.076)	-	$0.003^{+0.022}_{-0.016}$	$0.003^{+0.030}_{-0.019}$	1193^{+40}_{-42}	-	< 24.3
CoRoT-16b	E	$0.37^{+0.11}_{-0.12}$	161^{+33}_{-29}	$-0.30^{+0.12}_{-0.11}$	0.10 ± 0.18	$62.6^{+11}_{-9.9}$	-	< 7.0
CoRoT-17b	U	< 0.081 (< 0.19)	-	$-0.010^{+0.028}_{-0.040}$	$-0.003^{+0.054}_{-0.070}$	308^{+29}_{-27}	-	< 26.3
CoRoT-18b	C	< 0.025 (< 0.061)	-	$0.0028^{+0.012}_{-0.0083}$	$0.001^{+0.024}_{-0.015}$	588 ± 16	-	< 35.0
CoRoT-19b	U	< 0.056 (< 0.14)	-	$0.005^{+0.024}_{-0.017}$	$-0.010^{+0.029}_{-0.063}$	$131.5^{+7.5}_{-7.3}$	-	< 6.7
CoRoT-20b	E	$0.575^{+0.016}_{-0.014}$	$55.8^{+4.0}_{-3.9}$	$0.323^{+0.028}_{-0.031}$	$0.476^{+0.031}_{-0.030}$	459^{+16}_{-15}	-	< 9.2
CoRoT-21b	U	< 0.39 (< 0.53)	-	$-0.091^{+0.089}_{-0.045}$	$-0.29^{+0.22}_{-0.14}$	296^{+62}_{-66}	-	< 77.3
CoRoT-23b	U	$0.126^{+0.072}_{-0.060}$	56^{+77}_{-29}	$0.077^{+0.046}_{-0.047}$	$0.078^{+0.088}_{-0.077}$	378 ± 35	-	< 13.0
CoRoT-25b	U	< 0.22 (< 0.54)	-	$0.005^{+0.068}_{-0.070}$	$-0.09^{+0.10}_{-0.24}$	$33.5^{+7.4}_{-6.6}$	-	< 14.0
CoRoT-26b	U	< 0.41 (< 0.88)	-	$-0.019^{+0.31}_{-0.100}$	$0.15^{+0.38}_{-0.20}$	66^{+44}_{-13}	-	< 8.9
CoRoT-27b	C	< 0.034 (< 0.075)	-	$-0.010^{+0.011}_{-0.015}$	$-0.001^{+0.024}_{-0.030}$	1324^{+48}_{-51}	-	< 14.6
CoRoT-28b	U	< 0.071 (< 0.15)	-	$-0.002^{+0.026}_{-0.032}$	$0.020^{+0.071}_{-0.034}$	$56.3^{+4.0}_{-3.8}$	-	< 5.3
CoRoT-29b	U	< 0.12 (< 0.25)	-	$0.029^{+0.049}_{-0.037}$	$0.048^{+0.11}_{-0.060}$	125^{+14}_{-15}	-	< 6.3
HAT-P-1b	C	< 0.011 (< 0.044)	-	$-0.00066^{+0.00069}_{-0.00078}$	$-0.0018^{+0.0036}_{-0.021}$	59.5 ± 1.2	-	$4.5^{+1.6}_{-1.3}$
HAT-P-2b	E	$0.50833^{+0.00082}_{-0.00075}$	$186.96^{+0.87}_{-0.88}$	$-0.50456^{+0.00040}_{-0.00039}$	-0.0616 ± 0.0078	$938.1^{+10.}_{-9.9}$	CURV	$34.9^{+11}_{-9.3}$
HAT-P-3b	C	< 0.010 (< 0.022)	-	0.0048 ± 0.0012	$-0.0012^{+0.0079}_{-0.0094}$	90.3 ± 1.3	-	$4.0^{+1.7}_{-1.2}$
HAT-P-4b	C	< 0.0073 (< 0.032)	-	$-0.00052^{+0.00087}_{-0.0011}$	$-0.0000^{+0.0073}_{-0.0071}$	$78.6^{+2.4}_{-2.3}$	$0.0223^{+0.0034}_{-0.0033}$	$9.7^{+1.9}_{-1.4}$
HAT-P-5b	U	< 0.072 (< 0.18)	-	$0.015^{+0.050}_{-0.030}$	$-0.004^{+0.036}_{-0.059}$	135^{+13}_{-12}	-	< 18.9
HAT-P-6b	C	< 0.044 (< 0.065)	-	-0.00161 ± 0.00067	$0.035^{+0.018}_{-0.022}$	$120.7^{+2.3}_{-2.2}$	-	$6.9^{+1.9}_{-1.6}$
HAT-P-7b	C	< 0.0040 (< 0.012)	-	$-0.0003^{+0.0011}_{-0.0016}$	$-0.0003^{+0.0024}_{-0.0046}$	$211.9^{+1.6}_{-1.5}$	$0.0714^{+0.0035}_{-0.0037}$	$13.6^{+1.7}_{-1.4}$

Table 8. continued.

Planet	Flag	e	ω [deg]	$e\cos\omega$	$e\sin\omega$	K [m s^{-1}]	$\dot{\gamma}$ [m s^{-1} day^{-1}]	Jitter [m s^{-1}]
HAT-P-8b	C	< 0.0060 (< 0.022)	-	$-0.00005^{+0.00083}_{-0.00090}$	$0.0010^{+0.011}_{-0.0023}$	$160.4^{+2.4}_{-2.5}$	-	$7.8^{+2.3}_{-1.9}$
HAT-P-9b	U	< 0.16 (< 0.33)	-	$-0.067^{+0.058}_{-0.068}$	$0.051^{+0.13}_{-0.077}$	84.6 ± 8.9	-	< 6.3
HAT-P-12b	C	< 0.035 (< 0.069)	-	$0.012^{+0.020}_{-0.014}$	$0.002^{+0.026}_{-0.019}$	35.4 ± 1.5	-	$3.96^{+1.0}_{-0.86}$
HAT-P-13b	C	< 0.013 (< 0.022)	-	-0.0068 ± 0.0054	$0.0011^{+0.0089}_{-0.0065}$	105.7 ± 1.0	0.0511 ± 0.0017 PLC	$5.87^{+0.66}_{-0.56}$
HAT-P-14b	E	$0.1074^{+0.0076}_{-0.0079}$	$106.1^{+2.6}_{-2.5}$	$-0.0298^{+0.0042}_{-0.0041}$	$0.1031^{+0.0079}_{-0.0082}$	$225.8^{+2.1}_{-2.0}$	-	$10.7^{+2.8}_{-2.2}$
HAT-P-15b	E	$0.200^{+0.026}_{-0.028}$	$262.5^{+2.4}_{-2.9}$	$-0.0262^{+0.0082}_{-0.0084}$	$-0.198^{+0.028}_{-0.027}$	$181.2^{+5.1}_{-5.0}$	-	$18.5^{+3.0}_{-2.4}$
HAT-P-16b	E	$0.0462^{+0.0027}_{-0.0024}$	$213.0^{+5.1}_{-5.4}$	$-0.0388^{+0.0016}_{-0.0015}$	$-0.0251^{+0.0046}_{-0.0048}$	534.6 ± 1.8	-	< 1.9
HAT-P-17b	E	0.3417 ± 0.0036	200.5 ± 1.3	-0.3194 ± 0.0033	$-0.1293^{+0.0079}_{-0.0081}$	59.09 ± 0.65	PLC	1.4 ± 0.5
HAT-P-18b	U	< 0.087 (< 0.16)	-	$0.033^{+0.042}_{-0.034}$	$0.006^{+0.064}_{-0.047}$	27.5 ± 2.5	-	$16.6^{+2.6}_{-2.1}$
HAT-P-19b	C	< 0.024 (< 0.10)	-	$0.0013^{+0.0023}_{-0.0017}$	$-0.0029^{+0.0087}_{-0.050}$	$40.8^{+1.9}_{-1.8}$	0.440 ± 0.061	$9.8^{+2.7}_{-2.0}$
HAT-P-20b	E	$0.0158^{+0.0023}_{-0.0018}$	$324.2^{+12}_{-8.9}$	0.01278 ± 0.00056	$-0.0092^{+0.0035}_{-0.0034}$	$1249.7^{+4.2}_{-4.1}$	-	$15.5^{+3.7}_{-2.9}$
HAT-P-21b	E	0.217 ± 0.010	$305.8^{+2.1}_{-1.9}$	0.1267 ± 0.0043	-0.176 ± 0.012	533.8 ± 6.1	-	$30.2^{+6.9}_{-5.5}$
HAT-P-22b	C	< 0.0020 (< 0.0039)	-	$-0.00060^{+0.0014}_{-0.00080}$	$0.00024^{+0.0014}_{-0.00089}$	316.49 ± 0.60	CURV	$1.15^{+0.32}_{-0.29}$
HAT-P-23b	U	< 0.052 (< 0.16)	-	0.0042 ± 0.0014	$0.015^{+0.081}_{-0.021}$	346^{+21}_{-20}	-	$46.5^{+13}_{-8.8}$
HAT-P-24b	C	< 0.038 (< 0.070)	-	$-0.017^{+0.016}_{-0.018}$	$-0.000^{+0.022}_{-0.024}$	$87.4^{+3.1}_{-3.0}$	-	$10.3^{+3.0}_{-2.5}$
HAT-P-25b	C	< 0.033 (< 0.077)	-	$0.0056^{+0.011}_{-0.0085}$	$-0.010^{+0.017}_{-0.034}$	$74.3^{+2.4}_{-2.5}$	-	$3.9^{+2.5}_{-1.8}$
HAT-P-27b	C	< 0.028 (< 0.066)	-	$0.002^{+0.013}_{-0.010}$	$-0.005^{+0.014}_{-0.029}$	90.9 ± 2.1	-	$6.9^{+2.7}_{-1.6}$
HAT-P-28b	C	< 0.039 (< 0.088)	-	$-0.004^{+0.016}_{-0.023}$	$-0.003^{+0.021}_{-0.036}$	$85.9^{+4.0}_{-4.4}$	-	$12.2^{+6.9}_{-4.1}$
HAT-P-29b	E	$0.104^{+0.021}_{-0.018}$	159^{+20}_{-16}	-0.094 ± 0.016	0.036 ± 0.035	68.0 ± 3.0	CURV	$27.1^{+7.9}_{-8.3}$
HAT-P-30b	C	< 0.016 (< 0.031)	-	$0.0044^{+0.0089}_{-0.0055}$	$0.0018^{+0.013}_{-0.0075}$	92.4 ± 1.6	-	$2.8^{+1.4}_{-1.2}$
HAT-P-31b	E	$0.2617^{+0.0093}_{-0.0095}$	$276.3^{+1.2}_{-1.3}$	$0.0288^{+0.0035}_{-0.0060}$	$-0.2600^{+0.0094}_{-0.0093}$	232.8 ± 2.5	-	$7.4^{+2.5}_{-1.8}$
HAT-P-32b	C	< 0.044 (< 0.31)	-	0.00075 ± 0.00055	$0.0020^{+0.12}_{-0.0093}$	108 ± 18	-0.094 ± 0.023	$63.2^{+10.}_{-8.5}$
HAT-P-33b	U	< 0.22 (< 0.53)	-	$0.006^{+0.095}_{-0.085}$	$0.074^{+0.22}_{-0.097}$	73^{+16}_{-14}	-	$51.1^{+8.9}_{-6.8}$
HAT-P-34b	E	$0.432^{+0.029}_{-0.027}$	$21.9^{+5.2}_{-5.6}$	$0.399^{+0.027}_{-0.026}$	0.160 ± 0.042	343 ± 19	-	$52.3^{+13}_{-9.2}$
HAT-P-35b	C	< 0.020 (< 0.056)	-	$0.0003^{+0.0090}_{-0.0088}$	$-0.0032^{+0.0092}_{-0.022}$	$120.9^{+2.2}_{-2.1}$	-	$4.2^{+2.8}_{-1.9}$
HAT-P-36b	U	< 0.059 (< 0.11)	-	$-0.002^{+0.024}_{-0.028}$	$0.027^{+0.041}_{-0.029}$	336 ± 15	-	$37.5^{+13}_{-9.0}$
HAT-P-37b	U	< 0.14 (< 0.26)	-	$-0.026^{+0.031}_{-0.035}$	$-0.071^{+0.074}_{-0.12}$	184^{+16}_{-17}	-	$28^{+12}_{-10.}$
HAT-P-38b	U	< 0.055 (< 0.17)	-	$0.001^{+0.022}_{-0.019}$	$-0.003^{+0.034}_{-0.062}$	$35.3^{+2.4}_{-2.3}$	-	< 2.1
HAT-P-39b	U	< 0.17 (< 0.52)	-	$0.013^{+0.083}_{-0.072}$	-0.00 ± 0.13	64^{+13}_{-11}	-	$46.3^{+7.7}_{-6.1}$
HAT-P-40b	U	< 0.12 (< 0.19)	-	$0.011^{+0.021}_{-0.019}$	$0.089^{+0.056}_{-0.062}$	$55.5^{+2.8}_{-2.7}$	-	$4.8^{+2.1}_{-1.6}$
HAT-P-41b	U	< 0.22 (< 0.40)	-	$-0.060^{+0.040}_{-0.048}$	$-0.12^{+0.12}_{-0.16}$	96^{+13}_{-11}	-	$33.5^{+10.}_{-7.4}$
HAT-P-42b	U	< 0.11 (< 0.27)	-	$0.000^{+0.052}_{-0.056}$	$-0.007^{+0.067}_{-0.10}$	97 ± 14	-	< 33.4
HAT-P-43b	U	< 0.21 (< 0.96)	-	$-0.036^{+0.071}_{-0.17}$	$0.051^{+0.23}_{-0.085}$	93^{+42}_{-16}	-	< 13.4
HAT-P-45b	U	< 0.11 (< 0.37)	-	$0.000^{+0.063}_{-0.048}$	$0.006^{+0.10}_{-0.060}$	106^{+17}_{-14}	-	$29.3^{+11}_{-7.1}$
HAT-P-49b	U	< 0.12 (< 0.25)	-	$0.041^{+0.065}_{-0.048}$	$0.003^{+0.089}_{-0.072}$	195^{+24}_{-23}	-	93^{+45}_{-27}
HAT-P-50b	U	< 0.084 (< 0.14)	-	$-0.046^{+0.035}_{-0.038}$	$-0.030^{+0.033}_{-0.040}$	$162.5^{+6.3}_{-6.2}$	-	< 10.7
HAT-P-51b	U	< 0.070 (< 0.14)	-	$-0.019^{+0.022}_{-0.027}$	$-0.028^{+0.034}_{-0.059}$	$39.8^{+2.1}_{-2.4}$	-	$4.7^{+3.2}_{-2.1}$
HAT-P-52b	C	< 0.030 (< 0.082)	-	$-0.003^{+0.011}_{-0.016}$	$-0.000^{+0.022}_{-0.023}$	$128.2^{+5.6}_{-5.7}$	-	$8.9^{+5.6}_{-3.3}$
HAT-P-53b	U	¡ 0.085 (¡0.145)	-	-0.021 ± 0.036	$-0.060^{+0.028}_{-0.032}$	$227.2^{+4.5}_{-3.6}$	-	< 5.7

Table 8. continued.

Planet	Flag	e	ω [deg]	$e\cos\omega$	$e\sin\omega$	K [m s^{-1}]	$\dot{\gamma}$ [m s^{-1} day^{-1}]	Jitter [m s^{-1}]
HAT-P-54b	U	< 0.66 (< 0.96)	-	$0.056^{+0.57}_{-0.065}$	$0.17^{+0.35}_{-0.18}$	167^{+890}_{-35}	-	53^{+17}_{-13}
HAT-P-55b	U	< 0.17 (< 0.26)	-	0.026 ± 0.028	$-0.122^{+0.086}_{-0.082}$	$77.5^{+6.8}_{-6.6}$	-	$21.1^{+13}_{-9.6}$
HAT-P-56b	U	< 0.29 (< 0.53)	-	$-0.029^{+0.068}_{-0.12}$	$0.14^{+0.25}_{-0.15}$	240^{+54}_{-37}	$-6.4^{+1.6}_{-1.5}$	< 12.2
HATS-1b	U	< 0.082 (< 0.26)	-	$-0.028^{+0.028}_{-0.051}$	$0.019^{+0.098}_{-0.036}$	238^{+26}_{-23}	-	< 6.3
HATS-2b	U	< 0.29 (< 0.46)	-	$-0.093^{+0.057}_{-0.029}$	-0.20 ± 0.15	329^{+59}_{-51}	-	< 22.6
HATS-3b	U	$0.23^{+0.19}_{-0.10}$	155^{+54}_{-34}	$-0.174^{+0.091}_{-0.10}$	$0.07^{+0.25}_{-0.14}$	135 ± 20	-	56^{+29}_{-21}
HATS-4b	C	< 0.024 (< 0.060)	-	$-0.0017^{+0.0071}_{-0.0083}$	$-0.008^{+0.012}_{-0.027}$	$194.2^{+5.1}_{-6.2}$	-	$9.5^{+4.7}_{-3.3}$
HATS-5b	C	< 0.044 (< 0.12)	-	$0.004^{+0.021}_{-0.014}$	$-0.008^{+0.021}_{-0.053}$	$30.0^{+1.6}_{-1.7}$	-	< 3.3
HATS-7b	U	< 0.12 (< 0.34)	-	$0.015^{+0.073}_{-0.047}$	$0.002^{+0.082}_{-0.11}$	$19.1^{+2.2}_{-2.0}$	-	< 3.4
HATS-8b	U	< 0.25 (< 0.76)	-	$0.005^{+0.090}_{-0.046}$	$-0.05^{+0.13}_{-0.27}$	$19.2^{+5.2}_{-3.3}$	-	< 2.7
HATS-9b	U	< 0.075 (< 0.16)	-	$0.012^{+0.046}_{-0.028}$	$-0.014^{+0.036}_{-0.069}$	$132.3^{+5.5}_{-5.3}$	-	< 7.1
HATS-10b	U	< 0.28 (< 0.52)	-	$0.11^{+0.17}_{-0.11}$	$0.12^{+0.15}_{-0.12}$	79^{+22}_{-16}	-	< 4.7
HATS-13b	U	< 0.22 (< 0.41)	-	$0.073^{+0.032}_{-0.057}$	$-0.10^{+0.12}_{-0.19}$	89^{+19}_{-14}	-	< 6.0
HATS-14b	U	< 0.11 (< 0.26)	-	$0.000^{+0.039}_{-0.037}$	$-0.014^{+0.059}_{-0.13}$	159 ± 14	-	< 5.5
HD 149026b	C	< 0.013 (< 0.098)	-	$-0.00007^{+0.00046}_{-0.00052}$	$0.0010^{+0.023}_{-0.0025}$	$37.9^{+1.8}_{-1.3}$	-	$5.04^{+0.85}_{-0.55}$
HD 17156b	E	$0.6703^{+0.0014}_{-0.0013}$	121.32 ± 0.20	$-0.3484^{+0.0020}_{-0.0019}$	0.5727 ± 0.0018	$271.56^{+0.62}_{-0.63}$	-	$2.33^{+0.32}_{-0.28}$
HD 189733b	C	< 0.0039 (< 0.011)	-	$0.00089^{+0.0012}_{-0.00095}$	$-0.0000^{+0.0032}_{-0.0037}$	201.3 ± 1.6	-	$8.82^{+0.91}_{-0.78}$
HD 209458b	C	< 0.0081 (< 0.022)	-	$-0.00020^{+0.00030}_{-0.00036}$	$0.0027^{+0.012}_{-0.0029}$	$84.27^{+0.69}_{-0.70}$	-	$3.40^{+0.62}_{-0.59}$
HD 80606b	E	$0.93226^{+0.00064}_{-0.00069}$	$301.03^{+0.20}_{-0.19}$	$0.4803^{+0.0022}_{-0.0025}$	$-0.7988^{+0.0023}_{-0.0021}$	$474.9^{+2.5}_{-2.7}$	-	$1.85^{+0.64}_{-0.41}$
KELT-2Ab	U	< 0.081 (< 0.15)	-	$-0.008^{+0.028}_{-0.040}$	$0.032^{+0.064}_{-0.037}$	$162.3^{+8.9}_{-8.6}$	-	< 9.3
KELT-3b	C	< 0.035 (< 0.072)	-	$-0.007^{+0.012}_{-0.020}$	$-0.006^{+0.015}_{-0.032}$	$182.3^{+5.2}_{-4.7}$	-	< 9.1
KELT-6b	C	< 0.036 (< 0.058)	-	$0.022^{+0.009}_{-0.010}$	$-0.013^{+0.017}_{-0.022}$	41.8 ± 1.1	-	2.2 ± 1.1
KELT-8b	C	< 0.047 (< 0.13)	-	0.001 ± 0.018	$0.012^{+0.058}_{-0.022}$	$104.2^{+5.2}_{-5.3}$	-	< 8.0
Kepler-5b	C	< 0.043 (< 0.099)	-	$-0.008^{+0.017}_{-0.028}$	$0.000^{+0.029}_{-0.027}$	228.7 ± 8.8	-	$17.4^{+8.5}_{-5.3}$
Kepler-6b	U	< 0.060 (< 0.11)	-	$-0.0108^{+0.0048}_{-0.0046}$	$0.036^{+0.047}_{-0.034}$	$81.7^{+3.3}_{-3.4}$	-	< 3.7
Kepler-7b	C	< 0.026 (< 0.13)	-	0.0012 ± 0.0011	$0.0017^{+0.051}_{-0.0094}$	$42.6^{+4.3}_{-4.4}$	-	< 3.5
Kepler-8b	U	< 0.18 (< 0.50)	-	$0.022^{+0.070}_{-0.054}$	$-0.01^{+0.13}_{-0.17}$	67 ± 16	-	< 27.9
Kepler-12b	C	< 0.021 (< 0.13)	-	$0.0002^{+0.0013}_{-0.0012}$	$0.000^{+0.029}_{-0.014}$	48.3 ± 4.3	-	< 10.2
Kepler-15b	U	< 0.068 (< 0.16)	-	$0.008^{+0.045}_{-0.028}$	$-0.005^{+0.035}_{-0.062}$	$75.0^{+5.2}_{-5.1}$	-	< 5.0
Kepler-17b	C	< 0.020 (< 0.057)	-	$-0.0005^{+0.0072}_{-0.0094}$	$-0.000^{+0.014}_{-0.019}$	398 ± 12	-	< 11.0
Kepler-39b	U	$0.111^{+0.045}_{-0.052}$	98^{+17}_{-12}	$-0.015^{+0.022}_{-0.021}$	$0.108^{+0.046}_{-0.058}$	1256^{+57}_{-56}	-	86^{+50}_{-36}
Kepler-40b	U	< 0.15 (< 0.30)	-	$-0.018^{+0.038}_{-0.060}$	$-0.071^{+0.074}_{-0.12}$	174^{+25}_{-22}	-	< 20.3
Kepler-41b	U	< 0.21 (< 0.35)	-	$0.002^{+0.015}_{-0.014}$	$0.13^{+0.14}_{-0.13}$	86 ± 10	-	< 9
Kepler-43b	C	< 0.028 (< 0.049)	-	$-0.0125^{+0.0096}_{-0.0098}$	$0.008^{+0.021}_{-0.014}$	374.5 ± 6.9	-	$25.3^{+8.8}_{-6.9}$
Kepler-44b	U	< 0.07 (< 0.20)	-	$0.007^{+0.041}_{-0.023}$	$0.002^{+0.061}_{-0.041}$	125 ± 11	-	< 6.2
Kepler-45b	U	$0.186^{+0.11}_{-0.088}$	242^{+16}_{-32}	$-0.080^{+0.052}_{-0.047}$	$-0.16^{+0.12}_{-0.11}$	107^{+14}_{-13}	-	$27.6^{+10.}_{-7.9}$
Kepler-74b	U	$0.27^{+0.12}_{-0.13}$	60^{+42}_{-31}	0.14 ± 0.11	0.17 ± 0.15	$59.4^{+7.8}_{-7.6}$	-	< 6.9
Kepler-75b	E	$0.5704^{+0.0093}_{-0.0094}$	$63.5^{+1.5}_{-1.4}$	$0.254^{+0.012}_{-0.013}$	$0.510^{+0.011}_{-0.012}$	1285^{+22}_{-24}	-	< 7.4
Kepler-76b	U	< 0.078 (< 0.17)	-	$-0.016^{+0.026}_{-0.039}$	$-0.001^{+0.057}_{-0.061}$	307^{+23}_{-22}	-	< 15.2
Kepler-77b	U	< 0.079 (< 0.19)	-	$0.008^{+0.030}_{-0.022}$	$-0.026^{+0.038}_{-0.086}$	71.9 ± 5.3	-	< 6.1

Table 8. continued.

Planet	Flag	e	ω [deg]	$e\cos\omega$	$e\sin\omega$	K [m s^{-1}]	$\dot{\gamma}$ [m s^{-1} day^{-1}]	Jitter [m s^{-1}]
Kepler-412b	U	< 0.076 (< 0.28)	-	$-0.0009^{+0.0038}_{-0.0041}$	$-0.0089^{+0.158}_{-0.020}$	140.7 ± 8.1	-	< 6.0
Kepler-419b	E	$0.800^{+0.087}_{-0.097}$	$97.8^{+18.5}_{-11.1}$	$-0.10^{+0.15}_{-0.28}$	$0.761^{+0.060}_{-0.090}$	179^{+43}_{-31}	CURV	58^{+10}_{-14}
Kepler-422b	U	< 0.55 (< 0.94)	-	$0.07^{+0.40}_{-0.11}$	$0.12^{+0.45}_{-0.22}$	46^{+49}_{-13}	-	$24.5^{+8.5}_{-6.7}$
Kepler-423b	U	< 0.079 (< 0.17)	-	$-0.008^{+0.030}_{-0.045}$	$-0.004^{+0.049}_{-0.066}$	$99.3^{+9.3}_{-9.8}$	-	$27.0^{+9.2}_{-7.5}$
Kepler-424b	U	< 0.076 (< 0.18)	-	$0.007^{+0.035}_{-0.023}$	$0.024^{+0.087}_{-0.035}$	146 ± 12	PLC	< 10.9
Kepler-425b	U	< 0.20 (< 0.43)	-	$-0.021^{+0.075}_{-0.12}$	$0.01^{+0.16}_{-0.12}$	$31.7^{+6.5}_{-6.3}$	-	< 8.5
Kepler-426b	U	< 0.12 (< 0.32)	-	$0.004^{+0.057}_{-0.050}$	$-0.012^{+0.070}_{-0.13}$	$49.6^{+8.6}_{-8.3}$	-	< 4.5
Kepler-427b	U	< 0.27 (< 0.46)	-	$0.049^{+0.11}_{-0.091}$	$0.14^{+0.18}_{-0.15}$	$29.3^{+5.0}_{-4.9}$	-	< 3.2
Kepler-428b	U	< 0.11 (< 0.33)	-	$0.025^{+0.049}_{-0.031}$	$0.039^{+0.13}_{-0.051}$	189^{+19}_{-17}	-	< 9.4
Kepler-432b	E	0.4775 ± 0.0073	68.64 ± 1.05	0.1739 ± 0.0083	0.4446 ± 0.0079	29.1 ± 0.33	PLC	< 3.5
Kepler-433b	U	$0.124^{+0.064}_{-0.057}$	65^{+260}_{-41}	$0.076^{+0.050}_{-0.053}$	$0.053^{+0.095}_{-0.080}$	258^{+33}_{-34}	$-1.42^{+0.43}_{-0.42}$	< 16.5
Kepler-434b	U	< 0.13 (< 0.20)	-	$0.046^{+0.044}_{-0.045}$	$0.070^{+0.072}_{-0.065}$	232^{+19}_{-20}	-	< 8.7
Kepler-435b	U	< 0.18 (< 0.39)	-	$-0.017^{+0.037}_{-0.048}$	$-0.076^{+0.089}_{-0.20}$	64.2 ± 9.0	0.111 ± 0.021	< 5.2
OGLE-TR-10b	U	< 0.82 (< 0.99)	-	$-0.10^{+0.20}_{-0.55}$	$0.35^{+0.34}_{-0.32}$	134^{+530}_{-50}	-	< 39.2
OGLE-TR-56b	U	< 0.61 (< 0.97)	-	$-0.01^{+0.16}_{-0.17}$	$0.16^{+0.56}_{-0.18}$	313^{+1100}_{-69}	-	< 31.7
OGLE-TR-111b	U	< 0.54 (< 0.96)	-	$0.20^{+0.52}_{-0.11}$	$-0.03^{+0.21}_{-0.28}$	91^{+170}_{-29}	-	< 20.4
OGLE-TR-113b	U	< 0.15 (< 0.27)	-	$-0.032^{+0.042}_{-0.049}$	$0.076^{+0.10}_{-0.080}$	294^{+31}_{-33}	-	< 37.7
OGLE-TR-132b	U	< 0.60 (< 0.95)	-	$0.06^{+0.54}_{-0.12}$	$0.10^{+0.28}_{-0.20}$	216^{+960}_{-70}	-	< 32.7
OGLE-TR-182b	U	< 0.27 (< 0.76)	-	$0.001^{+0.093}_{-0.079}$	$0.12^{+0.34}_{-0.13}$	128^{+31}_{-23}	-	< 14.0
OGLE-TR-211b	U	< 0.58 (< 0.98)	-	$-0.03^{+0.15}_{-0.42}$	$0.02^{+0.40}_{-0.26}$	84^{+81}_{-40}	-	92^{+24}_{-19}
Qatar-1b	C	< 0.012 (< 0.048)	-	$-0.0001^{+0.0016}_{-0.0018}$	$-0.0018^{+0.0042}_{-0.022}$	$264.7^{+5.0}_{-5.2}$	-	$10.0^{+4.6}_{-3.5}$
Qatar-2b	C	< 0.011 (< 0.020)	-	$-0.0041^{+0.0042}_{-0.0055}$	$-0.0020^{+0.0055}_{-0.0087}$	$554.1^{+6.0}_{-5.8}$	-	$22.0^{+4.7}_{-4.5}$
TrES-1b	C	< 0.012 (< 0.041)	-	$0.00162^{+0.00057}_{-0.00058}$	$0.0018^{+0.018}_{-0.0059}$	$106.7^{+2.9}_{-2.8}$	-	$6.2^{+2.1}_{-1.6}$
TrES-2b	C	< 0.0030 (< 0.012)	-	$0.00036^{+0.00051}_{-0.00041}$	$-0.0000^{+0.0025}_{-0.0033}$	183.0 ± 1.5	-	< 2.3
TrES-3b	C	< 0.043 (< 0.065)	-	0.0025 ± 0.0014	$0.026^{+0.028}_{-0.027}$	$348.5^{+8.6}_{-4.9}$	-	< 12.5
TrES-4b	C	< 0.015 (< 0.069)	-	$0.0014^{+0.0016}_{-0.0014}$	$-0.000^{+0.014}_{-0.016}$	$51.4^{+3.2}_{-3.1}$	-	$14.0^{+6.7}_{-4.0}$
TrES-5b	C	< 0.030 (< 0.062)	-	$0.010^{+0.016}_{-0.011}$	$-0.000^{+0.019}_{-0.022}$	343 ± 12	-	< 7.4
WASP-1b	C	< 0.013 (< 0.038)	-	$0.00005^{+0.0010}_{-0.00091}$	$-0.0035^{+0.0045}_{-0.020}$	$118.7^{+1.9}_{-2.0}$	-	$4.2^{+2.1}_{-1.8}$
WASP-2b	C	< 0.013 (< 0.024)	-	-0.0001 ± 0.0011	$-0.0082^{+0.0080}_{-0.0095}$	156.5 ± 1.3	-	< 3.7
WASP-3b	C	< 0.0058 (< 0.029)	-	$0.00021^{+0.00071}_{-0.00056}$	$0.0001^{+0.0070}_{-0.0047}$	$266.7^{+9.4}_{-9.1}$	-	$17.6^{+5.9}_{-4.3}$
WASP-4b	C	< 0.0033 (< 0.013)	-	$-0.00029^{+0.00047}_{-0.00060}$	$0.0000^{+0.0036}_{-0.0028}$	$232.7^{+2.5}_{-2.2}$	-	$11.0^{+2.5}_{-1.9}$
WASP-5b	C	< 0.012 (0.026)	-	$0.0057^{+0.0028}_{-0.0029}$	$0.0024^{+0.011}_{-0.0074}$	$268.2^{+4.6}_{-4.2}$	-	$10.9^{+3.6}_{-2.5}$
WASP-6b	U	< 0.070 (< 0.12)	-	$0.0003^{+0.0018}_{-0.0017}$	$0.051^{+0.040}_{-0.047}$	$71.6^{+2.4}_{-2.6}$	-	$6.0^{+2.1}_{-1.9}$
WASP-7b	C	< 0.049 (< 0.11)	-	$0.007^{+0.028}_{-0.019}$	$-0.001^{+0.033}_{-0.038}$	$109.4^{+8.3}_{-8.1}$	-	$35.1^{+9.6}_{-6.8}$
WASP-8b	E	0.3057 ± 0.00046	274.21 ± 0.33	0.0225 ± 0.0018	-0.3049 ± 0.0046	221.65 ± 1.39	PLC	$2.6^{+1.5}_{-0.9}$
WASP-10b	E	$0.0601^{+0.0064}_{-0.0046}$	$151.9^{+11}_{-8.8}$	-0.0530 ± 0.0015	$0.028^{+0.011}_{-0.012}$	$543 \pm 10.$	$-0.088^{+0.021}_{-0.024}$	$15.0^{+7.9}_{-4.7}$
WASP-11b	C	< 0.030 (< 0.055)	-	$0.0040^{+0.0087}_{-0.0070}$	$0.017^{+0.023}_{-0.017}$	$80.6^{+1.8}_{-1.7}$	$-0.0199^{+0.0027}_{-0.0030}$	$7.0^{+2.2}_{-1.6}$
WASP-12b	C	< 0.020 (0.034)	-	$-0.0030^{+0.0038}_{-0.0044}$	$-0.013^{+0.011}_{-0.012}$	$219.9^{+2.2}_{-2.1}$	-	$9.1^{+1.8}_{-1.3}$
WASP-13b	C	< 0.016 (< 0.033)	-	$0.0044^{+0.010}_{-0.0062}$	$0.0005^{+0.012}_{-0.0099}$	$56.89^{+0.89}_{-0.93}$	-	< 1.7
WASP-14b	E	$0.0782^{+0.0014}_{-0.0012}$	251.61 ± 0.41	$-0.02468^{+0.00037}_{-0.00036}$	$-0.0742^{+0.0013}_{-0.0014}$	984.2 ± 1.4	-	$5.6^{+2.0}_{-1.4}$

Table 8. continued.

Planet	Flag	e	ω [deg]	$e\cos\omega$	$e\sin\omega$	K [m s^{-1}]	$\dot{\gamma}$ [m s^{-1} day^{-1}]	Jitter [m s^{-1}]
WASP-15b	U	< 0.055 (< 0.14)	-	$0.001^{+0.027}_{-0.021}$	$0.011^{+0.062}_{-0.027}$	$63.5^{+4.2}_{-4.6}$	-	< 8.7
WASP-16b	C	< 0.018(< 0.025)	-	$-0.0101^{+0.0036}_{-0.0033}$	$0.0104^{+0.0068}_{-0.0069}$	$123.8^{+1.0}_{-1.1}$	-	< 2.4
WASP-17b	C	< 0.020 (< 0.075)	-	$0.00292^{+0.00085}_{-0.00084}$	$-0.000^{+0.018}_{-0.021}$	$56.0^{+4.1}_{-4.0}$	-	$12.7^{+8.4}_{-5.3}$
WASP-18b	E	0.0076 ± 0.0010	$268.7^{+2.9}_{-2.7}$	$-0.00017^{+0.00038}_{-0.00037}$	$-0.00756^{+0.00100}_{-0.0010}$	1817.3 ± 2.3	-	< 3.5
WASP-19b	C	< 0.0061 (< 0.015)	-	$-0.0004^{+0.0021}_{-0.0027}$	$0.0004^{+0.0062}_{-0.0038}$	257.9 ± 2.9	-	$8.5^{+2.4}_{-2.1}$
WASP-20b	C	< 0.039 (< 0.096)	-	-0.000 ± 0.017	$-0.003^{+0.023}_{-0.041}$	32.9 ± 1.8	-	$7.07^{+1.2}_{-0.97}$
WASP-21b	C	< 0.048 (< 0.080)	-	$-0.025^{+0.019}_{-0.020}$	0.000 ± 0.029	36.9 ± 1.4	-	$3.9^{+1.6}_{-1.4}$
WASP-22b	C	< 0.021 (< 0.048)	-	$0.0011^{+0.0095}_{-0.0075}$	$0.0057^{+0.022}_{-0.0094}$	71.0 ± 1.7	$0.072^{+0.015}_{-0.012}$	$10.6^{+5.2}_{-3.4}$
WASP-23b	U	< 0.065 (< 0.11)	-	$-0.008^{+0.010}_{-0.011}$	$-0.047^{+0.035}_{-0.036}$	$147.4^{+3.8}_{-3.9}$	-	< 5.3
WASP-24b	C	< 0.0046 (< 0.017)	-	$0.00056^{+0.00089}_{-0.00069}$	$0.0001^{+0.0057}_{-0.0034}$	147.7 ± 2.0	-	< 4.2
WASP-25b	U	< 0.083 (< 0.18)	-	$-0.006^{+0.024}_{-0.032}$	$0.030^{+0.086}_{-0.039}$	$75.2^{+5.4}_{-5.1}$	-	$15.5^{+4.2}_{-3.8}$
WASP-26b	C	< 0.0039 (< 0.015)	-	$-0.00011^{+0.00064}_{-0.00076}$	$0.0000^{+0.0042}_{-0.0034}$	138.2 ± 1.2	-	< 1.5
WASP-28b	U	< 0.058 (< 0.11)	-	$0.004^{+0.016}_{-0.012}$	$-0.034^{+0.033}_{-0.045}$	$120.8^{+4.5}_{-4.7}$	-	< 2.6
WASP-29b	U	< 0.059 (< 0.15)	-	$-0.000^{+0.027}_{-0.026}$	$-0.002^{+0.043}_{-0.049}$	$36.0^{+3.2}_{-3.1}$	-	< 2.9
WASP-31b	C	< 0.047 (< 0.097)	-	$0.009^{+0.030}_{-0.017}$	$0.004^{+0.038}_{-0.025}$	$59.4^{+2.8}_{-2.9}$	-	< 2.4
WASP-32b	C	< 0.0040 (< 0.0088)	-	$0.0005^{+0.0022}_{-0.0016}$	$0.0000^{+0.0031}_{-0.0027}$	$483.5^{+2.6}_{-2.7}$	-	$9.6^{+4.2}_{-3.0}$
WASP-34b	C	< 0.024 (< 0.052)	-	$0.0052^{+0.014}_{-0.0089}$	$0.001^{+0.020}_{-0.015}$	72.0 ± 1.9	CURV	$6.7^{+1.8}_{-1.5}$
WASP-35b	C	< 0.028 (< 0.050)	-	0.013 ± 0.011	$0.011^{+0.018}_{-0.013}$	$92.8^{+1.9}_{-1.8}$	-	< 2.2
WASP-36b	C	< 0.019 (< 0.041)	-	$0.0015^{+0.0100}_{-0.0072}$	$0.0037^{+0.019}_{-0.0085}$	$391.5^{+8.5}_{-8.4}$	-	< 5.3
WASP-37b	U	< 0.052 (< 0.091)	-	$0.027^{+0.022}_{-0.020}$	$0.003^{+0.033}_{-0.031}$	241^{+12}_{-11}	-	< 7.9
WASP-38b	E	$0.0278^{+0.0030}_{-0.0028}$	340.6 ± 9.1	0.0261 ± 0.0025	$-0.0088^{+0.0046}_{-0.0047}$	246.6 ± 1.2	-	$7.3^{+1.9}_{-1.4}$
WASP-39b	C	< 0.048 (< 0.33)	-	$0.0007^{+0.0017}_{-0.0014}$	$0.000^{+0.049}_{-0.046}$	$36.9^{+6.0}_{-5.3}$	-	< 6.6
WASP-41b	U	< 0.12 (< 0.22)	-	$0.022^{+0.029}_{-0.023}$	$0.072^{+0.088}_{-0.071}$	$139.2^{+9.2}_{-9.1}$	-	$22.8^{+4.8}_{-3.8}$
WASP-42b	E	$0.062^{+0.013}_{-0.011}$	159^{+27}_{-22}	-0.054 ± 0.010	$0.020^{+0.026}_{-0.027}$	64.9 ± 1.6	-	< 1.5
WASP-43b	C	< 0.0062 (< 0.016)	-	0.00074 ± 0.00042	$-0.0024^{+0.0028}_{-0.0080}$	551.7 ± 4.7	-	$12.5^{+3.1}_{-2.6}$
WASP-44b	U	< 0.068 (< 0.17)	-	$0.001^{+0.023}_{-0.020}$	$-0.018^{+0.033}_{-0.080}$	140^{+12}_{-10}	-	< 5.8
WASP-45b	C	< 0.043 (< 0.10)	-	$0.009^{+0.017}_{-0.011}$	$0.014^{+0.048}_{-0.020}$	$148.2^{+4.4}_{-4.6}$	-	< 3.2
WASP-46b	C	< 0.022 (0.055)	-	0.0072 ± 0.0024	$0.008^{+0.024}_{-0.013}$	$386 \pm 10.$	-	< 13.9
WASP-48b	C	< 0.014 (< 0.064)	-	$0.0013^{+0.0020}_{-0.0016}$	$-0.000^{+0.011}_{-0.018}$	$142.6^{+4.8}_{-4.7}$	-	< 4.2
WASP-49b	C	< 0.026 (< 0.058)	-	$-0.0043^{+0.0083}_{-0.015}$	$0.000^{+0.019}_{-0.018}$	$60.0^{+2.4}_{-2.5}$	-	< 4.2
WASP-50b	C	< 0.022 (< 0.041)	-	$0.0041^{+0.0057}_{-0.0048}$	$-0.012^{+0.012}_{-0.017}$	$255.6^{+3.5}_{-3.6}$	-	$10.5^{+4.1}_{-2.8}$
WASP-52b	U	< 0.092 (< 0.15)	-	$0.016^{+0.019}_{-0.018}$	$0.065^{+0.049}_{-0.048}$	$85.0^{+3.4}_{-3.5}$	-	< 8.4
WASP-54b	U	< 0.060 (< 0.091)	-	$0.007^{+0.014}_{-0.013}$	$0.046^{+0.026}_{-0.027}$	$70.0^{+1.7}_{-1.6}$	-	$4.4^{+1.6}_{-1.2}$
WASP-55b	U	< 0.056 (< 0.13)	-	$-0.003^{+0.022}_{-0.030}$	$-0.007^{+0.028}_{-0.055}$	$70.1^{+5.2}_{-4.8}$	-	< 6.3
WASP-56b	U	< 0.082 (< 0.17)	-	$0.004^{+0.026}_{-0.022}$	$-0.040^{+0.042}_{-0.077}$	$68.7^{+4.5}_{-4.3}$	-	< 3.5
WASP-57b	U	< 0.059 (< 0.12)	-	$-0.015^{+0.021}_{-0.035}$	$0.004^{+0.044}_{-0.034}$	$100.3^{+7.1}_{-7.5}$	-	< 8.7
WASP-58b	C	< 0.044 (< 0.096)	-	$0.003^{+0.019}_{-0.014}$	$0.015^{+0.045}_{-0.020}$	$111.2^{+4.3}_{-4.5}$	-	< 3.7
WASP-59b	U	$0.101^{+0.046}_{-0.048}$	75^{+14}_{-17}	0.024 ± 0.022	$0.095^{+0.048}_{-0.053}$	$109.6^{+4.7}_{-4.8}$	-	< 5.1
WASP-60b	U	< 0.064 (< 0.14)	-	$0.007^{+0.034}_{-0.024}$	$0.001^{+0.052}_{-0.044}$	$60.1^{+5.4}_{-5.5}$	-	$16.6^{+5.0}_{-4.7}$
WASP-61b	U	< 0.074 (< 0.16)	-	$0.007^{+0.040}_{-0.025}$	$0.025^{+0.070}_{-0.035}$	234^{+17}_{-18}	-	< 10.7

Table 8. continued.

Planet	Flag	e	ω [deg]	$e\cos\omega$	$e\sin\omega$	K [m s^{-1}]	$\dot{\gamma}$ [m s^{-1} day^{-1}]	Jitter [m s^{-1}]
WASP-62b	U	< 0.075 (< 0.14)	-	$-0.030^{+0.029}_{-0.034}$	$-0.006^{+0.040}_{-0.058}$	60.8 ± 4.3	-	$10.7^{+3.5}_{-3.2}$
WASP-63b	U	< 0.086 (< 0.17)	-	$0.026^{+0.040}_{-0.029}$	$-0.020^{+0.039}_{-0.077}$	39.6 ± 3.3	-	$8.6^{+2.8}_{-2.3}$
WASP-64b	U	< 0.054 (< 0.12)	-	$0.017^{+0.021}_{-0.017}$	$-0.016^{+0.024}_{-0.053}$	213 ± 12	-	< 4.6
WASP-65b	C	< 0.016 (< 0.037)	-	$-0.0016^{+0.0056}_{-0.0080}$	$-0.0049^{+0.0073}_{-0.017}$	248.4 ± 5.0	-	< 5.1
WASP-66b	C	< 0.046 (< 0.10)	-	$0.005^{+0.018}_{-0.013}$	$-0.016^{+0.022}_{-0.047}$	253^{+11}_{-12}	-	< 14.8
WASP-67b	C	< 0.015 (< 0.084)	-	$0.00055^{+0.0011}_{-0.00086}$	$0.000^{+0.016}_{-0.013}$	$56.1^{+4.4}_{-4.5}$	-	< 3.4
WASP-68b	C	< 0.023 (< 0.041)	-	$0.0116^{+0.0089}_{-0.0092}$	$-0.003^{+0.011}_{-0.017}$	$97.9^{+2.0}_{-1.9}$	$0.0389^{+0.0054}_{-0.0057}$	$7.0^{+1.4}_{-1.3}$
WASP-69b	U	< 0.11 (< 0.23)	-	$0.005^{+0.033}_{-0.028}$	$-0.052^{+0.056}_{-0.10}$	$36.9^{+3.1}_{-3.3}$	-	$10.9^{+2.2}_{-1.7}$
WASP-70Ab	U	< 0.053 (< 0.10)	-	$0.002^{+0.014}_{-0.012}$	$0.030^{+0.042}_{-0.030}$	$73.3^{+2.7}_{-2.4}$	-	$7.3^{+5.2}_{-3.4}$
WASP-71b	C	< 0.019 (< 0.035)	-	$-0.0070^{+0.0073}_{-0.0096}$	$0.0017^{+0.014}_{-0.0099}$	$234.3^{+4.2}_{-4.1}$	-	< 3.4
WASP-72b	C	< 0.017 (< 0.038)	-	$-0.0005^{+0.0069}_{-0.0093}$	$-0.000^{+0.011}_{-0.014}$	$178.8^{+4.3}_{-4.6}$	-	< 8.9
WASP-73b	C	< 0.017 (< 0.043)	-	$-0.0011^{+0.0066}_{-0.0080}$	$0.0024^{+0.018}_{-0.0096}$	196.3 ± 4.3	-	$9.8^{+3.5}_{-3.0}$
WASP-74b	C	< 0.030 (< 0.073)	-	$0.0014^{+0.012}_{-0.0097}$	$-0.005^{+0.014}_{-0.034}$	$113.0^{+3.7}_{-3.6}$	-	$12.2^{+2.7}_{-2.1}$
WASP-75b	U	< 0.056 (< 0.11)	-	$-0.009^{+0.014}_{-0.020}$	$0.030^{+0.044}_{-0.030}$	$146.6^{+5.1}_{-4.9}$	-	< 7.6
WASP-77Ab	C	< 0.0075 (< 0.014)	-	$-0.0034^{+0.0032}_{-0.0036}$	$0.0000^{+0.0046}_{-0.0047}$	$322.9^{+2.6}_{-2.3}$	-	< 4.1
WASP-78b	U	< 0.092 (< 0.17)	-	$0.037^{+0.045}_{-0.038}$	$0.002^{+0.061}_{-0.058}$	$113.6^{+9.3}_{-9.6}$	-	< 4.9
WASP-79b	U	< 0.066 (< 0.14)	-	$-0.007^{+0.026}_{-0.037}$	$0.003^{+0.056}_{-0.040}$	$88.1^{+7.8}_{-8.0}$	-	< 8.5
WASP-80b	C	< 0.020 (< 0.046)	-	$0.0008^{+0.011}_{-0.0088}$	$-0.001^{+0.011}_{-0.019}$	110.0 ± 3.4	-	< 2.9
WASP-83b	U	< 0.12 (< 0.22)	-	$-0.055^{+0.038}_{-0.036}$	$-0.031^{+0.059}_{-0.093}$	34.2 ± 3.5	-	< 2.7
WASP-84b	U	< 0.077 (< 0.14)	-	$0.038^{+0.032}_{-0.031}$	$-0.007^{+0.041}_{-0.055}$	77.7 ± 4.9	-	$13.8^{+3.3}_{-2.7}$
WASP-88b	U	< 0.13 (< 0.29)	-	$-0.041^{+0.050}_{-0.069}$	$-0.004^{+0.088}_{-0.097}$	$53.3^{+7.5}_{-6.9}$	-	< 16.5
WASP-89b	E	$0.1928^{+0.010}_{-0.0094}$	$27.9^{+3.6}_{-3.9}$	$0.1699^{+0.0083}_{-0.0079}$	$0.090^{+0.013}_{-0.014}$	847^{+14}_{-13}	-	< 6.0
WASP-94Ab	U	< 0.064 (< 0.12)	-	$0.020^{+0.029}_{-0.022}$	$-0.021^{+0.028}_{-0.049}$	45.9 ± 2.9	-	$8.2^{+2.0}_{-1.9}$
WASP-95b	C	< 0.018 (< 0.045)	-	$0.0008^{+0.0083}_{-0.0062}$	$-0.001^{+0.011}_{-0.017}$	$175.5^{+4.1}_{-4.5}$	-	$10.6^{+3.4}_{-2.5}$
WASP-96b	U	< 0.11 (< 0.20)	-	$0.039^{+0.052}_{-0.040}$	$0.037^{+0.080}_{-0.048}$	$64.0^{+5.3}_{-4.8}$	-	< 4.2
WASP-97b	C	< 0.019 (< 0.047)	-	$0.0006^{+0.0085}_{-0.0068}$	$-0.0031^{+0.0083}_{-0.022}$	$195.5^{+4.8}_{-4.6}$	-	$9.2^{+3.8}_{-2.6}$
WASP-98b	U	< 0.070 (< 0.14)	-	$-0.026^{+0.026}_{-0.032}$	$0.002^{+0.054}_{-0.044}$	154^{+11}_{-12}	-	< 6.3
WASP-99b	C	< 0.010 (< 0.025)	-	$0.0004^{+0.0051}_{-0.0040}$	$-0.0011^{+0.0057}_{-0.010}$	$244.5^{+3.4}_{-3.6}$	$0.172^{+0.038}_{-0.037}$	$9.5^{+2.7}_{-2.4}$
WASP-100b	C	< 0.044 (< 0.091)	-	$0.010^{+0.021}_{-0.014}$	$0.014^{+0.040}_{-0.020}$	$211.6^{+8.6}_{-8.2}$	-	< 6.4
WASP-101b	U	< 0.068 (< 0.16)	-	$0.002^{+0.030}_{-0.028}$	$-0.007^{+0.041}_{-0.069}$	54.3 ± 4.9	-	< 7.0
WASP-103b	U	< 0.15 (< 0.24)	-	$0.040^{+0.044}_{-0.037}$	$0.090^{+0.082}_{-0.079}$	268 ± 15	-	< 7.7
WASP-104b	C	< 0.015 (< 0.036)	-	$-0.0006^{+0.0056}_{-0.0075}$	$0.0011^{+0.015}_{-0.0087}$	$202.0^{+5.0}_{-4.6}$	-	< 5.5
WASP-106b	C	< 0.046 (< 0.088)	-	$-0.010^{+0.012}_{-0.016}$	$0.024^{+0.036}_{-0.024}$	164.5 ± 4.6	-	< 5.8
WASP-117b	E	0.300 ± 0.026	$241.5^{+2.8}_{-3.2}$	$-0.1429^{+0.0086}_{-0.0087}$	-0.264 ± 0.029	$25.21^{+0.79}_{-0.73}$	-	< 1.3
WTS-2b	U	$0.27^{+0.19}_{-0.11}$	293^{+29}_{-15}	$0.126^{+0.040}_{-0.028}$	$-0.22^{+0.19}_{-0.23}$	302^{+94}_{-50}	-	< 20.0
XO-1b	C	< 0.019 (< 0.043)	-	0.0012 ± 0.0011	$-0.0081^{+0.0087}_{-0.022}$	$115.3^{+1.9}_{-1.7}$	-	< 3.5
XO-2Nb	C	< 0.006 (< 0.014)	-	$-0.0009^{+0.0034}_{-0.0022}$	$-0.0004^{+0.0040}_{-0.0061}$	90.17 ± 0.82	CURV	2.6 ± 0.7
XO-3b	E	$0.27587^{+0.00071}_{-0.00067}$	$349.35^{+0.67}_{-0.68}$	$0.27111^{+0.00034}_{-0.00033}$	$-0.0510^{+0.0033}_{-0.0034}$	$1468.9^{+4.6}_{-4.5}$	-	$29.2^{+10.}_{-7.8}$
XO-4b	C	< 0.0039 (< 0.017)	-	$0.00012^{+0.00061}_{-0.00051}$	$0.0001^{+0.0050}_{-0.0029}$	$169.6^{+2.3}_{-2.4}$	-	$10.2^{+4.2}_{-2.8}$
XO-5b	C	< 0.021 (< 0.042)	-	$-0.0057^{+0.0079}_{-0.014}$	$-0.001^{+0.012}_{-0.015}$	143.5 ± 3.0	-	$10.8^{+2.2}_{-1.8}$

Table 8. continued.

Planet	Flag	e	ω [deg]	$e\cos\omega$	$e\sin\omega$	K [m s^{-1}]	$\dot{\gamma}$ [m s^{-1} day^{-1}]	Jitter [m s^{-1}]

Table 9. Orbital and physical parameters of the 231 transiting giant planets considered in this work. They were derived from our orbital fits and the system parameters listed in Table 7. Upper limits of 1σ on the eccentricity are given for both well-determined circular orbits and undetermined eccentricities, as reported in the second column of Table 8 ('C' or 'U').

Planet	P	a	e	$M_{\rm p}$	$\rho_{\rm p}$	$\log g_{\rm p}$
	[days]	au		[$M_{\rm Jup}$]	[g cm^{-3}]	[cgs]
CoRoT-1b	1.509	$0.02752^{+0.00022}_{-0.00023}$	< 0.036	1.23 ± 0.10	$0.302^{+0.031}_{-0.028}$	$3.015^{+0.038}_{-0.040}$
CoRoT-2b	1.743	$0.02810^{+0.00057}_{-0.00058}$	< 0.024	$3.30^{+0.19}_{-0.18}$	$1.30^{+0.14}_{-0.13}$	3.581 ± 0.036
CoRoT-3b	4.257	$0.0574^{+0.0012}_{-0.0013}$	< 0.016	$21.44^{+0.96}_{-0.97}$	$25.9^{+6.4}_{-4.9}$	$4.718^{+0.065}_{-0.063}$
CoRoT-4b	9.202	$0.09025^{+0.00068}_{-0.00055}$	< 0.14	$0.703^{+0.071}_{-0.073}$	$0.517^{+0.099}_{-0.082}$	$3.090^{+0.058}_{-0.062}$
CoRoT-5b	4.038	$0.04963^{+0.00033}_{-0.00032}$	< 0.087	0.478 ± 0.035	$0.221^{+0.030}_{-0.026}$	$2.788^{+0.043}_{-0.044}$
CoRoT-6b	8.887	$0.0854^{+0.0013}_{-0.0014}$	< 0.18	2.95 ± 0.28	$2.30^{+0.32}_{-0.29}$	$3.730^{+0.048}_{-0.050}$
CoRoT-8b	6.212	$0.06339^{+0.00096}_{-0.00098}$	< 0.19	$0.218^{+0.033}_{-0.041}$	1.45 ± 0.29	$3.219^{+0.069}_{-0.093}$
CoRoT-9b	95.273	$0.4029^{+0.0054}_{-0.0056}$	$0.134^{+0.040}_{-0.034}$	$0.846^{+0.056}_{-0.057}$	$0.91^{+0.21}_{-0.16}$	$3.280^{+0.062}_{-0.060}$
CoRoT-10b	13.241	$0.1055^{+0.0019}_{-0.0020}$	0.524 ± 0.018	2.73 ± 0.14	$3.69^{+0.96}_{-0.70}$	$3.855^{+0.069}_{-0.063}$
CoRoT-11b	2.994	$0.04407^{+0.00056}_{-0.00059}$	< 0.36	$2.62^{+0.59}_{-0.62}$	$1.11^{+0.26}_{-0.27}$	$3.502^{+0.090}_{-0.12}$
CoRoT-12b	2.828	$0.04013^{+0.00090}_{-0.00093}$	< 0.050	$0.915^{+0.071}_{-0.069}$	$0.381^{+0.13}_{-0.091}$	$3.040^{+0.086}_{-0.082}$
CoRoT-13b	4.035	$0.05107^{+0.00030}_{-0.00031}$	< 0.067	1.331 ± 0.073	$2.38^{+0.18}_{-0.17}$	$3.624^{+0.027}_{-0.028}$
CoRoT-14b	1.512	$0.02691^{+0.00070}_{-0.00073}$	< 0.036	7.42 ± 0.47	$7.1^{+1.7}_{-1.3}$	$4.190^{+0.064}_{-0.061}$
CoRoT-16b	5.352	0.0618 ± 0.0015	$0.37^{+0.11}_{-0.12}$	$0.529^{+0.098}_{-0.096}$	$0.41^{+0.22}_{-0.14}$	$2.98^{+0.14}_{-0.13}$
CoRoT-17b	3.768	$0.0481^{+0.0015}_{-0.0016}$	< 0.081	$2.41^{+0.27}_{-0.26}$	$2.81^{+0.77}_{-0.58}$	$3.758^{+0.080}_{-0.076}$
CoRoT-18b	1.900	$0.0295^{+0.0015}_{-0.0017}$	< 0.025	3.46 ± 0.38	$1.91^{+1.1}_{-0.62}$	$3.70^{+0.14}_{-0.12}$
CoRoT-19b	3.897	$0.05166^{+0.00069}_{-0.00070}$	< 0.056	1.155 ± 0.072	$0.668^{+0.063}_{-0.061}$	$3.236^{+0.033}_{-0.035}$
CoRoT-20b	9.243	$0.0901^{+0.0021}_{-0.0022}$	$0.575^{+0.016}_{-0.014}$	$4.23^{+0.26}_{-0.25}$	$8.9^{+1.5}_{-1.2}$	$4.172^{+0.051}_{-0.048}$
CoRoT-21b	2.725	$0.04160^{+0.00094}_{-0.00100}$	< 0.39	2.22 ± 0.56	$1.24^{+0.62}_{-0.43}$	$3.51^{+0.14}_{-0.15}$
CoRoT-23b	3.631	$0.0484^{+0.0011}_{-0.0012}$	< 0.16	3.09 ± 0.33	$3.3^{+1.7}_{-1.0}$	$3.84^{+0.13}_{-0.11}$
CoRoT-25b	4.861	$0.05789^{+0.0019}_{-0.00093}$	< 0.22	$0.293^{+0.061}_{-0.060}$	$0.24^{+0.14}_{-0.12}$	$2.74^{+0.15}_{-0.21}$
CoRoT-26b	4.205	$0.05250^{+0.00094}_{-0.00098}$	< 0.41	$0.58^{+0.20}_{-0.11}$	$0.360^{+0.036}_{-0.026}$	$2.952^{+0.070}_{-0.044}$
CoRoT-27b	3.575	$0.0467^{+0.0015}_{-0.0017}$	< 0.034	$10.30^{+0.81}_{-0.83}$	$12.5^{+2.1}_{-1.7}$	4.400 ± 0.051
CoRoT-28b	5.209	$0.0590^{+0.0027}_{-0.0028}$	< 0.071	0.481 ± 0.056	$0.68^{+0.19}_{-0.14}$	$3.115^{+0.081}_{-0.078}$
CoRoT-29b	2.851	$0.0390^{+0.0018}_{-0.0020}$	< 0.12	$0.84^{+0.13}_{-0.12}$	$1.44^{+1.2}_{-0.58}$	$3.41^{+0.18}_{-0.16}$
HAT-P-1b	4.465	$0.0553^{+0.0012}_{-0.0013}$	< 0.011	0.525 ± 0.026	$0.339^{+0.052}_{-0.042}$	$2.925^{+0.044}_{-0.041}$
HAT-P-2b	5.633	$0.06880^{+0.00065}_{-0.00070}$	$0.50833^{+0.00082}_{-0.00075}$	$8.70^{+0.19}_{-0.20}$	$7.3^{+1.4}_{-1.1}$	$4.221^{+0.053}_{-0.048}$
HAT-P-3b	2.900	$0.03899^{+0.00062}_{-0.00065}$	< 0.0100	$0.609^{+0.021}_{-0.022}$	$1.04^{+0.18}_{-0.15}$	$3.271^{+0.048}_{-0.045}$
HAT-P-4b	3.057	$0.04449^{+0.00083}_{-0.0012}$	< 0.0073	$0.651^{+0.033}_{-0.037}$	$0.380^{+0.029}_{-0.030}$	2.988 ± 0.019
HAT-P-5b	2.788	$0.04073^{+0.00050}_{-0.00093}$	< 0.072	1.02 ± 0.10	$0.642^{+0.12}_{-0.097}$	$3.207^{+0.057}_{-0.059}$
HAT-P-6b	3.853	$0.05239^{+0.00080}_{-0.00082}$	< 0.044	$1.106^{+0.039}_{-0.040}$	$0.583^{+0.091}_{-0.078}$	$3.190^{+0.044}_{-0.043}$
HAT-P-7b	2.205	0.03813 ± 0.00036	< 0.0040	1.806 ± 0.036	$0.651^{+0.029}_{-0.028}$	3.293 ± 0.014
HAT-P-8b	3.076	$0.04496^{+0.00046}_{-0.00045}$	< 0.0060	1.354 ± 0.035	$0.497^{+0.078}_{-0.065}$	$3.173^{+0.043}_{-0.041}$
HAT-P-9b	3.923	$0.0529^{+0.0017}_{-0.0018}$	< 0.16	$0.761^{+0.10}_{-0.092}$	$0.344^{+0.069}_{-0.058}$	$2.983^{+0.066}_{-0.069}$
HAT-P-12b	3.213	$0.03838^{+0.00031}_{-0.00033}$	< 0.035	$0.2084^{+0.0096}_{-0.0094}$	0.296 ± 0.026	$2.752^{+0.029}_{-0.030}$
HAT-P-13b	2.916	$0.04270^{+0.00058}_{-0.0012}$	< 0.013	$0.883^{+0.027}_{-0.047}$	$0.517^{+0.11}_{-0.087}$	$3.121^{+0.059}_{-0.056}$
HAT-P-14b	4.628	$0.06062^{+0.00065}_{-0.00067}$	$0.1074^{+0.0076}_{-0.0079}$	2.303 ± 0.054	$1.88^{+0.29}_{-0.24}$	$3.635^{+0.042}_{-0.040}$
HAT-P-15b	10.863	$0.0965^{+0.0013}_{-0.0014}$	$0.200^{+0.026}_{-0.028}$	$1.949^{+0.080}_{-0.078}$	$1.96^{+0.27}_{-0.23}$	3.624 ± 0.039
HAT-P-16b	2.776	$0.04134^{+0.00044}_{-0.00045}$	$0.0462^{+0.0027}_{-0.0024}$	4.221 ± 0.092	$2.45^{+0.42}_{-0.34}$	$3.800^{+0.046}_{-0.044}$
HAT-P-17b	10.339	$0.0882^{+0.0013}_{-0.0014}$	0.3417 ± 0.0036	0.537 ± 0.017	$0.647^{+0.062}_{-0.056}$	$3.116^{+0.029}_{-0.028}$
HAT-P-18b	5.508	0.05596 ± 0.00074	< 0.087	0.200 ± 0.019	$0.251^{+0.052}_{-0.042}$	$2.698^{+0.062}_{-0.061}$
HAT-P-19b	4.009	$0.04664^{+0.00076}_{-0.00078}$	< 0.024	0.284 ± 0.016	$0.242^{+0.055}_{-0.043}$	$2.740^{+0.062}_{-0.059}$
HAT-P-20b	2.875	$0.03617^{+0.00043}_{-0.00045}$	$0.0158^{+0.0023}_{-0.0018}$	7.27 ± 0.18	$13.8^{+1.7}_{-1.5}$	$4.380^{+0.035}_{-0.034}$
HAT-P-21b	4.124	$0.04950^{+0.00072}_{-0.00075}$	0.2170 ± 0.0100	3.97 ± 0.13	$4.6^{+1.5}_{-1.0}$	$3.971^{+0.083}_{-0.075}$
HAT-P-22b	3.212	$0.04142^{+0.00053}_{-0.00054}$	< 0.0020	$2.172^{+0.055}_{-0.056}$	$2.14^{+0.39}_{-0.31}$	$3.664^{+0.050}_{-0.046}$
HAT-P-23b	1.213	0.02320 ± 0.00024	< 0.052	1.97 ± 0.12	$0.96^{+0.23}_{-0.18}$	$3.418^{+0.064}_{-0.063}$
HAT-P-24b	3.355	$0.04651^{+0.00055}_{-0.00056}$	< 0.038	$0.723^{+0.031}_{-0.030}$	$0.467^{+0.089}_{-0.070}$	$3.065^{+0.052}_{-0.049}$
HAT-P-25b	3.653	$0.04659^{+0.00049}_{-0.00050}$	< 0.033	0.567 ± 0.022	$0.427^{+0.074}_{-0.070}$	$3.002^{+0.049}_{-0.053}$
HAT-P-27b	3.040	$0.03998^{+0.00084}_{-0.00091}$	< 0.028	0.616 ± 0.030	$0.76^{+0.17}_{-0.13}$	$3.183^{+0.059}_{-0.055}$
HAT-P-28b	3.257	$0.04337^{+0.00066}_{-0.00070}$	< 0.039	0.637 ± 0.037	$0.459^{+0.12}_{-0.098}$	$3.041^{+0.069}_{-0.071}$
HAT-P-29b	5.723	$0.06669^{+0.00084}_{-0.00086}$	$0.104^{+0.021}_{-0.018}$	$0.676^{+0.035}_{-0.034}$	0.62 ± 0.18	$3.138^{+0.077}_{-0.096}$

Table 9. continued.

Planet	P [days]	a au	e	M_p [M_{Jup}]	ρ_p [g cm^{-3}]	$\log g_p$ [cgs]
HAT-P-30b	2.811	0.04190 ± 0.00046	< 0.016	$0.746^{+0.020}_{-0.021}$	$0.385^{+0.062}_{-0.053}$	3.013 ± 0.044
HAT-P-31b	5.005	$0.0610^{+0.0013}_{-0.0011}$	$0.2617^{+0.0093}_{-0.0095}$	$2.147^{+0.090}_{-0.078}$	$2.30^{+1.5}_{-0.92}$	3.68 ± 0.14
HAT-P-32b	2.150	$0.03427^{+0.00040}_{-0.00042}$	< 0.044	0.75 ± 0.13	$0.163^{+0.029}_{-0.028}$	$2.767^{+0.070}_{-0.080}$
HAT-P-33b	3.474	$0.04995^{+0.00048}_{-0.00049}$	< 0.22	0.66 ± 0.14	$0.170^{+0.039}_{-0.037}$	$2.758^{+0.087}_{-0.10}$
HAT-P-34b	5.453	$0.06774^{+0.00074}_{-0.00076}$	$0.432^{+0.029}_{-0.027}$	$3.33^{+0.21}_{-0.20}$	$2.50^{+0.75}_{-0.60}$	$3.772^{+0.078}_{-0.080}$
HAT-P-35b	3.647	$0.04978^{+0.00064}_{-0.00066}$	< 0.020	1.056 ± 0.033	$0.55^{+0.14}_{-0.11}$	$3.169^{+0.067}_{-0.063}$
HAT-P-36b	1.327	$0.02382^{+0.00038}_{-0.00039}$	< 0.059	1.85 ± 0.10	$1.13^{+0.23}_{-0.18}$	$3.457^{+0.055}_{-0.053}$
HAT-P-37b	2.797	$0.03793^{+0.00056}_{-0.00058}$	< 0.14	$1.20^{+0.12}_{-0.11}$	$0.91^{+0.23}_{-0.17}$	$3.332^{+0.072}_{-0.068}$
HAT-P-38b	4.640	$0.05231^{+0.00085}_{-0.00089}$	< 0.055	0.267 ± 0.020	$0.60^{+0.19}_{-0.15}$	$2.994^{+0.084}_{-0.087}$
HAT-P-39b	3.544	$0.05095^{+0.00062}_{-0.00063}$	< 0.17	$0.569^{+0.089}_{-0.11}$	$0.1836^{+0.0060}_{-0.0080}$	$2.761^{+0.019}_{-0.036}$
HAT-P-40b	4.457	$0.06076^{+0.00062}_{-0.0015}$	< 0.12	$0.581^{+0.033}_{-0.034}$	$0.138^{+0.018}_{-0.015}$	$2.681^{+0.040}_{-0.039}$
HAT-P-41b	2.694	$0.04258^{+0.00047}_{-0.00048}$	< 0.22	$0.795^{+0.056}_{-0.091}$	$0.2040^{+0.0060}_{-0.0088}$	$2.836^{+0.015}_{-0.023}$
HAT-P-42b	4.642	0.0575 ± 0.0011	< 0.11	$0.88^{+0.14}_{-0.13}$	$0.52^{+0.25}_{-0.16}$	3.13 ± 0.12
HAT-P-43b	3.333	$0.04445^{+0.00045}_{-0.00053}$	< 0.21	$0.73^{+0.32}_{-0.14}$	$0.431^{+0.11}_{-0.054}$	$3.042^{+0.12}_{-0.070}$
HAT-P-45b	3.129	$0.04521^{+0.00069}_{-0.00070}$	< 0.11	$0.86^{+0.11}_{-0.12}$	$0.358^{+0.025}_{-0.067}$	$3.001^{+0.019}_{-0.034}$
HAT-P-49b	2.692	$0.04378^{+0.00048}_{-0.00049}$	< 0.12	1.77 ± 0.22	$0.78^{+0.20}_{-0.18}$	$3.341^{+0.078}_{-0.091}$
HAT-P-50b	3.122	$0.04527^{+0.00058}_{-0.0015}$	< 0.084	$1.359^{+0.070}_{-0.086}$	$0.79^{+0.14}_{-0.11}$	3.306 ± 0.050
HAT-P-51b	4.218	$0.05067^{+0.00048}_{-0.00047}$	< 0.070	0.311 ± 0.019	$0.178^{+0.027}_{-0.022}$	$2.662^{+0.046}_{-0.044}$
HAT-P-52b	2.754	$0.03696^{+0.00037}_{-0.00038}$	< 0.030	$0.817^{+0.041}_{-0.039}$	$0.98^{+0.25}_{-0.18}$	$3.298^{+0.068}_{-0.063}$
HAT-P-53b	1.962	$0.03160^{+0.00041}_{-0.00043}$	< 0.085	$1.477^{+0.042}_{-0.044}$	$0.80^{+0.19}_{-0.14}$	$3.323^{+0.064}_{-0.058}$
HAT-P-54b	3.800	0.04122 ± 0.00043	< 0.66	$1.82^{+2.3}_{-0.98}$	$2.7^{+3.4}_{-1.5}$	$3.70^{+0.35}_{-0.34}$
HAT-P-55b	3.585	$0.04604^{+0.00056}_{-0.00055}$	< 0.17	$0.580^{+0.053}_{-0.054}$	$0.435^{+0.080}_{-0.066}$	3.012 ± 0.057
HAT-P-56b	2.791	$0.04232^{+0.00038}_{-0.00041}$	< 0.29	$1.90^{+0.22}_{-0.28}$	$0.75^{+0.11}_{-0.12}$	$3.342^{+0.051}_{-0.073}$
HATS-1b	3.446	$0.04446^{+0.00080}_{-0.00084}$	< 0.082	1.75 ± 0.19	$0.99^{+0.31}_{-0.29}$	$3.409^{+0.089}_{-0.11}$
HATS-2b	1.354	0.02298 ± 0.00032	< 0.29	$1.53^{+0.12}_{-0.23}$	$1.17^{+0.14}_{-0.18}$	$3.440^{+0.042}_{-0.072}$
HATS-3b	3.548	$0.04852^{+0.00053}_{-0.00054}$	< 0.30	$1.10^{+0.18}_{-0.19}$	$0.516^{+0.096}_{-0.091}$	$3.154^{+0.070}_{-0.081}$
HATS-4b	2.517	$0.03623^{+0.00024}_{-0.00025}$	< 0.024	$1.309^{+0.040}_{-0.039}$	$1.53^{+0.19}_{-0.16}$	3.494 ± 0.034
HATS-5b	4.763	$0.05428^{+0.00056}_{-0.00060}$	< 0.044	0.238 ± 0.014	$0.389^{+0.041}_{-0.039}$	$2.851^{+0.034}_{-0.036}$
HATS-7b	3.185	$0.04012^{+0.00043}_{-0.00044}$	< 0.12	0.123 ± 0.014	$0.88^{+0.24}_{-0.19}$	$2.994^{+0.077}_{-0.082}$
HATS-8b	3.584	$0.04668^{+0.00053}_{-0.00057}$	< 0.25	0.145 ± 0.026	$0.277^{+0.026}_{-0.052}$	$2.671^{+0.015}_{-0.031}$
HATS-9b	1.915	$0.03048^{+0.00038}_{-0.00037}$	< 0.075	$0.823^{+0.041}_{-0.039}$	$0.84^{+0.29}_{-0.20}$	$3.255^{+0.087}_{-0.080}$
HATS-10b	3.313	$0.04493^{+0.00071}_{-0.00076}$	< 0.28	$0.585^{+0.097}_{-0.12}$	$0.799^{+0.040}_{-0.067}$	$3.191^{+0.028}_{-0.057}$
HATS-13b	3.044	$0.04059^{+0.00041}_{-0.00042}$	< 0.22	$0.592^{+0.087}_{-0.098}$	$0.413^{+0.067}_{-0.074}$	$3.001^{+0.060}_{-0.083}$
HATS-14b	2.767	$0.03815^{+0.00032}_{-0.00031}$	< 0.11	$1.069^{+0.094}_{-0.097}$	1.19 ± 0.14	$3.391^{+0.045}_{-0.048}$
HD-149026b	2.876	0.04364 ± 0.00022	< 0.013	$0.322^{+0.014}_{-0.012}$	$0.750^{+0.089}_{-0.077}$	$3.085^{+0.035}_{-0.034}$
HD-17156b	21.216	0.16278 ± 0.00076	$0.6703^{+0.0014}_{-0.0013}$	3.235 ± 0.032	$3.123^{+0.066}_{-0.063}$	3.8316 ± 0.0068
HD-189733b	2.219	$0.03100^{+0.00059}_{-0.00061}$	< 0.0039	1.123 ± 0.045	$0.943^{+0.081}_{-0.072}$	$3.332^{+0.027}_{-0.026}$
HD-209458b	3.525	$0.04707^{+0.00045}_{-0.00047}$	< 0.0081	$0.682^{+0.014}_{-0.015}$	$0.333^{+0.014}_{-0.013}$	$2.958^{+0.014}_{-0.013}$
HD-80606b	111.437	$0.4565^{+0.0051}_{-0.0053}$	$0.93226^{+0.00064}_{-0.00069}$	$4.116^{+0.097}_{-0.100}$	$5.06^{+0.38}_{-0.35}$	4.006 ± 0.022
KELT-2Ab	4.114	0.05497 ± 0.00037	< 0.081	$1.527^{+0.087}_{-0.088}$	$0.91^{+0.13}_{-0.12}$	$3.365^{+0.044}_{-0.047}$
KELT-3b	2.703	0.04123 ± 0.00066	< 0.035	$1.478^{+0.063}_{-0.062}$	$0.75^{+0.15}_{-0.11}$	$3.307^{+0.052}_{-0.050}$
KELT-6b	7.846	0.0804 ± 0.0014	< 0.036	0.442 ± 0.019	$0.333^{+0.12}_{-0.079}$	$2.895^{+0.088}_{-0.079}$
KELT-8b	3.244	$0.04550^{+0.00083}_{-0.00088}$	< 0.047	$0.858^{+0.053}_{-0.051}$	$0.165^{+0.054}_{-0.039}$	$2.788^{+0.085}_{-0.081}$
Kepler-5b	3.548	$0.05071^{+0.00051}_{-0.00064}$	< 0.043	$2.126^{+0.095}_{-0.093}$	$0.898^{+0.10}_{-0.091}$	3.410 ± 0.034
Kepler-6b	3.235	$0.04448^{+0.0019}_{-0.00084}$	< 0.060	$0.647^{+0.055}_{-0.041}$	$0.490^{+0.026}_{-0.028}$	3.062 ± 0.018
Kepler-7b	4.885	$0.0633^{+0.0012}_{-0.0013}$	< 0.026	$0.449^{+0.051}_{-0.048}$	$0.124^{+0.016}_{-0.015}$	$2.612^{+0.048}_{-0.052}$
Kepler-8b	3.522	$0.04835^{+0.00083}_{-0.00089}$	< 0.18	$0.56^{+0.14}_{-0.13}$	$0.244^{+0.069}_{-0.064}$	$2.84^{+0.10}_{-0.12}$
Kepler-12b	4.438	$0.05563^{+0.00084}_{-0.00085}$	< 0.021	$0.433^{+0.042}_{-0.040}$	$0.110^{+0.013}_{-0.012}$	$2.572^{+0.043}_{-0.045}$
Kepler-15b	4.943	$0.05705^{+0.00069}_{-0.00066}$	< 0.068	$0.633^{+0.046}_{-0.045}$	$0.89^{+0.21}_{-0.17}$	$3.232^{+0.066}_{-0.064}$
Kepler-17b	1.486	$0.02680^{+0.00046}_{-0.00048}$	< 0.020	$2.47^{+0.12}_{-0.11}$	$1.30^{+0.14}_{-0.12}$	3.539 ± 0.033
Kepler-39b	21.087	$0.1635^{+0.0027}_{-0.0028}$	< 0.13	20.1 ± 1.1	$13.0^{+3.7}_{-2.7}$	$4.510^{+0.074}_{-0.069}$
Kepler-40b	6.873	$0.0804^{+0.0031}_{-0.0035}$	< 0.15	2.07 ± 0.33	$0.86^{+0.27}_{-0.21}$	$3.392^{+0.095}_{-0.097}$
Kepler-41b	1.856	0.03097 ± 0.00036	< 0.21	$0.566^{+0.069}_{-0.067}$	$0.327^{+0.043}_{-0.041}$	$2.926^{+0.052}_{-0.057}$
Kepler-43b	3.024	$0.04436^{+0.00046}_{-0.00047}$	< 0.028	$3.140^{+0.087}_{-0.088}$	$2.53^{+0.24}_{-0.22}$	3.766 ± 0.028
Kepler-44b	3.247	$0.0446^{+0.0011}_{-0.0010}$	< 0.070	$0.981^{+0.10}_{-0.097}$	$0.94^{+0.23}_{-0.18}$	$3.310^{+0.071}_{-0.070}$

Table 9. continued.

Planet	P [days]	a au	e	M_p [M_{Jup}]	ρ_p [g cm^{-3}]	$\log g_p$ [cgs]
Kepler-45b	2.455	$0.02987^{+0.00099}_{-0.0010}$	< 0.23	$0.484^{+0.073}_{-0.071}$	$0.68^{+0.33}_{-0.21}$	3.11 ± 0.12
Kepler-74b	7.341	$0.07813^{+0.00084}_{-0.00088}$	< 0.32	$0.604^{+0.088}_{-0.094}$	0.85 ± 0.14	$3.211^{+0.061}_{-0.076}$
Kepler-75b	8.885	0.0817 ± 0.0012	$0.5704^{+0.0093}_{-0.0094}$	$10.10^{+0.36}_{-0.35}$	$10.83^{+1.1}_{-0.93}$	4.357 ± 0.029
Kepler-76b	1.545	$0.0278^{+0.0015}_{-0.0016}$	< 0.078	$2.00^{+0.27}_{-0.26}$	$1.26^{+0.34}_{-0.27}$	$3.499^{+0.081}_{-0.082}$
Kepler-77b	3.579	$0.04502^{+0.00063}_{-0.00065}$	< 0.079	$0.522^{+0.042}_{-0.040}$	$0.732^{+0.070}_{-0.066}$	$3.147^{+0.036}_{-0.037}$
Kepler-412b	1.721	$0.02961^{+0.00075}_{-0.00079}$	< 0.076	$0.927^{+0.076}_{-0.071}$	$0.494^{+0.065}_{-0.057}$	$3.117^{+0.044}_{-0.043}$
Kepler-419b	69.755	$0.3704^{+0.0064}_{-0.0068}$	$0.800^{+0.087}_{-0.097}$	$2.58^{+0.78}_{-0.75}$	$3.5^{+2.3}_{-1.4}$	$3.84^{+0.17}_{-0.18}$
Kepler-422b	7.891	0.0813 ± 0.0014	< 0.55	$0.49^{+0.23}_{-0.12}$	$0.42^{+0.22}_{-0.15}$	2.99 ± 0.16
Kepler-423b	2.684	$0.03582^{+0.00056}_{-0.00057}$	< 0.079	$0.606^{+0.063}_{-0.061}$	$0.443^{+0.082}_{-0.068}$	$3.024^{+0.059}_{-0.061}$
Kepler-424b	3.312	$0.04365^{+0.00077}_{-0.00081}$	< 0.076	$1.076^{+0.096}_{-0.092}$	$1.97^{+0.56}_{-0.44}$	$3.540^{+0.076}_{-0.080}$
Kepler-425b	3.797	$0.04652^{+0.00082}_{-0.00086}$	< 0.20	0.226 ± 0.046	$0.299^{+0.068}_{-0.063}$	$2.767^{+0.085}_{-0.10}$
Kepler-426b	3.218	$0.04135^{+0.00088}_{-0.00095}$	< 0.12	$0.337^{+0.058}_{-0.060}$	$0.321^{+0.065}_{-0.060}$	$2.845^{+0.075}_{-0.087}$
Kepler-427b	10.291	0.0913 ± 0.0019	< 0.27	0.292 ± 0.054	$0.195^{+0.15}_{-0.078}$	$2.68^{+0.18}_{-0.16}$
Kepler-428b	3.526	$0.04331^{+0.00080}_{-0.00083}$	< 0.11	1.28 ± 0.13	$1.26^{+0.18}_{-0.16}$	$3.435^{+0.049}_{-0.052}$
Kepler-432b	52.501	$0.3025^{+0.0064}_{-0.0056}$	0.4775 ± 0.0073	$0.575^{+0.025}_{-0.023}$	$0.476^{+0.056}_{-0.048}$	$3.037^{+0.035}_{-0.034}$
Kepler-433b	5.334	$0.0678^{+0.0025}_{-0.0028}$	< 0.15	$2.81^{+0.45}_{-0.41}$	$1.14^{+0.53}_{-0.34}$	3.52 ± 0.12
Kepler-434b	12.875	$0.1142^{+0.0029}_{-0.0030}$	< 0.13	$2.98^{+0.31}_{-0.29}$	$2.8^{+2.2}_{-1.2}$	3.79 ± 0.17
Kepler-435b	8.600	$0.0949^{+0.0018}_{-0.0019}$	< 0.18	0.85 ± 0.13	$0.134^{+0.051}_{-0.035}$	2.73 ± 0.10
OGLE-TR-10b	3.101	$0.04350^{+0.00091}_{-0.0012}$	< 0.82	$1.13^{+1.6}_{-0.39}$	$0.815^{+0.87}_{-0.073}$	$3.292^{+0.33}_{-0.093}$
OGLE-TR-56b	1.212	$0.02385^{+0.00047}_{-0.00049}$	< 0.67	$3.3^{+4.0}_{-1.6}$	$1.59^{+2.0}_{-0.81}$	$3.64^{+0.35}_{-0.30}$
OGLE-TR-111b	4.014	$0.04689^{+0.00099}_{-0.0010}$	< 0.54	$0.78^{+0.62}_{-0.28}$	$0.84^{+0.65}_{-0.33}$	$3.24^{+0.25}_{-0.20}$
OGLE-TR-113b	1.432	0.02290 ± 0.00016	< 0.15	$1.36^{+0.16}_{-0.15}$	$1.32^{+0.18}_{-0.17}$	$3.456^{+0.051}_{-0.057}$
OGLE-TR-132b	1.690	0.03036 ± 0.00055	< 0.60	$2.7^{+3.4}_{-1.5}$	$2.01^{+1.8}_{-0.75}$	$3.68^{+0.30}_{-0.25}$
OGLE-TR-182b	3.979	$0.05205^{+0.00057}_{-0.00059}$	< 0.27	$1.07^{+0.15}_{-0.20}$	$0.41^{+0.16}_{-0.11}$	3.08 ± 0.11
OGLE-TR-211b	3.677	$0.05106^{+0.00073}_{-0.00076}$	< 0.58	$0.68^{+0.24}_{-0.28}$	$0.420^{+0.058}_{-0.12}$	$3.023^{+0.078}_{-0.17}$
Qatar-1b	1.420	0.02343 ± 0.00028	< 0.012	$1.321^{+0.041}_{-0.040}$	$0.99^{+0.27}_{-0.19}$	$3.370^{+0.071}_{-0.065}$
Qatar-2b	1.337	$0.02153^{+0.00020}_{-0.00019}$	< 0.011	2.470 ± 0.052	$1.552^{+0.057}_{-0.054}$	$3.590^{+0.013}_{-0.012}$
TrES-1b	3.030	$0.03926^{+0.00058}_{-0.00060}$	< 0.012	$0.697^{+0.028}_{-0.027}$	$0.712^{+0.055}_{-0.050}$	3.181 ± 0.025
TrES-2b	2.471	$0.03557^{+0.00073}_{-0.00074}$	< 0.0028	$1.212^{+0.051}_{-0.050}$	$0.820^{+0.092}_{-0.085}$	$3.302^{+0.033}_{-0.034}$
TrES-3b	1.306	$0.02284^{+0.00024}_{-0.00037}$	< 0.043	$1.801^{+0.078}_{-0.083}$	0.917 ± 0.024	$3.3914^{+0.0021}_{-0.0013}$
TrES-4b	3.554	$0.05159^{+0.00059}_{-0.00061}$	< 0.015	$0.498^{+0.033}_{-0.032}$	$0.099^{+0.017}_{-0.014}$	$2.562^{+0.052}_{-0.048}$
TrES-5b	1.482	$0.02452^{+0.00021}_{-0.00022}$	< 0.030	$1.790^{+0.071}_{-0.070}$	$1.257^{+0.085}_{-0.079}$	3.482 ± 0.023
WASP-1b	2.520	$0.03958^{+0.00047}_{-0.00049}$	< 0.013	$0.948^{+0.029}_{-0.028}$	$0.339^{+0.037}_{-0.034}$	$3.011^{+0.031}_{-0.032}$
WASP-2b	2.152	$0.0314^{+0.0013}_{-0.0015}$	< 0.013	$0.925^{+0.081}_{-0.088}$	$0.93^{+0.27}_{-0.20}$	$3.301^{+0.078}_{-0.077}$
WASP-3b	1.847	$0.03182^{+0.00080}_{-0.00085}$	< 0.0058	1.89 ± 0.12	$0.822^{+0.10}_{-0.089}$	$3.368^{+0.040}_{-0.039}$
WASP-4b	1.338	0.022870 ± 0.000090	< 0.0033	1.170 ± 0.015	$0.61^{+0.30}_{-0.18}$	$3.213^{+0.12}_{-0.098}$
WASP-5b	1.628	0.02739 ± 0.00039	< 0.012	$1.590^{+0.053}_{-0.052}$	$1.21^{+0.20}_{-0.16}$	$3.455^{+0.044}_{-0.043}$
WASP-6b	3.361	$0.04217^{+0.00079}_{-0.0012}$	< 0.070	$0.483^{+0.026}_{-0.030}$	$0.326^{+0.048}_{-0.043}$	$2.902^{+0.043}_{-0.046}$
WASP-7b	4.955	$0.06188^{+0.00098}_{-0.0010}$	< 0.049	$1.083^{+0.093}_{-0.088}$	$0.53^{+0.14}_{-0.10}$	$3.159^{+0.071}_{-0.068}$
WASP-8b	8.159	0.0801 ± 0.0015	0.3057 ± 0.0046	$2.132^{+0.080}_{-0.081}$	$2.47^{+0.39}_{-0.17}$	$3.706^{+0.043}_{-0.026}$
WASP-10b	3.093	$0.0378^{+0.0013}_{-0.0014}$	$0.0601^{+0.0064}_{-0.0046}$	$3.21^{+0.23}_{-0.24}$	$3.28^{+0.71}_{-0.58}$	3.844 ± 0.061
WASP-11b	3.722	$0.04376^{+0.00067}_{-0.00071}$	< 0.030	$0.532^{+0.021}_{-0.020}$	$0.679^{+0.054}_{-0.049}$	3.128 ± 0.025
WASP-12b	1.091	$0.02312^{+0.00094}_{-0.0010}$	< 0.020	1.39 ± 0.12	$0.283^{+0.054}_{-0.044}$	$3.015^{+0.057}_{-0.059}$
WASP-13b	4.353	$0.0558^{+0.0018}_{-0.0019}$	< 0.016	$0.525^{+0.035}_{-0.037}$	$0.182^{+0.036}_{-0.030}$	2.745 ± 0.057
WASP-14b	2.244	$0.0358^{+0.0012}_{-0.0013}$	$0.0782^{+0.0014}_{-0.0012}$	$7.22^{+0.49}_{-0.50}$	$4.23^{+0.95}_{-0.73}$	$4.035^{+0.063}_{-0.060}$
WASP-15b	3.752	$0.0499^{+0.0017}_{-0.0018}$	< 0.055	$0.542^{+0.054}_{-0.053}$	$0.231^{+0.049}_{-0.040}$	2.819 ± 0.065
WASP-16b	3.119	$0.0422^{+0.0010}_{-0.0017}$	< 0.018	$0.908^{+0.045}_{-0.071}$	$1.14^{+0.14}_{-0.17}$	$3.355^{+0.020}_{-0.041}$
WASP-17b	3.735	0.05151 ± 0.00035	< 0.020	0.512 ± 0.037	$0.080^{+0.013}_{-0.011}$	2.504 ± 0.048
WASP-18b	0.941	$0.02030^{+0.00069}_{-0.00073}$	0.00757 ± 0.00100	$10.20^{+0.70}_{-0.72}$	$9.6^{+1.8}_{-1.6}$	$4.323^{+0.055}_{-0.058}$
WASP-19b	0.789	$0.01649^{+0.00053}_{-0.00056}$	< 0.0061	$1.157^{+0.076}_{-0.078}$	$0.637^{+0.10}_{-0.089}$	$3.222^{+0.049}_{-0.048}$
WASP-20b	4.900	$0.05999^{+0.00069}_{-0.00068}$	< 0.039	$0.311^{+0.019}_{-0.018}$	$0.123^{+0.018}_{-0.015}$	$2.557^{+0.044}_{-0.043}$
WASP-21b	4.323	$0.05212^{+0.00051}_{-0.00052}$	< 0.048	0.297 ± 0.013	$0.301^{+0.058}_{-0.047}$	$2.808^{+0.053}_{-0.050}$
WASP-22b	3.533	$0.04700^{+0.00036}_{-0.00037}$	< 0.021	$0.570^{+0.017}_{-0.016}$	$0.459^{+0.053}_{-0.060}$	$3.024^{+0.033}_{-0.041}$
WASP-23b	2.944	$0.0370^{+0.0019}_{-0.0022}$	< 0.065	$0.879^{+0.095}_{-0.10}$	$1.17^{+0.24}_{-0.20}$	$3.359^{+0.064}_{-0.068}$
WASP-24b	2.341	$0.03607^{+0.00044}_{-0.00045}$	< 0.0046	$1.060^{+0.030}_{-0.029}$	$0.597^{+0.060}_{-0.052}$	$3.191^{+0.029}_{-0.028}$

Table 9. continued.

Planet	P [days]	a au	e	M_p [M_{Jup}]	ρ_p [g cm^{-3}]	$\log g_p$ [cgs]
WASP-25b	3.765	0.04738 ± 0.00047	< 0.083	0.574 ± 0.042	$0.406^{+0.065}_{-0.056}$	2.990 ± 0.050
WASP-26b	2.757	$0.03997^{+0.00035}_{-0.00036}$	< 0.0039	$1.038^{+0.020}_{-0.021}$	$0.560^{+0.12}_{-0.092}$	$3.170^{+0.055}_{-0.053}$
WASP-28b	3.409	$0.04465^{+0.00073}_{-0.00074}$	< 0.058	$0.906^{+0.046}_{-0.044}$	$0.629^{+0.078}_{-0.068}$	$3.183^{+0.038}_{-0.036}$
WASP-29b	3.923	$0.04566^{+0.00060}_{-0.00062}$	< 0.059	$0.245^{+0.023}_{-0.022}$	0.61 ± 0.12	$2.985^{+0.059}_{-0.067}$
WASP-31b	3.406	0.04663 ± 0.00034	< 0.047	0.489 ± 0.025	$0.163^{+0.019}_{-0.017}$	2.703 ± 0.036
WASP-32b	2.719	$0.03904^{+0.00062}_{-0.00061}$	< 0.0040	$3.49^{+0.12}_{-0.11}$	$3.24^{+0.40}_{-0.34}$	$3.853^{+0.036}_{-0.033}$
WASP-34b	4.318	0.0521 ± 0.0012	< 0.025	$0.583^{+0.030}_{-0.031}$	$0.412^{+0.10}_{-0.087}$	$2.997^{+0.067}_{-0.070}$
WASP-35b	3.162	$0.04313^{+0.00040}_{-0.00041}$	< 0.028	0.701 ± 0.019	$0.378^{+0.049}_{-0.041}$	$2.999^{+0.036}_{-0.035}$
WASP-36b	1.537	$0.02643^{+0.00025}_{-0.00027}$	< 0.019	$2.296^{+0.068}_{-0.067}$	$1.354^{+0.10}_{-0.098}$	3.540 ± 0.023
WASP-37b	3.577	$0.0447^{+0.0018}_{-0.0020}$	< 0.052	1.72 ± 0.17	$1.43^{+0.30}_{-0.24}$	3.514 ± 0.064
WASP-38b	6.872	$0.07584^{+0.00080}_{-0.00082}$	$0.0278^{+0.0030}_{-0.0028}$	$2.648^{+0.057}_{-0.058}$	$2.54^{+0.15}_{-0.14}$	3.742 ± 0.018
WASP-39b	4.055	$0.04859^{+0.00051}_{-0.00053}$	< 0.048	$0.275^{+0.042}_{-0.043}$	$0.166^{+0.032}_{-0.029}$	$2.626^{+0.068}_{-0.078}$
WASP-41b	3.052	0.04022 ± 0.00044	< 0.12	$0.941^{+0.065}_{-0.064}$	$0.672^{+0.13}_{-0.099}$	$3.208^{+0.054}_{-0.052}$
WASP-42b	4.982	$0.0548^{+0.0017}_{-0.0018}$	$0.062^{+0.013}_{-0.011}$	0.501 ± 0.034	$0.514^{+0.094}_{-0.074}$	$3.039^{+0.053}_{-0.050}$
WASP-43b	0.813	$0.01528^{+0.00017}_{-0.00018}$	< 0.0062	$2.050^{+0.050}_{-0.052}$	$2.28^{+0.14}_{-0.13}$	3.675 ± 0.019
WASP-44b	2.424	$0.03474^{+0.00040}_{-0.00043}$	< 0.068	$0.878^{+0.065}_{-0.067}$	$0.74^{+0.27}_{-0.19}$	$3.224^{+0.093}_{-0.087}$
WASP-45b	3.126	$0.04054^{+0.00087}_{-0.00093}$	< 0.043	1.003 ± 0.054	$0.79^{+0.39}_{-0.37}$	$3.26^{+0.12}_{-0.19}$
WASP-46b	1.430	$0.02334^{+0.00061}_{-0.00065}$	< 0.022	1.90 ± 0.11	$1.45^{+0.16}_{-0.14}$	3.533 ± 0.036
WASP-48b	2.144	$0.03449^{+0.00047}_{-0.00049}$	< 0.014	$1.031^{+0.046}_{-0.045}$	$0.275^{+0.056}_{-0.046}$	$2.962^{+0.055}_{-0.054}$
WASP-49b	2.782	$0.0379^{+0.0010}_{-0.0011}$	< 0.026	$0.399^{+0.029}_{-0.027}$	$0.356^{+0.057}_{-0.048}$	2.899 ± 0.048
WASP-50b	1.955	$0.02945^{+0.00084}_{-0.00087}$	< 0.022	1.460 ± 0.087	$1.18^{+0.18}_{-0.15}$	$3.434^{+0.045}_{-0.044}$
WASP-52b	1.750	$0.02713^{+0.00031}_{-0.00032}$	< 0.092	$0.459^{+0.022}_{-0.021}$	$0.277^{+0.025}_{-0.023}$	$2.848^{+0.030}_{-0.029}$
WASP-54b	3.694	$0.04988^{+0.00043}_{-0.00045}$	< 0.060	0.606 ± 0.018	$0.167^{+0.029}_{-0.024}$	$2.741^{+0.047}_{-0.046}$
WASP-55b	4.466	0.05326 ± 0.00071	< 0.056	$0.571^{+0.045}_{-0.042}$	$0.321^{+0.038}_{-0.039}$	$2.921^{+0.041}_{-0.045}$
WASP-56b	4.617	$0.05614^{+0.00040}_{-0.00041}$	< 0.082	$0.599^{+0.040}_{-0.039}$	$0.571^{+0.069}_{-0.062}$	$3.096^{+0.039}_{-0.040}$
WASP-57b	2.839	$0.03772^{+0.00083}_{-0.00089}$	< 0.059	$0.643^{+0.056}_{-0.054}$	$0.69^{+0.13}_{-0.11}$	$3.161^{+0.057}_{-0.056}$
WASP-58b	5.017	$0.0562^{+0.0019}_{-0.0020}$	< 0.044	$0.899^{+0.074}_{-0.072}$	$0.44^{+0.27}_{-0.15}$	$3.08^{+0.14}_{-0.12}$
WASP-59b	7.920	0.0697 ± 0.0011	< 0.12	$0.857^{+0.046}_{-0.047}$	$2.28^{+0.74}_{-0.53}$	$3.548^{+0.083}_{-0.078}$
WASP-60b	4.305	$0.05311^{+0.00058}_{-0.00059}$	< 0.064	0.505 ± 0.048	$0.99^{+0.57}_{-0.34}$	$3.23^{+0.14}_{-0.12}$
WASP-61b	3.856	$0.05146^{+0.00097}_{-0.00099}$	< 0.074	$2.05^{+0.18}_{-0.17}$	$1.33^{+0.16}_{-0.14}$	$3.519^{+0.042}_{-0.044}$
WASP-62b	4.412	$0.05672^{+0.00075}_{-0.00079}$	< 0.075	$0.568^{+0.043}_{-0.042}$	$0.262^{+0.043}_{-0.036}$	2.862 ± 0.050
WASP-63b	4.378	$0.05417^{+0.00067}_{-0.00089}$	< 0.086	0.339 ± 0.030	$0.179^{+0.14}_{-0.070}$	$2.68^{+0.17}_{-0.15}$
WASP-64b	1.573	$0.02652^{+0.00024}_{-0.00025}$	< 0.054	$1.221^{+0.073}_{-0.071}$	$0.737^{+0.087}_{-0.077}$	3.272 ± 0.038
WASP-65b	2.311	$0.0334^{+0.0016}_{-0.0018}$	< 0.016	$1.54^{+0.15}_{-0.16}$	$1.38^{+0.29}_{-0.24}$	$3.488^{+0.063}_{-0.066}$
WASP-66b	4.086	$0.05461^{+0.00099}_{-0.00096}$	< 0.046	2.37 ± 0.14	$1.09^{+0.25}_{-0.19}$	$3.482^{+0.064}_{-0.059}$
WASP-67b	4.614	$0.05179^{+0.00080}_{-0.00078}$	< 0.015	0.420 ± 0.035	$0.200^{+0.14}_{-0.084}$	$2.74^{+0.15}_{-0.16}$
WASP-68b	5.084	$0.06219^{+0.00049}_{-0.00051}$	< 0.023	$0.957^{+0.025}_{-0.024}$	$0.63^{+0.11}_{-0.12}$	$3.190^{+0.048}_{-0.063}$
WASP-69b	3.868	$0.04527^{+0.00053}_{-0.00054}$	< 0.11	0.250 ± 0.023	$0.262^{+0.047}_{-0.039}$	$2.743^{+0.056}_{-0.055}$
WASP-70Ab	3.713	$0.04855^{+0.00061}_{-0.00063}$	< 0.053	0.597 ± 0.026	$0.454^{+0.13}_{-0.080}$	$3.029^{+0.071}_{-0.059}$
WASP-71b	2.904	$0.04622^{+0.00068}_{-0.00069}$	< 0.019	2.222 ± 0.078	$0.89^{+0.29}_{-0.20}$	$3.412^{+0.084}_{-0.074}$
WASP-72b	2.217	$0.03711^{+0.00048}_{-0.00051}$	< 0.017	$1.446^{+0.054}_{-0.053}$	$0.87^{+0.58}_{-0.31}$	$3.34^{+0.15}_{-0.13}$
WASP-73b	4.087	$0.05517^{+0.00068}_{-0.00069}$	< 0.017	$1.879^{+0.061}_{-0.062}$	$1.53^{+0.41}_{-0.35}$	$3.546^{+0.069}_{-0.076}$
WASP-74b	2.138	$0.03705^{+0.00096}_{-0.0010}$	< 0.030	$0.944^{+0.061}_{-0.059}$	$0.309^{+0.043}_{-0.037}$	$2.983^{+0.042}_{-0.043}$
WASP-75b	2.484	$0.03751^{+0.00075}_{-0.00077}$	< 0.056	$1.073^{+0.059}_{-0.056}$	$0.649^{+0.089}_{-0.075}$	$3.217^{+0.041}_{-0.039}$
WASP-77Ab	1.360	0.02405 ± 0.00036	< 0.0075	$1.763^{+0.055}_{-0.054}$	$1.234^{+0.073}_{-0.070}$	3.475 ± 0.020
WASP-78b	2.175	$0.03488^{+0.00070}_{-0.00076}$	< 0.092	$0.817^{+0.075}_{-0.069}$	$0.251^{+0.061}_{-0.045}$	$2.903^{+0.068}_{-0.064}$
WASP-79b	3.662	$0.0521^{+0.0011}_{-0.0010}$	< 0.066	$0.843^{+0.085}_{-0.080}$	$0.178^{+0.088}_{-0.068}$	$2.80^{+0.12}_{-0.13}$
WASP-80b	3.068	$0.03427^{+0.00096}_{-0.0010}$	< 0.020	$0.540^{+0.036}_{-0.035}$	$0.776^{+0.088}_{-0.078}$	$3.169^{+0.038}_{-0.037}$
WASP-83b	4.971	$0.0590^{+0.0015}_{-0.0016}$	< 0.12	$0.305^{+0.037}_{-0.035}$	$0.338^{+0.076}_{-0.074}$	$2.845^{+0.070}_{-0.082}$
WASP-84b	8.523	0.0771 ± 0.0011	< 0.077	$0.694^{+0.049}_{-0.047}$	$1.029^{+0.11}_{-0.098}$	3.287 ± 0.037
WASP-88b	4.954	$0.06438^{+0.00073}_{-0.00074}$	< 0.13	$0.570^{+0.077}_{-0.078}$	$0.141^{+0.032}_{-0.031}$	$2.681^{+0.075}_{-0.087}$
WASP-89b	3.356	$0.0428^{+0.0012}_{-0.0013}$	$0.1928^{+0.0100}_{-0.0094}$	$5.80^{+0.34}_{-0.36}$	$6.37^{+0.89}_{-0.79}$	4.122 ± 0.043
WASP-94Ab	3.950	$0.0554^{+0.0011}_{-0.0012}$	< 0.064	$0.456^{+0.036}_{-0.034}$	$0.114^{+0.014}_{-0.013}$	$2.590^{+0.042}_{-0.044}$
WASP-95b	2.185	$0.03415^{+0.00093}_{-0.00096}$	< 0.018	$1.204^{+0.071}_{-0.074}$	$0.84^{+0.15}_{-0.12}$	$3.308^{+0.052}_{-0.048}$
WASP-96b	3.425	0.0454 ± 0.0013	< 0.11	$0.490^{+0.049}_{-0.047}$	$0.352^{+0.068}_{-0.059}$	$2.926^{+0.060}_{-0.062}$

Table 9. continued.

Planet	P [days]	a au	e	M_p [M_{Jup}]	ρ_p [g cm^{-3}]	$\log g_p$ [cgs]
WASP-97b	2.073	$0.03305^{+0.00058}_{-0.00059}$	< 0.019	$1.323^{+0.057}_{-0.056}$	$1.13^{+0.21}_{-0.16}$	$3.409^{+0.051}_{-0.049}$
WASP-98b	2.963	$0.03571^{+0.0010}_{-0.0010}$	< 0.070	$0.848^{+0.084}_{-0.076}$	$0.79^{+0.12}_{-0.11}$	3.240 ± 0.052
WASP-99b	5.753	0.0717 ± 0.0016	< 0.0100	2.80 ± 0.13	$2.63^{+0.45}_{-0.47}$	$3.760^{+0.048}_{-0.058}$
WASP-100b	2.849	$0.04574^{+0.00093}_{-0.00100}$	< 0.044	$2.01^{+0.12}_{-0.11}$	$0.52^{+0.39}_{-0.19}$	$3.24^{+0.17}_{-0.14}$
WASP-101b	3.586	$0.05057^{+0.00085}_{-0.00090}$	< 0.068	$0.497^{+0.049}_{-0.048}$	$0.219^{+0.034}_{-0.030}$	$2.791^{+0.051}_{-0.052}$
WASP-103b	0.926	$0.01987^{+0.00020}_{-0.00021}$	< 0.15	$1.455^{+0.090}_{-0.091}$	$0.511^{+0.068}_{-0.073}$	$3.191^{+0.043}_{-0.050}$
WASP-104b	1.755	0.02920 ± 0.00044	< 0.015	$1.268^{+0.050}_{-0.049}$	$1.07^{+0.12}_{-0.10}$	$3.386^{+0.034}_{-0.032}$
WASP-106b	9.290	0.0917 ± 0.0014	< 0.046	1.909 ± 0.079	$1.86^{+0.18}_{-0.21}$	$3.604^{+0.031}_{-0.037}$
WASP-117b	10.022	0.09464 ± 0.00082	0.300 ± 0.026	$0.2761^{+0.0099}_{-0.0096}$	$0.341^{+0.078}_{-0.061}$	$2.834^{+0.062}_{-0.057}$
WTS-2b	1.019	$0.01856^{+0.00059}_{-0.00062}$	< 0.35	$1.27^{+0.19}_{-0.21}$	$0.62^{+0.13}_{-0.12}$	$3.229^{+0.071}_{-0.085}$
XO-1b	3.942	$0.04930^{+0.00091}_{-0.00096}$	< 0.019	0.913 ± 0.038	$0.645^{+0.081}_{-0.071}$	$3.191^{+0.037}_{-0.036}$
XO-2b	2.616	0.03665 ± 0.00064	< 0.0060	$0.595^{+0.022}_{-0.021}$	$0.698^{+0.073}_{-0.066}$	3.153 ± 0.031
XO-3b	3.192	$0.04539^{+0.00081}_{-0.00084}$	$0.27587^{+0.00071}_{-0.00067}$	$11.70^{+0.42}_{-0.43}$	$8.1^{+1.6}_{-1.3}$	$4.293^{+0.055}_{-0.053}$
XO-4b	4.125	$0.05524^{+0.00027}_{-0.00028}$	< 0.0039	$1.612^{+0.027}_{-0.028}$	$0.830^{+0.10}_{-0.088}$	$3.347^{+0.034}_{-0.033}$
XO-5b	4.188	$0.04874^{+0.00054}_{-0.00057}$	< 0.021	1.046 ± 0.033	$0.95^{+0.15}_{-0.12}$	$3.324^{+0.043}_{-0.041}$

[1] INAF – Osservatorio Astrofisico di Torino, Via Osservatorio 20, I-10025 Pino Torinese, Italy
[2] INAF – Osservatorio Astronomico di Padova, Vicolo dell'Osservatorio 5, I-35122 Padova, Italy
[3] INAF – Osservatorio Astronomico di Brera, Via E. Bianchi 46, I-23807 Merate (LC), Italy
[4] Dipartimento di Fisica, Università Degli Studi di Milano, Via Celoria 16, I-20133 Milano, Italy
[5] INAF – Osservatorio Astrofisico di Catania, Via S. Sofia 78, I-95123 Catania, Italy
[6] Dipartimento di Fisica e Astronomia Galileo Galilei – Università di Padova, Vicolo dellOsservatorio 3, I-35122 Padova, Italy
[7] Fundación Galileo Galilei - INAF, Rambla José Ana Fernandez Pérez 7, E-38712 Breña Baja, TF - Spain
[8] INAF – Osservatorio Astronomico di Capodimonte, Salita Moiariello 16, I-80131 Napoli, Italy
[9] INAF – Osservatorio Astronomico di Palermo, Piazza del Parlamento, 1, I-90134 Palermo, Italy
[10] INAF – Osservatorio Astronomico di Trieste, via Tiepolo 11, I-34143 Trieste, Italy
[11] Institut d'Astrophysique de Paris, UMR7095 CNRS, Université Pierre & Marie Curie, 98bis boulevard Arago, 75014 Paris, France
[12] Observatoire de Haute-Provence, Université Aix-Marseille & CNRS, F-04870 St. Michel l'Observatoire, France
[13] Max-Planck-Institut für Astronomie, Königstuhl 17, D-69117 Heidelberg, Germany
[14] GAL Hassin, Centro Internazionale per le Scienze Astronomiche, I-90010 Isnello, Italy